

Recovery Performance and Relative Permeabilities of Composite Cores

by

Ashiq Hussain

A Thesis Presented to the

FACULTY OF THE COLLEGE OF GRADUATE STUDIES

KING FAHD UNIVERSITY OF PETROLEUM & MINERALS

DHAHRAN, SAUDI ARABIA

In Partial Fulfillment of the
Requirements for the Degree of

MASTER OF SCIENCE

In

PETROLEUM ENGINEERING

April, 1995

INFORMATION TO USERS

This manuscript has been reproduced from the microfilm master. UMI films the text directly from the original or copy submitted. Thus, some thesis and dissertation copies are in typewriter face, while others may be from any type of computer printer.

The quality of this reproduction is dependent upon the quality of the copy submitted. Broken or indistinct print, colored or poor quality illustrations and photographs, print bleedthrough, substandard margins, and improper alignment can adversely affect reproduction.

In the unlikely event that the author did not send UMI a complete manuscript and there are missing pages, these will be noted. Also, if unauthorized copyright material had to be removed, a note will indicate the deletion.

Oversize materials (e.g., maps, drawings, charts) are reproduced by sectioning the original, beginning at the upper left-hand corner and continuing from left to right in equal sections with small overlaps. Each original is also photographed in one exposure and is included in reduced form at the back of the book.

Photographs included in the original manuscript have been reproduced xerographically in this copy. Higher quality 6" x 9" black and white photographic prints are available for any photographs or illustrations appearing in this copy for an additional charge. Contact UMI directly to order.

UMI

A Bell & Howell Information Company
300 North Zeeb Road, Ann Arbor, MI 48106-1346 USA
313/761-4700 800/521-0600



Recovery Performance and Relative Permeabilities of Composite Cores

BY

ASHIQ HUSSAIN

A Thesis Presented to the
FACULTY OF THE COLLEGE OF GRADUATE STUDIES
KING FAHD UNIVERSITY OF PETROLEUM & MINERALS
DHAHRAN, SAUDI ARABIA

In Partial Fulfillment of the
Requirements for the Degree of

MASTER OF SCIENCE
In
PETROLEUM ENGINEERING

April 1995

UMI Number: 1375317

UMI Microform 1375317
Copyright 1995, by UMI Company. All rights reserved.

**This microform edition is protected against unauthorized
copying under Title 17, United States Code.**

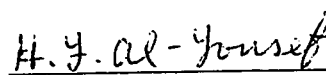
UMI
300 North Zeeb Road
Ann Arbor, MI 48103

KING FAHD UNIVERSITY OF PETROLEUM AND MINERALS
DHAHRAN, SAUDI ARABIA

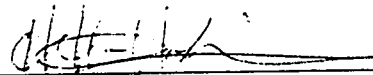
COLLEGE OF GRADUATE STUDIES

This thesis, written by **Mr. Ashiq Hussain** under the direction of his Thesis Advisor and approved by his Thesis Committee, has been presented to and accepted by the Dean of the College of Graduate Studies, in partial fulfillment of the requirements for the degree of **MASTER OF SCIENCE** in **Petroleum Engineering**.

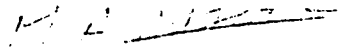
Thesis Committee:



Dr. Hasan Y. Al-Yousef
Thesis Advisor



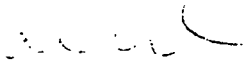
Dr. Hasan S. Al-Hashim
Member



Dr. Mohamed A. Aggour
Member

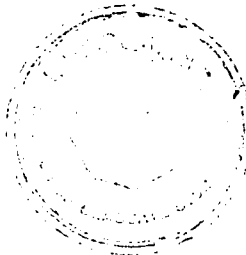


Dr. Khalid A. Al-Fossail
Department Chairman



Dr. Ala H. Al-Rabeh
Dean, College of Graduate Studies

Date: _____



Dedicated

to

Mahr Mohammad Iqbal

Acknowledgement

In the name of Allah, Most Gracious, Most Merciful.

First and foremost, all praise to Allah, the Almighty, Who gave me an opportunity, courage and patience to carry out this work.

I am indebted to my thesis advisor Dr. Hasan Y. Al-yousef for his constant help, co-operation, and guidance. Working with him was indeed a learning experience.

Thanks are due to my thesis committee member Dr. Hasan S. Al-Hashim and Dr. Mohammad A. Aggour for their deep interest, and valuable comments. I am also thankful to Dr. Abdulaziz U. Al-Kaabi for allowing me to utilize the laboratories in Division-1 at the Research Institute for this experimental work. Acknowledgement is also due to King Fahd University of Petroleum & Minerals for providing support to this work.

I would also thank my friends Atif, Mansoor and Sabih for helping me in typing and compiling this report. Thanks are due to Dr. Subarao Ghanta for allowing to utilize computing facilities at Optical Lab. and making useful comments, suggestions and advice throughout my stay at KFUPM.

Last but not the least, thanks are due to my family members for their understanding throughout my academic career, and all my friends in and out of the campus who shared my happiness and were partners in tough times.

Contents

Acknowledgement	i
List of Tables	vi
List of Figures	vii
Abstract (English)	
Abstract (Arabic)	i
1 INTRODUCTION	1
1.1 Relative Permeability	2
1.2 Composite Core	3
1.3 Uses of Relative Permeability	4
1.4 Measurement of Relative Permeability	5
1.4.1 Steady-State Method	5
1.4.2 Unsteady-State Method	6
1.4.3 Centrifuge Method	7

2	LITERATURE REVIEW	8
3	STATEMENT OF THE PROBLEM AND PROPOSED APPROACH	14
3.1	Proposed Approach	15
4	EXPERIMENTAL EQUIPMENT AND PROCEDURES	16
4.1	Centrifuge	16
4.2	Displacement Setup	17
4.2.1	Main Flow System	17
4.2.2	Core Holder	20
4.2.3	Confining Pressure System	20
4.2.4	Injection System	22
4.2.5	Effluent Measurement System	22
4.2.6	Pressure Measurement System	22
4.2.7	Data Acquisition System	24
4.3	Fluids	24
4.4	Experimental Procedures	26
4.4.1	Core Cleaning	26
4.4.2	Drying of the Core Samples	26
4.4.3	Porosity Measurement	27
4.4.4	Air Permeability Determination	29
4.4.5	Brine Saturation	31

4.4.6	Aging of Core Samples	31
4.4.7	Wettability Measurement	33
4.4.8	Displacement Experiments	33
4.4.9	Determination of S_{wi} and S_{or}	34
5	RESULTS AND DISCUSSION	36
5.1	Wettability of Core Samples	36
5.2	Recovery Performance	43
5.3	JBN Relative Permeabilities	47
5.4	Comparison of Experimental and Calculated Results	48
5.5	History Match Relative Permeabilities	72
5.6	Numerical Simulation	73
5.6.1	No Capillary Pressure Included	83
5.6.2	Capillary Pressure Included	84
6	CONCLUSIONS	104
6.1	Experimental	104
6.2	Numerical	104
	Nomenclature	106
	Bibliography	108
	Appendix A	113

Appendix B	117
B.1 Wettability	118
B.1.1 USBM Method	118
B.2 Johnson-Bossler-Naumann Method	121
Vita	123

List of Tables

4.1	Porosities and Permeabilities of Core Samples	31
5.1	Wettability Indices of Core Samples	43
5.2	Recovery Performance of Core Samples	44
5.3	Input parameters for the simulation runs	73
A.1	Oil and Brine Drive of Core Plug-2	114
A.2	Oil and Brine Drive of Core Plug-12	114
A.3	Oil and Brine Drive of Core Plug-3	115
A.4	Oil and Brine Drive of Core Plug-4	115
A.5	Oil and Brine Drive of Core Plug-16	116

List of Figures

4.1	Rotor head of Centrifuge	18
4.2	Beckman Centrifuge	19
4.3	Main Flow System for Displacement Experiment	19
4.4	Core Holder	21
4.5	Confining Pressure System	21
4.6	Fluids Injection System	23
4.7	Effluent Measurement System	23
4.8	Pressure Measurement System	25
4.9	Data Acquisition System	25
4.10	Forced through System for Core Cleaning	27
4.11	Electric Vacuum Oven for Drying of Samples	28
4.12	Helium Porosimeter	28
4.13	Air Permeameter	30
4.14	Brine Saturator	32
5.1	Capillary Pressure Curves for Core Plug P-2	38

5.2	Capillary Pressure Curves for Core Plug P-12	39
5.3	Capillary Pressure Curves for Core Plug P-3	40
5.4	Capillary Pressure Curves for Core Plug P-4	41
5.5	Capillary Pressure Curves for Core Plug P-16	42
5.6	Recovery Performance Comparison of Composite-1	45
5.7	Recovery Performance Comparison of Composite-2	46
5.8	JBN Relative Permeabilities of Core Plug P-2	49
5.9	JBN Relative Permeabilities of Core Plug P-12	50
5.10	JBN Relative Permeabilities of Composite Core-1	51
5.11	JBN Relative Permeabilities of Core Plug P-3	52
5.12	JBN Relative Permeabilities of Core Plug P-4	53
5.13	JBN Relative Permeabilities of Core Plug P-16	54
5.14	JBN Relative Permeabilities of Composite Core-2	55
5.15	JBN Relative Permeabilities Comparison of Composite-1	56
5.16	JBN Relative Permeabilities Comparison of Composite-2	57
5.17	Recovery Performance for Core Plug P-2	58
5.18	Pressure differential Curves for Core Plug P-2	59
5.19	Recovery Performance for Core Plug P-12	60
5.20	Pressure differential Curves for Core Plug P-12	61
5.21	Recovery Performance for Composite-1	62
5.22	Pressure differential Curves for Composite-1	63

5.23 Recovery Performance Curves for Core Plug P-3	64
5.24 Pressure differential Curves for Core Plug P-3	65
5.25 Recovery Performance Curves for Core Plug P-4	66
5.26 Pressure differential Curves for Core Plug P-4	67
5.27 Recovery Performance Curves for Core Plug P-16	68
5.28 Pressure differential Curves for Core Plug P-16	69
5.29 Recovery Performance Curves for Composite-2	70
5.30 Pressure differential Curves for Composite-2	71
5.31 History Match Recovery for Core Plug P-3	74
5.32 History Match Pressure drop for Core Plug P-3	75
5.33 History Match Relative Permeabilities for Core Plug P-3	76
5.34 History Match Recovery for Core Plug P-4	77
5.35 History Match Pressure drop for Core Plug P-4	78
5.36 History Match Relative Permeabilities for Core Plug P-4	79
5.37 History Match Recovery for Composite-2	80
5.38 History Match Pressure drop for Composite-2	81
5.39 History Match Relative Permeabilities for Composite-2	82
5.40 Recovery comparison for 2-plug composites without Capillary Pressure	85
5.41 Pressure drop comparison for 2-plug composites without Capillary Pressure	86
5.42 Recovery comparison for 3-plug composites without Capillary Pressure	87

5.43 Pressure drop comparison for 3-plug composites without Capillary	
Pressure	88
5.44 Relative permeabilities for 2-plug composites without Capillary Pres-	
sure	89
5.45 Relative permeabilities for 3-plug composites without Capillary Pres-	
sure	90
5.46 Averaging of relative permeabilities for 2-plug composites without	
Capillary Pressure	91
5.47 Averaging of relative permeabilities for 3-plug composites without	
Capillary Pressure	92
5.48 Recovery comparison for 2-plug composites with Capillary Pressure .	94
5.49 Pressure drop comparison for 2-plug composites with Capillary Pressure	95
5.50 Recovery comparison for 3-plug composites with Capillary Pressure .	96
5.51 Pressure drop comparison for 3-plug composites with Capillary Pressure	97
5.52 Relative permeabilities for 2-plug composites with Capillary Pressure	98
5.53 Relative permeabilities for 3-plug composites with Capillary Pressure	99
5.54 Averaging of relative permeabilities for 2-Plug composites with Cap-	
illary Pressure	100
5.55 Averaging of relative permeabilities for 3-Plug composites with Cap-	
illary Pressure	101

5.56 Comparison of relative permeabilities for 2-plug composites with and without Capillary Pressure	102
5.57 Comparison of relative permeabilities for 3-plug composites with and without Capillary Pressure	103

THESIS ABSTRACT

Full Name of the Student: **Ashiq Hussain**

Title of Study : **RECOVERY PERFORMANCE AND RELATIVE
PERMEABILITIES OF COMPOSITE CORES**

Major Field : **Petroleum Engineering**

Date of Degree : **April 1995**

An experimental and numerical investigation was carried out to study the recovery performance and the averaging process of relative permeabilities of composite cores. The displacement experiments were conducted using carbonate reservoir rock samples. The results indicated that the oil recovery obtained from the composite cores was less than that obtained from the individual core plugs. The observed decrease in oil recovery is attributed to viscous fingering and bypassing due to the heterogeneous nature of the carbonate rocks. The relative permeabilities of the composite cores did not represent any kind of average of the individual plugs relative permeabilities.

The numerical simulation results showed that the oil recovery of the composite core is the average of the individual plugs recoveries. The relative permeability of the composite core is the harmonic average of the relative permeabilities of the individual plugs and the ordering of the plugs making the composite has no effect on the calculated average relative permeability curves.

MASTER OF SCIENCE DEGREE

**KING FAHD UNIVERSITY OF PETROLEUM AND MINERALS
Dhahran, Saudi Arabia**

Date: April 1995

ملخص الرسالة

الاسم : عاشق حسين

العنوان : أداء الانتاج والنفاذية النسبية للعينات اللبية المركبة .

التخصص : هندسة البترول

تاريخ التخرج : أبريل ١٩٩٥ م

لقد تم إجراء تجارب مختبرية وأخرى حسابية لدراسة أداء الانتاج وطرق احتساب متوسط النفاذية النسبية للعينات اللبية المركبة . ولقد إستخدمت عينات لبية من صخور مكن جييري في إجراء تجارب الإزاحة ولقد أظهرت نتائج التجارب المخبرية أن إنتاج الزيت من العينات اللبية المركبة أقل من إنتاج الزيت من العينات اللبية المنفردة ويعزى ذلك إلى الإختراق اللزوجي والهروب الجانبي بسبب عدم التجانس الطبيعي للصخور الجيرية التى استخدمت في الدراسة . كما أظهرت النتائج المخبرية أن النفاذية النسبية المتحصلة في العينات اللبية المركبة لاتمثل إلا متوسط النفاذية النسبية للعينات اللبية المنفردة .

ولقد بينت نتائج المحاكاة الحسابية أن إنتاج الزيت من العينات اللبية المركبة يساوي متوسط إنتاج العينات اللبية المنفردة وأن النفاذية النسبية للعينات المركبة يساوي المتوسط التوافقي للنفاذية النسبية للعينات اللبية المنفردة ووجد أيضاً أن ترتيب العينات اللبية في تكوين العينات المركبة لا يؤثر على منحنيات النفاذية النسبية المتوسط والمحتسبة .

درجة الماجستير في العلوم

جامعة الملك فهد للبترول والمعادن

الظهران - المملكة العربية السعودية

Chapter 1

INTRODUCTION

Permeability is defined as the fluid conductance capacity of the rock. Petroleum reservoir rocks are usually saturated with two or three fluid phases. Describing the simultaneous flow of two or more immiscible fluids through naturally occurring porous media is an important consideration in reservoir engineering. Relative permeability is used to describe multiphase flow behavior of the fluids in the rock.

Relative permeability is measured in the laboratory on small core plug samples which are cut parallel to the bedding planes of the reservoir rock. The representativeness of the results from these small plugs are often questionable due to the very small size of the samples as compared to the reservoir.

Composite cores are usually formed by combining small core samples side by side to have a longer core sample. Composite cores are preferred to use because they provide better material balance accuracy and decreased capillary end effects which usually affect the relative permeability measurements on small core samples.

1.1 Relative Permeability

The absolute permeability concept is not adequate to describe multiphase flow in petroleum reservoirs. The effective permeability of a porous medium to a fluid is a measure of the ability of the medium to transmit this fluid when the medium is saturated with more than one fluid. Effective permeability is a property that is dependent on both rock properties and the fluid saturations.

The relative permeability, a dimensionless quantity, to a fluid is defined as the ratio of effective permeability at a given saturation of that fluid to a reference permeability. The reference permeability is usually the absolute permeability or the effective permeability to oil at irreducible water saturation. Relative permeability is a direct measure of the ability of the porous system to conduct one fluid when one or more fluids are present. It is dependent upon both fluid saturation and the distribution of various fluids in the interstices of the porous network. This distribution is directly related to wettability characteristics of the rock.[13]

One of the most important properties needed to make a waterflood prediction is the water-oil relative permeability characteristics of the reservoir rock. The relative permeabilities are usually obtained from displacement experiments conducted using single core plugs or composite cores. The laboratory determination of the relative permeabilities of a sample should give the same relative permeability-saturation relationship that would exist if the sample were in place in the reservoir. The

attainment of this objective is complicated by the fact that the use of small core samples for laboratory measurement is necessary.

Errors in measuring relative permeability arise from the boundary effects. At the inlet end of the sample, a boundary effect exists if the injected fluid is not uniformly distributed at the face of the core. At the outlet end of the sample a boundary effect exists as a result of discontinuity of the capillary properties of the system. Here the flowing fluids leave the small flow channels and enter a collecting system having much enlarged flow channels. Thus, there is a tendency for the wetting phase to be retained by the core sample because of the attraction of the core sample for the wetting fluid.[17]

Relative permeabilities are functions of wettability, pore geometry, fluid distribution, saturation, and saturation history. The saturation gradient (end effect) may cause a variable permeability measurement, since the extent and character of this gradient can vary with fluid flowrate. Wettability affects relative permeability by controlling the flow and spatial distribution of fluids in porous medium.[14]

1.2 Composite Core

A Composite core is formed by splicing core plugs side by side to form a longer core. Determining the relative permeabilities from composite core is more advantageous due to the following reasons.

- Combining core plugs to form a composite core increases the volume of the core for material balance accuracy.
- For 2 inch core plug the end effects are very significant and that result in an extra pressure drop that affects the analysis. For long composite core (composed of three or more individual plugs) the end effects are minimized. The end effect zone may be viewed as a zone that causes an extra pressure drop similar to a damaged zone around a producing well. Since the zone width increases with decrease in flow rate, the additional pressure drop due to viscous forces will be relatively higher for high displacement rates.

1.3 Uses of Relative Permeability

Relative permeability data enter in a vital way in many reservoir engineering calculations. Relative permeability data are used to describe multiphase flow in porous medium. Such data may have the following applications[13]

- Aid in evaluating drill stem and production tests.
- Determination of residual fluid saturations.
- Fractional flow and frontal advance calculations to determine fluid distributions.
- Input in reservoir simulation models

1.4 Measurement of Relative Permeability

The relative permeability of a rock to each fluid phase can be measured on a core sample in the laboratory by the steady-state, unsteady-state or the centrifuge methods. In most reservoir conditions, the displacement is dynamic and thus the application of steady-state relative permeabilities to describe unsteady-state behavior is questionable from a conceptual point of view. It has been found by several researchers [e.g., 20,21] that there is a disagreement between unsteady-state and steady-state relative permeabilities values for the same samples of the reservoir. Other researchers, [1,3,12] however, found a good match between the two. The centrifuge method is faster than the steady-state technique and is not subject to the viscous fingering problems which sometimes interfere with the unsteady-state measurements.

1.4.1 Steady-State Method

In the various steady-state methods, oil and water are injected at constant rates into the core until the saturations reach equilibrium values. The pressure drop across the core is then measured to determine the relative permeabilities using the Darcy's law. The primary concern in designing the experiment is to eliminate or reduce the saturation gradient which is caused by capillary pressure end effects at the outflow boundary of the core.

Some of the most commonly used laboratory methods for measuring steady-state relative permeability are Penn-State method, Single-sample Dynamic method, Stationary Fluid method, Hassler method, Hafford method and Dispersed Feed method. Steady-state methods are generally very slow, taking days or weeks, because the saturations must reach equilibrium after each change in the injection flow rates. The main difference between the various steady-state methods is the procedure used to minimize outlet end effects.[16]

1.4.2 Unsteady-State Method

The unsteady-state method is the most common because it qualitatively resembles the actual flooding behavior in the field. The unsteady-state external drive method is fast, requiring only hours to determine the entire relative permeability curve. A core is fully saturated with brine and then driven to S_{wi} by oil flooding. Water is then injected into the core at a steady rate, and the relative permeability is calculated from the pressure drop across the core and produced fluids using the JBN method.[3]

The JBN method was derived from the theory developed by Buckley and Leverett [22] and Welge[16] and is based on the following assumptions.

- Capillary pressure forces are negligible compared to viscous forces.
- The core is a linear homogeneous body.

- Flow is stable and one dimensional.
- Gravity segregation effects are negligible.

1.4.3 Centrifuge Method

The centrifuge technique for measuring relative permeabilities involves monitoring liquid produced from rock samples. The samples are initially saturated uniformly with one or two phases. Liquids are collected in transparent tubes connected to the rock sample holders and production is monitored throughout the test. The centrifuge method has not been used widely, although it offers some advantages over other methods[17]. This method is becoming more popular because of improvements in automatic techniques to determine saturation.

Chapter 2

LITERATURE REVIEW

Reservoir rocks have complex nature of flow paths and fluid flow characteristics of these porous media are not easy to determine. There are several methods to measure multiphase flow properties of a porous medium. One of the methods is to measure relative permeabilities in the laboratory. There are some commonly used methods of measuring relative permeability in the laboratory; the steady-state, unsteady-state and centrifuge method. Effects of different parameters as wettability, capillary pressure and temperature on relative permeabilities have been studied by many researchers.

In 1952, Richardson et al. [1] applied the steady-state technique of relative permeability determination. They demonstrated that for two-phase flow in a core, a relatively uniform saturation distribution is obtained toward the inflow end. However, a zone of increasing wetting phase saturation existed toward the outflow end. The width of the zone decreased with increased flow rate.

Rapoport and Leas [2] in 1953, studied the properties of linear waterfloods. They established a scaling factor (product of length of the core, fluid velocity and viscosity) and showed that for a particular porous medium, there is a critical value of the factor. Above this value the flooding behavior is stabilized and recovery is independent of rate and length while below this value, floods are sensitive to rate and length.

In 1958, Sandberg et al.[29] investigated the effect of flow rate and viscosity on relative permeability. They showed that relative permeability is a function of saturation and is independent of flow rate and non-wetting phase saturation. They proposed to increase flow rate to minimize boundary effects.

The most widely used method to calculate relative permeabilities was developed in 1959 by Johnson, Bossler and Naumann [3], called the JBN method. It is used to calculate individual gas and oil and water and oil relative permeabilities from linear displacement experiments on nominal size core samples. They assumed that the flowing pressure gradient is high compared to the capillary pressure difference between the flowing phases and constant flow velocity at each cross section of the linear porous body. They derived equations, using Welge's method, to calculate the relative permeabilities.

Jones and Roszelle [6] presented a graphical technique for determining relative permeabilities. The graphical technique is equivalent to JBN and Welge equations. From the graphs of average saturation versus pore volumes of injected fluid, material

balance and relative injectivity versus pore volumes injected, the tangent to the curves give the saturation at the outlet end of the core, oil fractional flow and consequently relative permeabilities can be computed.

Odeh and Dotson [21] devised a technique to correct the values of relative permeabilities computed by Jones and Roszelle by taking into account the effect of flow rate. They suggested to make a graph (expected to be a straight line) of q/k_r (ratio of flow rate to relative permeability for both water and oil) versus average water saturation and compute the corrected values by

$$(k_r)_{cor} = k_r \frac{(q/k_r)_c}{(q/k_r)_{SL}} \quad (2.1)$$

where subscripts 'cor' , 'c' and 'SL' refer to the relative permeabilities corrected, computed from Jones and Roszelle's technique and from graph, respectively.

In 1989, Civan and Donaldson [28] developed a semianalytical method for calculation of relative permeabilities from unsteady-state displacement. They solved the fraction flow equation and integro-differential equation, derived from the material balance and Darcy's equation, including the capillary pressure.

In 1969, Huppler [4] introduced an ordering scheme of the core plugs for forming a composite core from length and permeability of each individual core plug. It was suggested that core sections should be ordered such that the harmonic average permeability between sections is as close as possible to the over-all average permeability for the composite core.

Huppler [5] in 1970, also investigated the effects of heterogeneities on waterflood relative permeabilities. The permeability and porosity distribution of the heterogeneous core to be studied was specified in the numerical simulator and relative permeabilities were calculated from the output. Deviations from the input curves gave an indication of the effect of heterogeneity.

Owens and Archer [20] showed that the wettability has a strong effect on relative permeability. Oil displacement efficiency decreases, as wettability changes from water-wet to oil-wet. The improper estimation of wettability leads to errors in recovery performance and overestimation of residual oil for tertiary recovery.

Labastie, Guy, Delclaud and Ifly [7] conducted experiments with direct measurement of saturation and pressure in each phase at different points in the core and found that relative permeabilities are independent of flow rate except near the residual oil saturation. However capillary pressures depend on wettability and flow rate.

Watson, Kerig and Otter [32] devised a simple test for detecting nonuniformities in core samples. They showed that deviation from linear behavior of pressure drop across the core with time indicates the heterogeneity of the core and its location might be approximately determined.

In 1986, Hinkley and Davis [9] studied the construction methodology of composite cores. They found that the interface between core segments of a composite core had a strong effect on saturation distributions when capillary contact was not

maintained between the segments.

Wu et al. [30] presented Buckley-Leverett type analytical solution for a composite core, comprising two cores of different rock properties. Their results showed discontinuities in saturation profiles across the interface.

Results presented by Heaviside, Brown, and Gamble [10] showed that end effects in cores from reservoirs having intermediate wettability were not present at low flow rates and relative permeabilities are rate dependent. The flood front is less dispersed at low flow rates.

Mohanty and Miller [12] studied the effect of heterogeneity, capillarity and viscous fingering using Computer Tomographic (CT) Scanner for relative permeability determination. They showed that as the capillary number (ratio of viscous forces to capillary forces) increases, both the relative permeabilities to oil and water increase. The early part of the relative permeability curve is affected by heterogeneity and fingering and as the flow rate decreases, fingering becomes less severe.

Donaldson et al. [23] studied the relative permeabilities at reservoir conditions (high temperature and pressure) and found an increase in the relative permeability to oil and decrease in the residual oil saturation with increase in temperature which resulted from change of wettability to more water-wet.

Several investigators [24,25,26,27] presented results of temperature effects on waterflood. They observed an increase in relative permeability to oil and irreducible water saturation and a decrease in residual oil saturation. They showed that these

effects were more pronounced for crude oils than for the refined oils. They stated that the data implied a change of wettability to a more water-wet condition at higher temperature.

In 1983, Miller [19] conducted experiments on Berea sandstone and concluded that there is no effect of temperature on relative permeability.

Kossack, Aasen and Opdal [11] developed an averaging technique of laboratory determined relative permeabilities using pseudofunctions for reservoir simulation studies. In the multistep pseudofunctions generation process, several scales (fine grid) of heterogeneities are incorporated in one set (coarse grid) to reduce the number of grid blocks to a smaller number. They made comparison of both grids and concluded that the effect of increased numerical dispersion and the decreased detail of reservoir description in the coarse grid is overcome by pseudofunctions.

Although considerable research has been made to study various factors affecting relative permeabilities determination, no attempt was made to study the averaging process of relative permeabilities from composite core plugs. Therefore the objective of this study is to investigate the recovery performance and averaging of relative permeabilities of both individual and composite core plugs.

Chapter 3

STATEMENT OF THE PROBLEM AND PROPOSED APPROACH

Measurement of relative permeability is a complex job. The most common methods for determination of relative permeabilities are applied on small core samples in the laboratory. Composite cores, made of series of small core plugs, are used to determine relative permeabilities to minimize end effects which result in incorrect pressure drop and ultimately wrong relative permeability curves.

The goal of the study is three-fold.

1. To study the recovery performance of core samples and compare the values with the recovery of composite core formed by the individual core samples.
2. To determine and compare relative permeabilities of individual core plugs and composite core, and
3. To study the averaging process of relative permeabilities of composite cores.

3.1 Proposed Approach

- Evaluating wettability of cores using USBM method.
- Displacement experiments with individual core plugs and composite cores.
- Calculation of relative permeabilities of core samples using the JBN method.
- Comparison of experimental and simulation results using the JBN relative permeabilities in the simulator as input parameters.
- Comparison of experimental and history match results.
- Averaging of relative permeabilities and comparison of results with and without including capillary pressure end effects.

Chapter 4

EXPERIMENTAL EQUIPMENT AND PROCEDURES

In this chapter, the experimental equipment setups, materials used and experimental procedures will be presented.

4.1 Centrifuge

One of the capillary pressure measurement methods is the centrifuge method. Both drainage and imbibition capillary pressure curves can be obtained using the centrifuge. Core samples are loaded in a bucket which is fixed to the rotor head. The centrifuge is started at a certain speed. The volume of oil or brine expelled from the core samples into graduated glass tubes which are attached to it, is recorded for each speed with the help of a stroboscope and an eye-piece at the top of the centrifuge. In the oil-drive case the brine-saturated sample is placed near the axis

of rotation and brine is expelled due to centrifugal force, while in brine-drive case the oil saturated sample is placed at the outer periphery of the rotor in the bucket. The rotor heads for both oil and brine drive and the centrifuge (Beckman Model L8M/P) is shown in Figure 4.1 and Figure 4.2 respectively.

Capillary pressure and average saturation of fluid can be calculated from the rotational speed and produced volume of oil/or brine respectively. The method will be discussed in the next chapter.

4.2 Displacement Setup

The apparatus used in this study was designed to carry out dynamic displacement experiments for relative permeability measurements using two immiscible fluids (oil and brine). A schematic diagram of the flow system is shown in Figure 4.3. A detailed description of the systems used for displacement experiments is given below.

4.2.1 Main Flow System

A schematic diagram of the main flooding system is shown in Figure 4.3. It consists of: (1) Syringe pump, (2) Air bath to control the temperature, (3) Floating-piston cell for oil, (4) Floating-piston cell for brine, (5) Two-way valve (6) Core sample, (7) core holder, (8) Inlet pressure gauge, (9) Differential pressure transducer, (10) Two phase separator, (11) Back pressure regulator, (12) Beaker for effluent

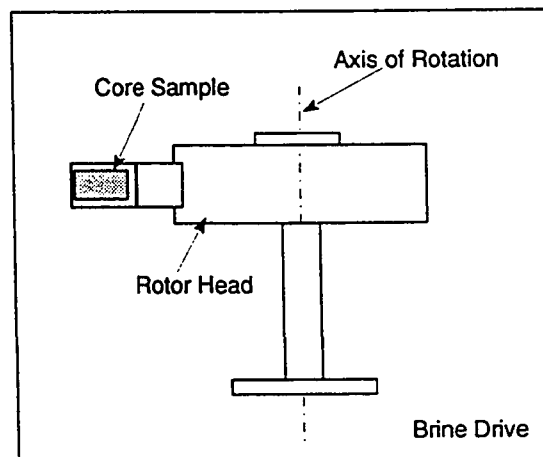
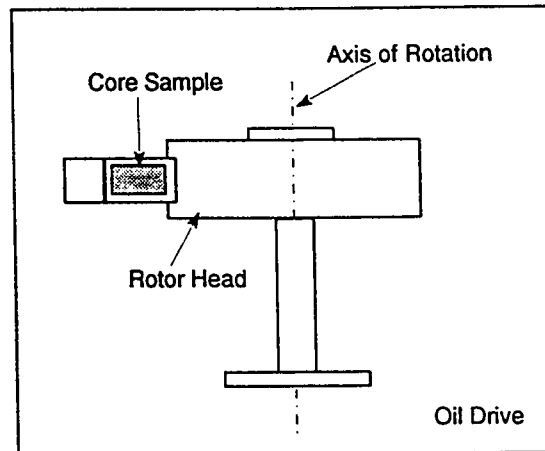


Figure 4.1: Rotor head of Centrifuge

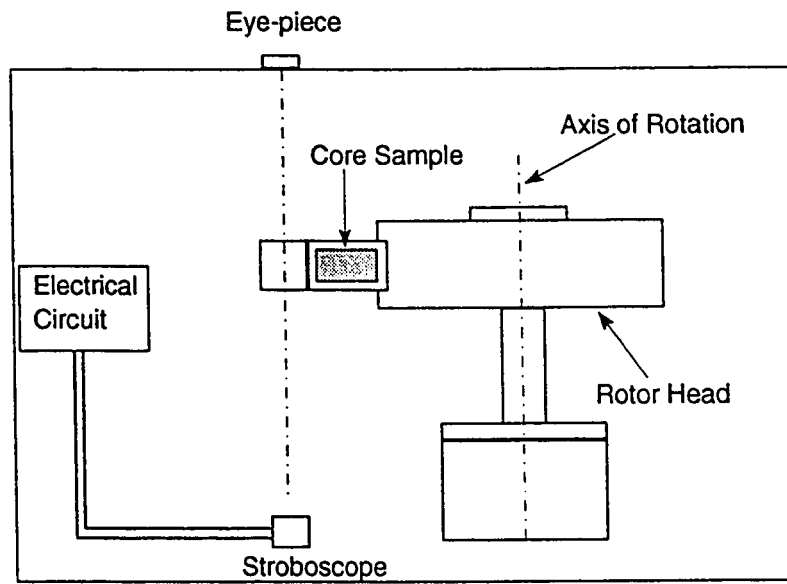


Figure 4.2: Beckman Centrifuge

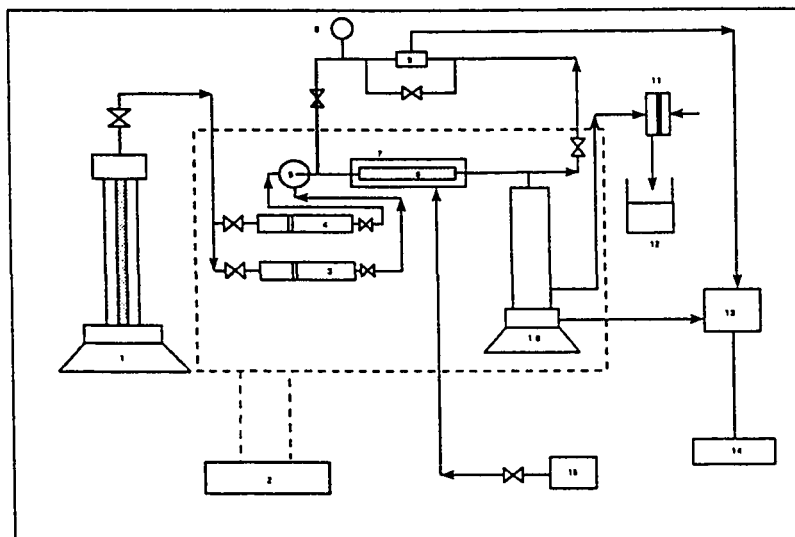


Figure 4.3: Main Flow System for Displacement Experiment

collection, (13) Interface for data acquisition system, (14) Computer, and (15) Confining pressure control(Pump). Stainless steel tubing of size 1/8 inch was used to make all connections in the system. A two-way valve was used at the inlet of the core to switch flow between oil and water injection. The two phase separator was connected to the core outlet.

4.2.2 Core Holder

The core holder is constructed of a stainless steel cylinder threaded on both ends for retaining caps. To contain the core sample, a viton rubber sleeve was used. After putting the core in the rubber sleeve, two stainless steel end plugs were fixed against the core. Each end plug has a central hole and circular and radial grooves on the face to distribute fluid across the core face. The upstream and downstream dead volumes (between the two-way valve and the core inlet face and core outlet face to separator inlet) were measured. The core holder is shown in the Figure 4.4.

4.2.3 Confining Pressure System

Confining pressure on the core is applied by pumping distilled water in the core holder outside the rubber sleeve. The pressure was raised to 1500 psi with the help of a small reciprocating pump. The confining pressure system is shown in Figure 4.5.

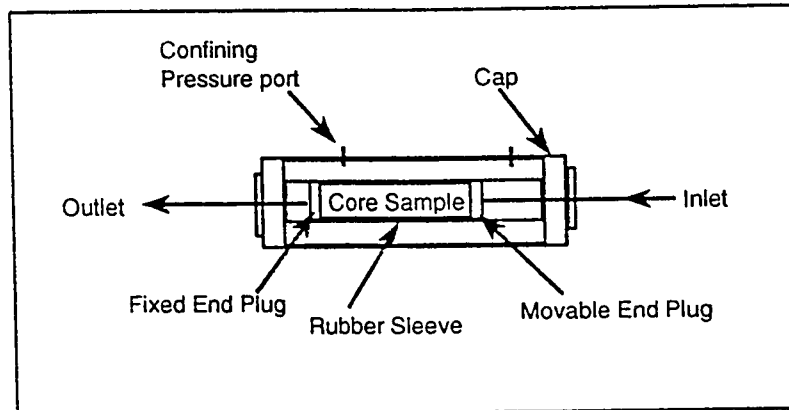


Figure 4.4: Core Holder

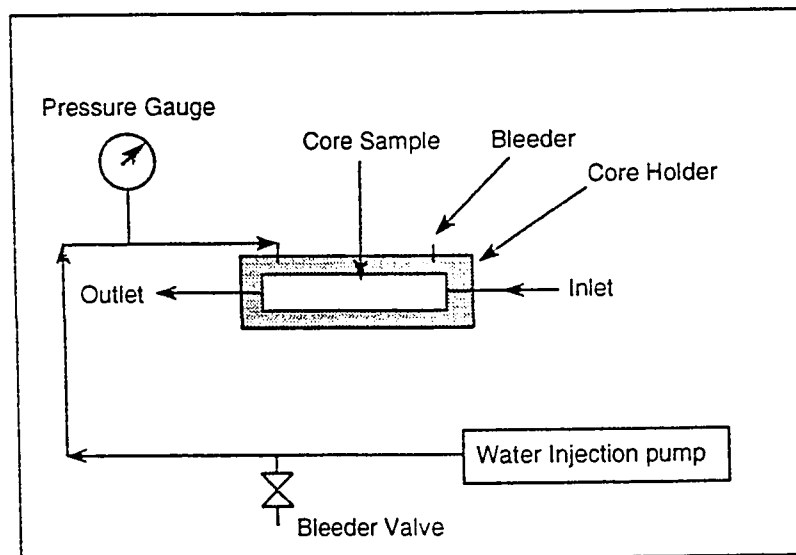


Figure 4.5: Confining Pressure System

4.2.4 Injection System

An automatic refill syringe pump, ISCO model 260D, was used at a constant flow rate mode. The pump injected distilled water into the oil and brine floating piston cells and the pistons moved in the cell to inject brine or oil to the core inlet through the two-way valve. The injection system is shown in Figure 4.6.

4.2.5 Effluent Measurement System

A vertical dual column separator was employed to collect produced brine and oil from the system as shown in Figure 4.7. The separator had an acoustic level measuring device at the bottom of it which detects the oil-water interface in the measurement column of the separator. This level is transformed into volume of oil produced. Initially the separator was completely filled with brine and then 10 cubic centimeter of oil was pumped in it to form an interface for calibration of the separator.

4.2.6 Pressure Measurement System

The differential pressure across the core was measured with a Valedyne pressure transducer (Range 0-12.5 psi and 0-125 psi). The pressure range selection was estimated from the absolute brine permeability and dimensions of the core samples. Another pressure gauge (Heise, Range 0-5000 psi) was installed at the inlet

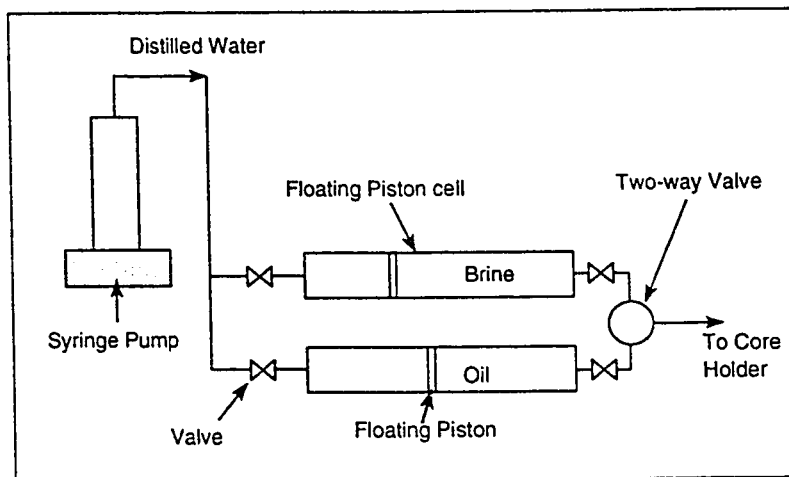


Figure 4.6: Fluids Injection System

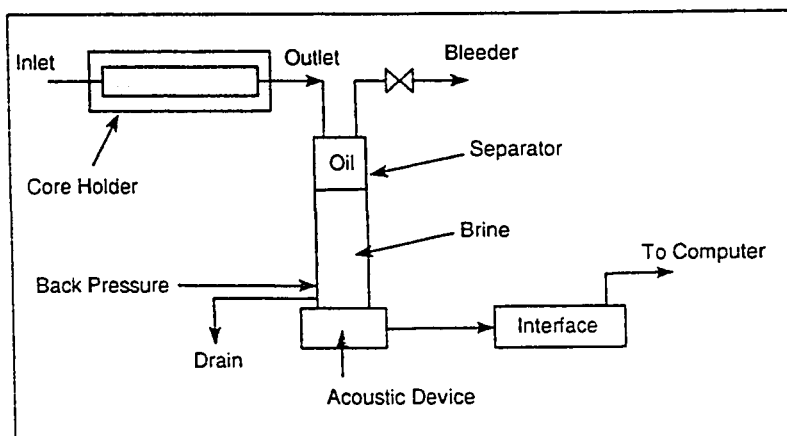


Figure 4.7: Effluent Measurement System

of the core holder to monitor the injection pressure of the system. The pressure measurement system is shown in Figure 4.8

4.2.7 Data Acquisition System

The oil volume produced from the separator and pressure differential across the core from the pressure transducer are sent to a computer through interface for recording. This system is shown in Figure 4.9.

4.3 Fluids

Dead oil was used as the displaced fluid and sodium chloride brine as the displacing fluid. The dead oil was prepared by mixing kerosene and crude oil in the ratio 2:1 to reduce the viscosity of the crude oil. A 2.20 percent (22,000 ppm) sodium chloride brine was used. The brine was prepared by mixing 2.20 grams of sodium chloride (NaCl) to a litre of distilled water. Brine and crude oil viscosity were determined using a viscometer at atmospheric pressure and 75°C. The brine viscosity was 0.54 centipoise and the oil viscosity was 1.81 centipoise. The densities were measured by weighing a specific volume of oil and brine. The density of crude oil and brine were calculated as 0.7584 gm/cc and 1.005 gm/cc respectively at room temperature and pressure (25°C, 14.7 psia).

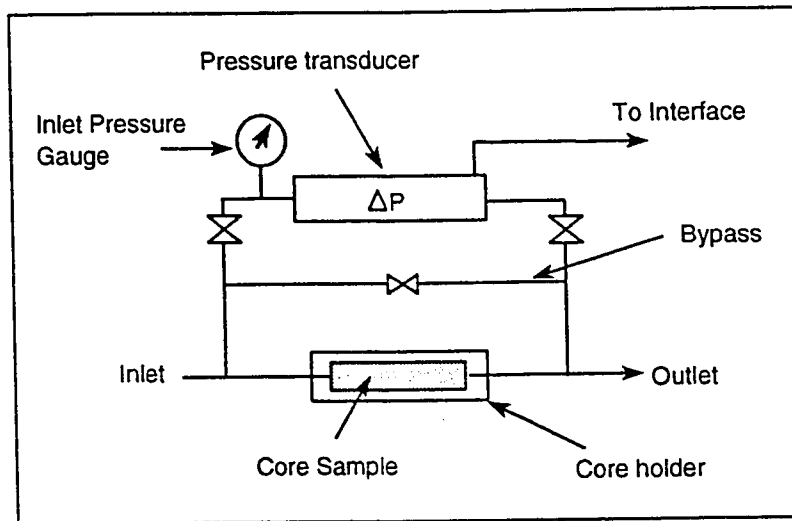


Figure 4.8: Pressure Measurement System

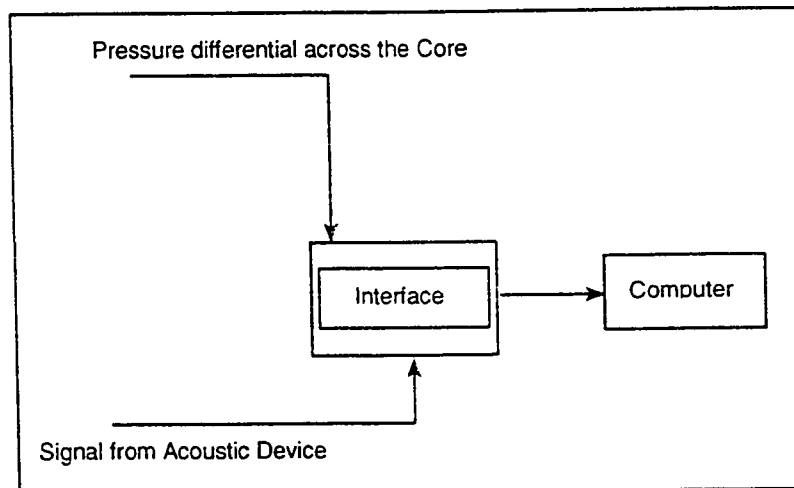


Figure 4.9: Data Acquisition System

4.4 Experimental Procedures

Procedures for core cleaning, core saturation with brine and oil, wettability measurement, and displacement experiment are summarized in the following sections.

4.4.1 Core Cleaning

Limestone core samples of 3.8 centimeters (1.5 inch) in diameter and 5 centimeters (2 inch) in length were cut from the reservoir rock. An attempt was made to remove all fluids and adsorbed material, leaving a clean rock surface by cleaning the core samples. A forced-through system as shown in Figure 4.10 was used to clean core samples by injecting solvents under pressure into the core samples.

The core samples were cleaned with series of solvents in the forced through cleaning system. The solvents used for cleaning were toluene followed by chloroform and methanol. Single solvent is relatively ineffective in core cleaning and good results are obtained with a series of solvents. The toluene is effective in removing the hydrocarbons, including asphaltenes and some polar compounds. Methanol and chloroform remove strongly adsorbed polar compounds.[14]

4.4.2 Drying of the Core Samples

The core samples were put in a Precision Electric Vacuum oven system, as shown in Figure 4.11, for drying. The temperature in the oven was maintained at 200°F

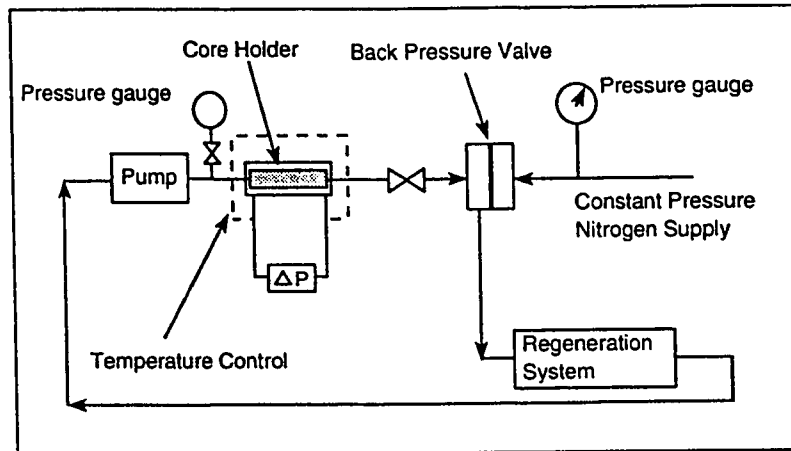


Figure 4.10: Forced through System for Core Cleaning

along with vacuum pulled over the rock samples for 48 hours to evaporate all solvents from the core and have a clean, dry rock samples.

4.4.3 Porosity Measurement

Porosity is defined as the ratio of pore volume to bulk volume of the core. Helium Porosimeter was used to measure the porosity of the core samples. A typical Helium porosimeter is shown in Figure 4.12. A known volume (reference cell) of Helium gas, at a measured preset pressure (100 psi) is expanded into an unknown void volume: the equilibrium pressure is dependent upon the magnitude of the unknown volume which may be calculated using Boyle's Law. The procedure used for calculating porosity is described below.

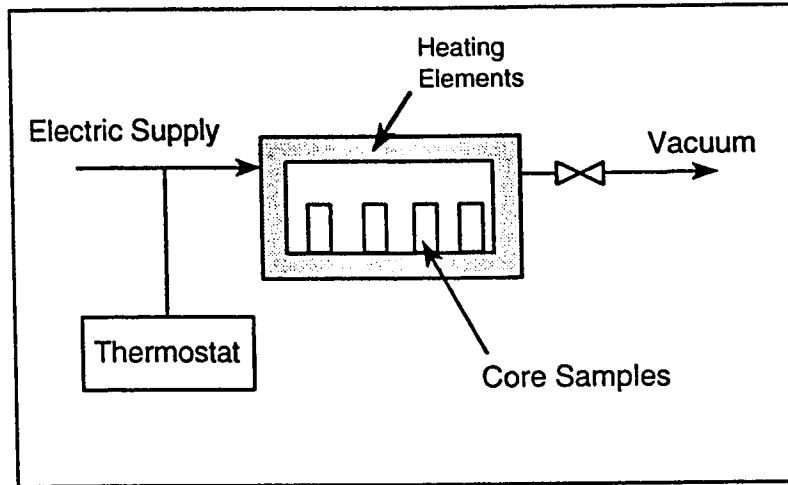


Figure 4.11: Electric Vacuum Oven for Drying of Samples

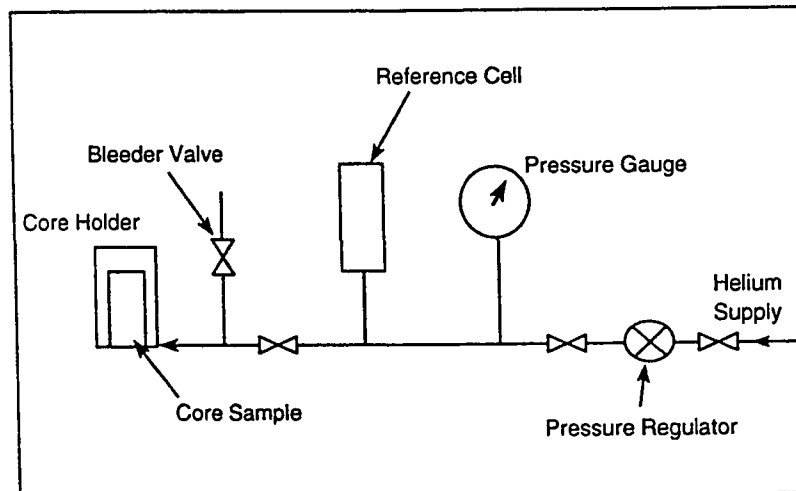


Figure 4.12: Helium Porosimeter

Helium Porosity Determination

Gauge reading with empty core holder = 96.2 cc.

Then for each sample in the core holder, the gauge readings were determined. The grain volume was measured by subtracting each reading from 96.2 cc.

Sample gauge reading = R

Grain volume = 96.2-R

Pore volume = Bulk volume - Grain volume

Porosity = Pore Volume/Bulk Volume

4.4.4 Air Permeability Determination

Absolute air permeabilities of the rock samples were determined to select the core samples according to their permeabilities for displacement experiments. The air permeameter is shown in Figure 4.13.

Air Permeability was determined by using Darcy's law for gas as follows

$$q = \frac{kA(P_1^2 - P_2^2)}{\mu L P_2} \quad (4.1)$$

where

q = Flow rate, cc/sec

k = Permeability, darcies

A = Cross sectional area, cm^2

L = length of the core, cm

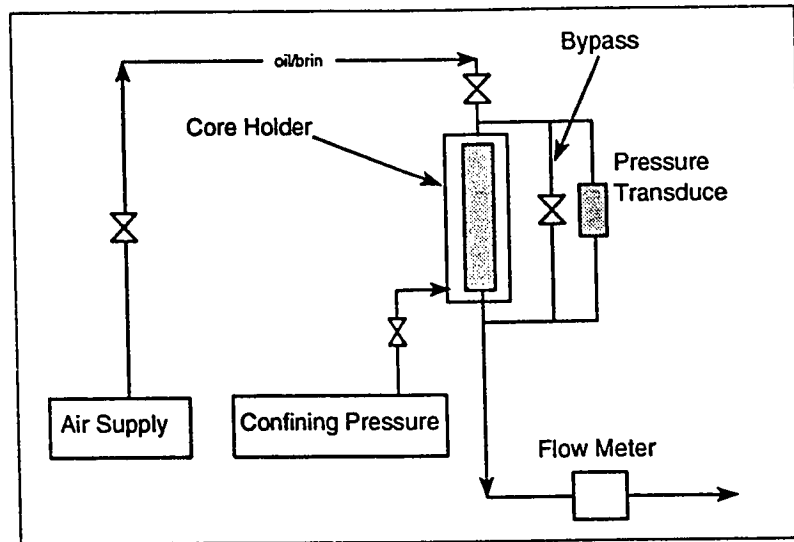


Figure 4.13: Air Permeameter

P_2 = Downstream pressure, (1.0) atm.

P_1 = Upstream pressure, atm.

μ = air viscosity = 0.0186 cp

$$\Delta P = P_1 - P_2$$

$$P_1 = \Delta P + P_2$$

ΔP is measured using a pressure transducer fixed on the apparatus. The absolute permeabilities and porosities of the core samples are given in Table 4.1.

Table 4.1: Porosities and Permeabilities of Core Samples

Core Sample	Length cm	Area cm^2	Porosity percent	k_a md
P-2	5.08	11.34	25.91	87.29
P-12	5.08	11.34	18.78	112.90
P-3	5.08	11.34	20.50	564.00
P-4	5.08	11.34	18.50	1014.00
P-16	5.08	11.34	17.09	481.00

4.4.5 Brine Saturation

The core samples were placed in a high pressure cell (saturator) and vacuum was pulled on the cores for 5 hours. The saturator is shown in Figure 4.14. Samples were then saturated by admitting deaerated synthetic 2.2 percent sodium chloride brine into the vessel. A pressure of 2000 psi of brine was applied for 24 hours to diffuse brine into the pores completely. Samples were put in the same brine for a week to establish equilibrium between brine and the core samples.

4.4.6 Aging of Core Samples

Brine saturated samples were weighed and put in the centrifuge for spinning at 9000 rpm equivalent to 100 psi capillary pressure to establish irreducible brine saturation by driving out the brine from the cores.

Reservoir rock changes its original, strongly water wet condition by adsorption of polar compounds and the deposition of organic matter originally in the crude oil. Some crude oils make a rock oil-wet by depositing a thick organic film on

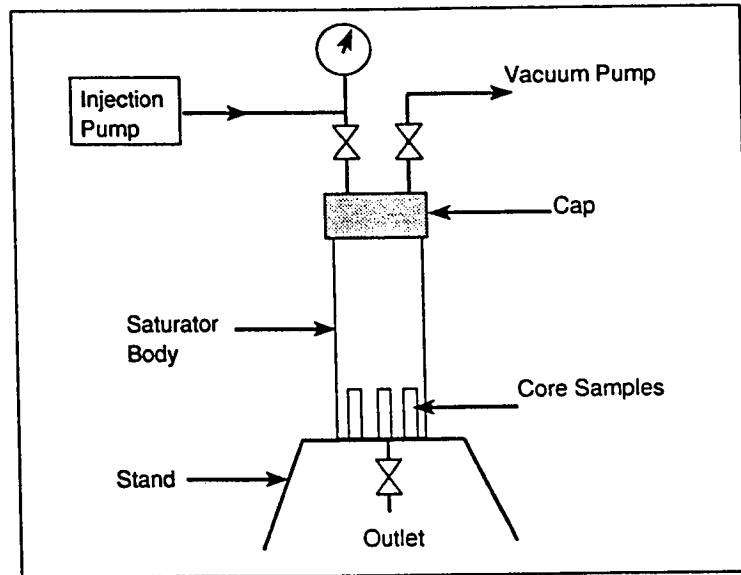


Figure 4.14: Brine Saturator

the mineral surface. During cleaning the adsorbed matter is removed by different solvents. Therefore after saturation with brine and then oil, a certain time is required to restore the wettability of the core samples.[14]

Cores were placed in aging cell filled with oil at 2000 psi and it was put in the electric oven at 75°C (167°F) for a month to age the samples for wettability restoration. Due to the limitation of the centrifuge maximum temperature (75°C), the samples were aged and the displacement experiments were carried out at this temperature.

4.4.7 Wettability Measurement

Core samples were centrifuged to determine oil and brine drives capillary pressure curves. In the oil-drive case brine saturated cores at S_{or} were centrifuged under oil. Oil saturated cores at S_{wi} were centrifuged under brine. For each speed of the centrifuge, the produced volume of brine and oil were determined. The centrifuge speed was increased stepwise to a maximum of 9000 RPM. The capillary pressure and the average water saturation can be computed from the speed of the centrifuge and the produced volumes respectively. The USBM wettability index is calculated by taking the logarithm of the ratio of the areas under the oil and brine drive curves. The theory and calculation procedure of USBM method are presented in Appendix-B.

4.4.8 Displacement Experiments

After loading the core sample in the core holder, a confining pressure of 1500 psi was applied on the core and a back pressure of 150 psi was applied at the core outlet. The temperature of the oven was set at 75°C in which the whole setup was placed. The effective permeability of the sample to oil at S_{wi} was determined by measuring pressure differential across the core sample at constant oil flow rates of 0.5, 1.0, 1.5, and 2.0 cc/min. The effective permeability to oil, k_o was determined by using the slope of the graph of flow rate vs. pressure drop. The effective permeability was

calculated using Darcy's law.

$$k = \frac{\Delta q}{\Delta P} \frac{\mu L}{A} \quad (4.2)$$

After the k_o measurement, the brine displacement run was initiated by switching the two way valve to brine cell and oil volume and differential pressure were recorded. After injecting sufficient amount of brine (about 12 pore volumes) at 2 cc/min , when the pressure differential across the core and oil volume reading in the separator stabilized, the displacement test was terminated.

Effective permeability to brine at S_{or} was calculated by measuring pressure drops at various constant flow rates in the same way as k_o was determined.

4.4.9 Determination of S_{wi} and S_{or}

Core samples saturated with brine at S_{or} (after the displacement experiment) were put in the Dean Stark solvent extractor, where Xylene was used as extraction solvent. The volume of extracted water was collected and measured over a 24 hours period. The value of irreducible water saturation and residual oil saturations were calculated as follows:

$$S_{wi} = \frac{V_w}{V_p} - \frac{V_o}{V_p} \quad (4.3)$$

$$S_{or} = 1 - \frac{V_w}{V_p} \quad (4.4)$$

where

V_w = Extracted water volume, cc

V_o = Oil volume produced during displacement experiment, cc

V_p = Pore volume, cc

Chapter 5

RESULTS AND DISCUSSION

Waterflood experiments were conducted on single core plugs and two composite cores of carbonate rock samples. The first composite consisted of two core samples; core sample P-2 and P-12 while the other composite consisted of core plugs; P-3, P-4 and P-16.

5.1 Wettability of Core Samples

The displacement processes described by relative permeability result from the interaction between the rock and the fluids moving through it. Interfacial tension and wettability can have significant impact on these processes. In selecting the appropriate fluids for the displacement test, one of the most important considerations is wettability, which has the biggest influence on oil recovery by water flooding.[31]

Wettability of the samples was determined using the USBM Method. This is a

rapid method for determining the wettability but it gives the average wettability of the samples. The method, however, cannot determine whether the wettability of the samples is fractional or mixed wet. The volume of oil expelled during the brine drive and brine volume during the oil drive were measured at various rotational speeds. The recorded values of speed, produced volumes, capillary pressure and average water saturation are shown in Tables A.1 through A.5 in Appendix-A.

A computer program that implements the method described by Rajan [18] was used to calculate the end face saturations from the average saturation and capillary pressure measurements. The procedure for calculating wettability index is discussed in Appendix-B. The capillary pressure curves both for the oil and brine drives of the core plugs are shown in Figures 5.1 to 5.5.

It can be seen from these figures that the oil drive curve becomes vertical at S_{wi} while the brine drive curve becomes vertical at S_{or} indicating that no considerable amount of fluid is produced at 9000 RPM rotational speed which is equivalent to 110 psi capillary pressure.

The USBM wettability indices of the five core samples are shown in Table 5.1. The wettability indices indicate that the samples were neutral. When the rock has no strong preference for either oil or water, the system is said to be neutral or of intermediate wettability.

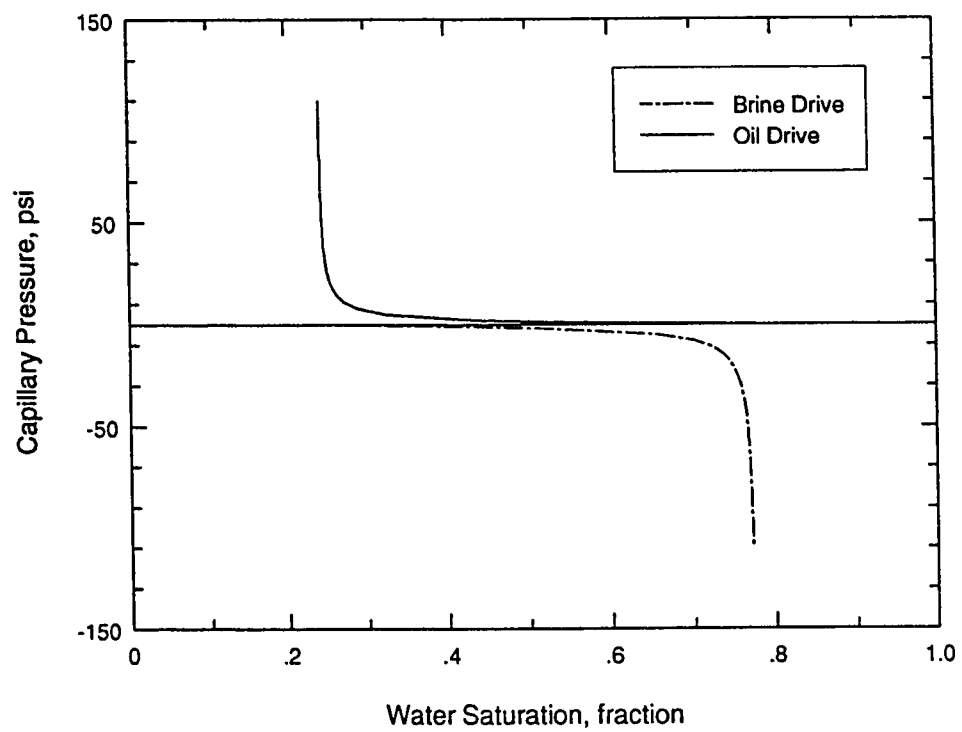


Figure 5.1: Capillary Pressure Curves for Core Plug P-2

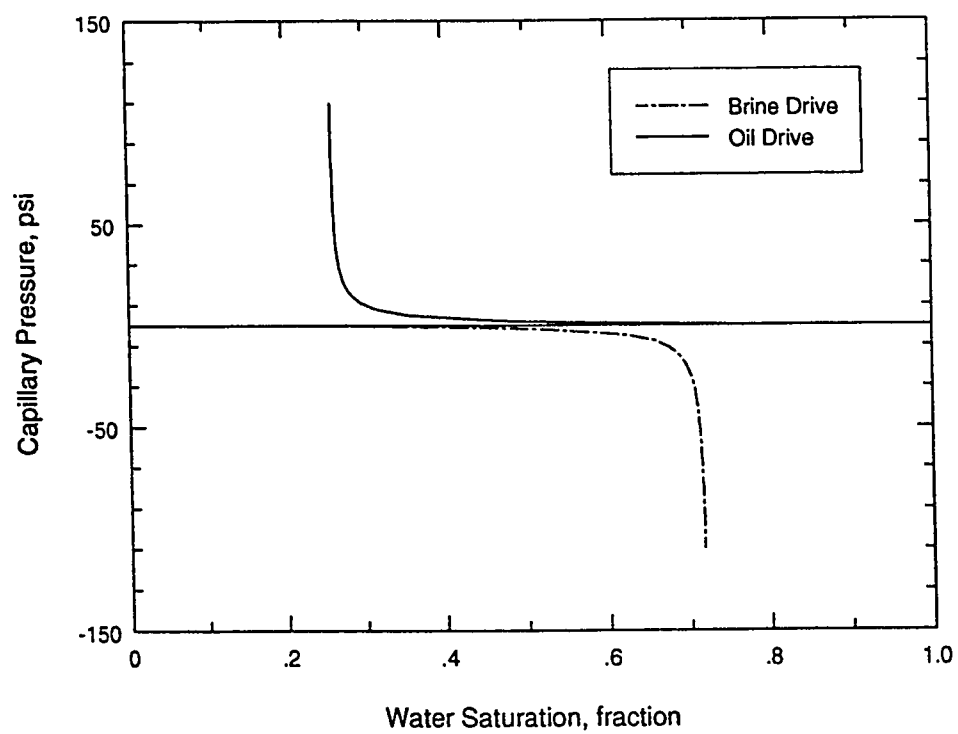


Figure 5.2: Capillary Pressure Curves for Core Plug P-12

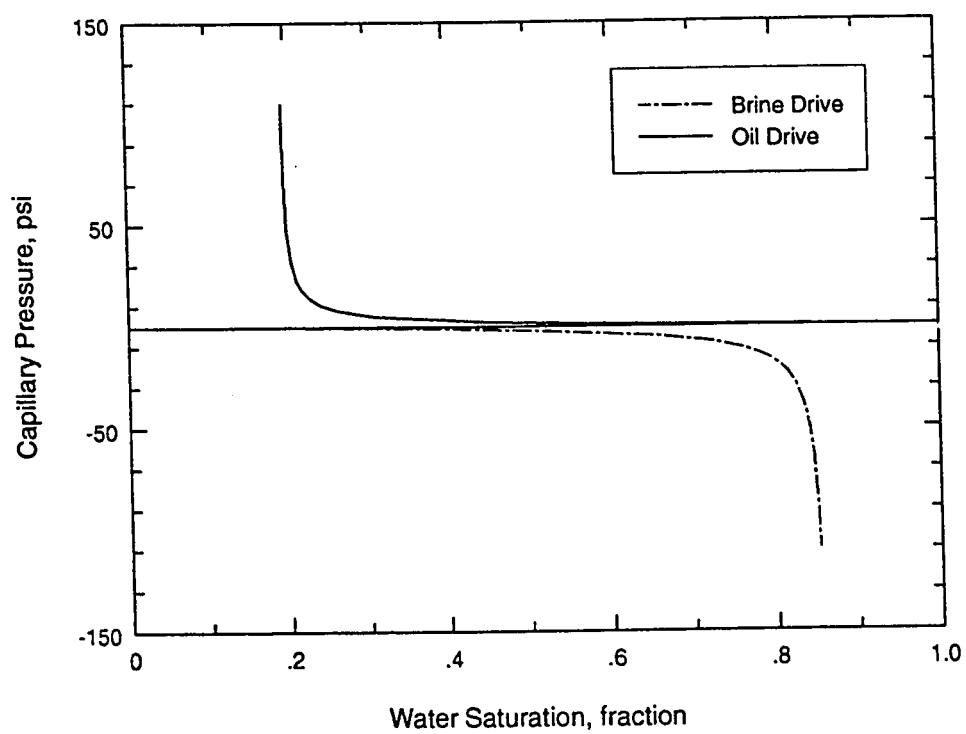


Figure 5.3: Capillary Pressure Curves for Core Plug P-3

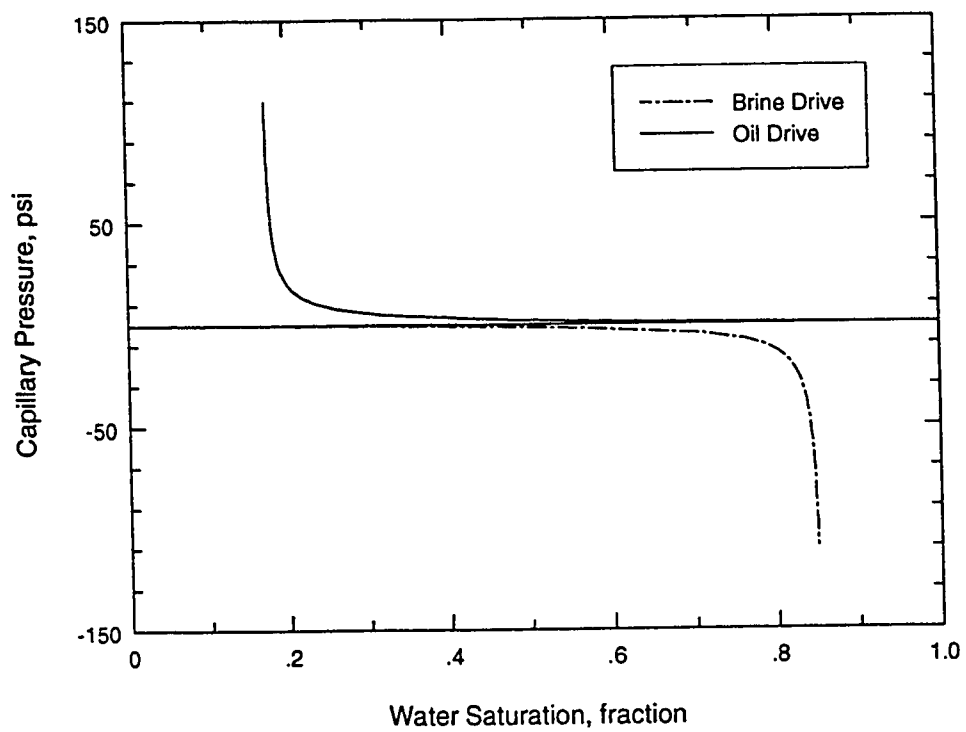


Figure 5.4: Capillary Pressure Curves for Core Plug P-4

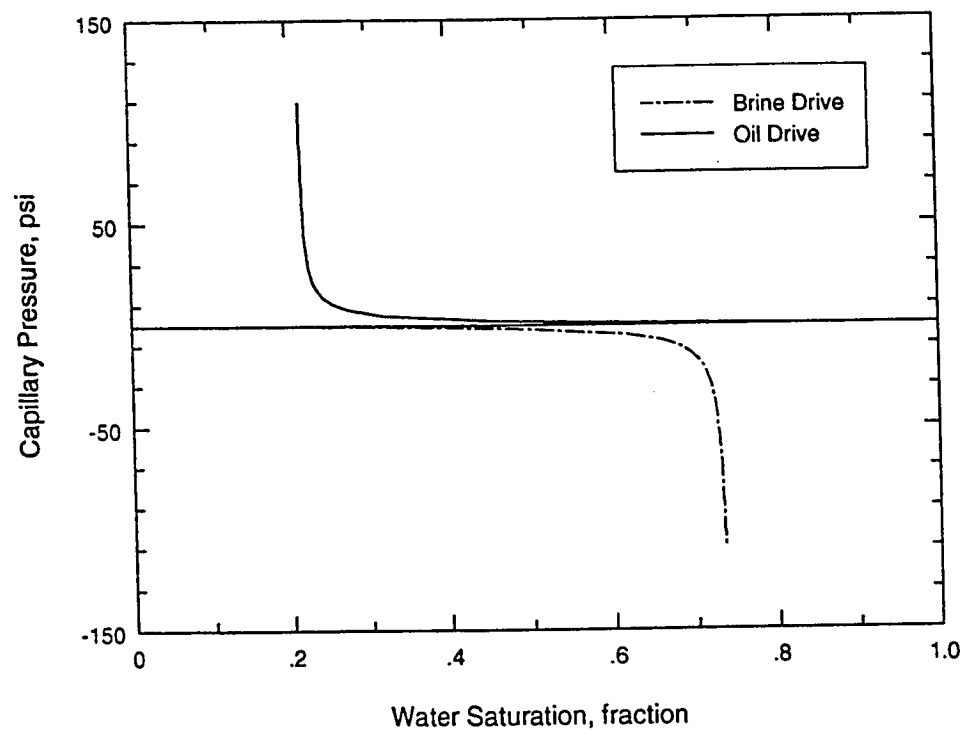


Figure 5.5: Capillary Pressure Curves for Core Plug P-16

Table 5.1: Wettability Indices of Core Samples

Composite	Core Sample	A_1	A_2	WI
Comp-1	P-2	4.029	4.637	-0.06
	P-12	4.330	3.745	0.06
Comp-2	P-3	5.159	7.001	-0.13
	P-4	6.139	5.541	0.04
	P-16	4.889	4.529	0.02

5.2 Recovery Performance

Breakthrough and total recovery at the end of the displacement experiments for the core samples and composite cores are shown in Table 5.2.

For strongly water wet systems, oil behind the displacement front losses connectivity so that the oil recovery reaches maximum after injection of about one pore volume of water. There is little production of oil no matter how many pore volumes of water are passed through the core sample after breakthrough. For intermediate wet, mixed wet or oil wet, oil connectivity is never lost completely and oil continues to be produced.[8]

Carbonate rocks are heterogeneous in nature and displacement phenomenon in these rock samples is always subjected to frontal instability and the associated formation of viscous fingers. The carbonate rocks are unlikely to undergo one dimensional displacement. It is shown in Figures 5.6 and 5.7 that oil recovery continues to increase by increasing the volume of injected water. According to Buckley Leverette theory[22], higher recovery should be obtained in longer core samples when the core

Table 5.2: Recovery Performance of Core Samples

Core Plug	S_{wi} frac.	S_{oi} frac.	S_{or} frac.	B.Through Recovery percent OOIP	Total Recovery percent OOIP
P-2	0.248	0.752	0.189	57.0	74.86
P-12	0.258	0.742	0.332	28.0	55.25
Comp-1	0.252	0.748	0.362	17.0	51.60
P-3	0.185	0.815	0.402	25.0	50.67
P-4	0.165	0.835	0.357	33.0	57.25
P-16	0.210	0.790	0.157	40.0	80.12
Comp-2	0.186	0.814	0.393	41.0	51.72

is homogeneous. In composite-1 and composite-2, due to the heterogeneous nature of the carbonate rocks, the breakthrough generally occurs much earlier resulting in lower breakthrough recovery as shown in Figures 5.6 and 5.7 due to viscous fingering and bypassing of the displacing fluid. In these figures, comparison of oil recovery with the individual plugs is shown. The maximum breakthrough recovery for individual plug P-2 is about 57 percent of original oil in place (OOIP). The minimum breakthrough recovery was for the composite-1, where 17 percent of OOIP was recovered at breakthrough and 52 percent were recovered after 12 pore volumes of water injection. In composite-2, most of the oil (41 percent of OOIP) was produced at breakthrough and the total recovered oil was also equal to the amount recovered from Composite-1, i.e., 52 percent of OOIP.

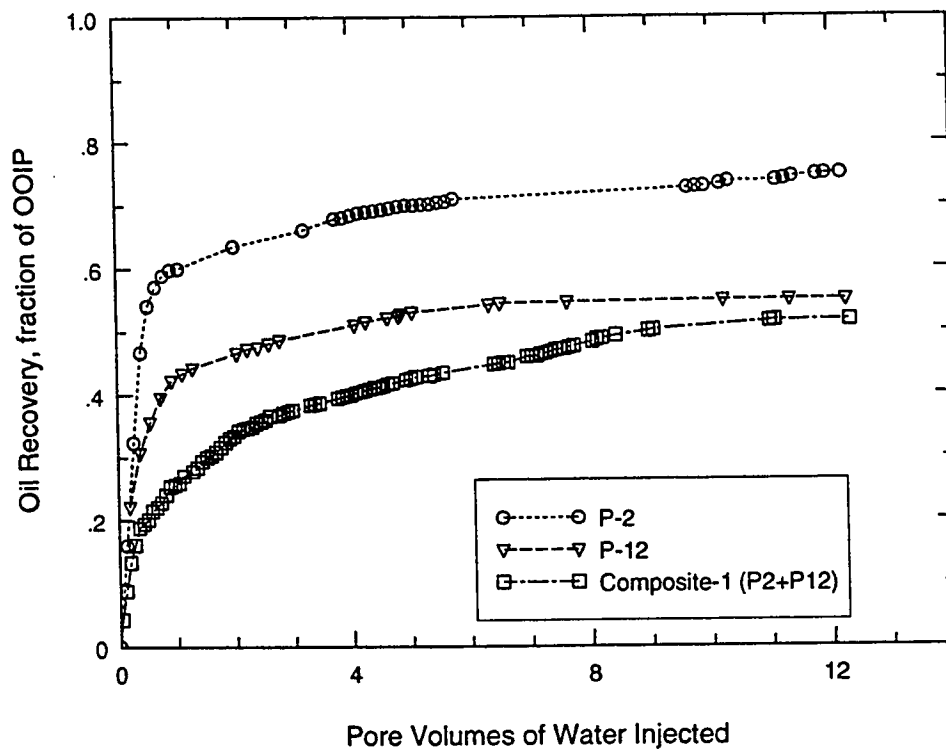


Figure 5.6: Recovery Performance Comparison of Composite-1

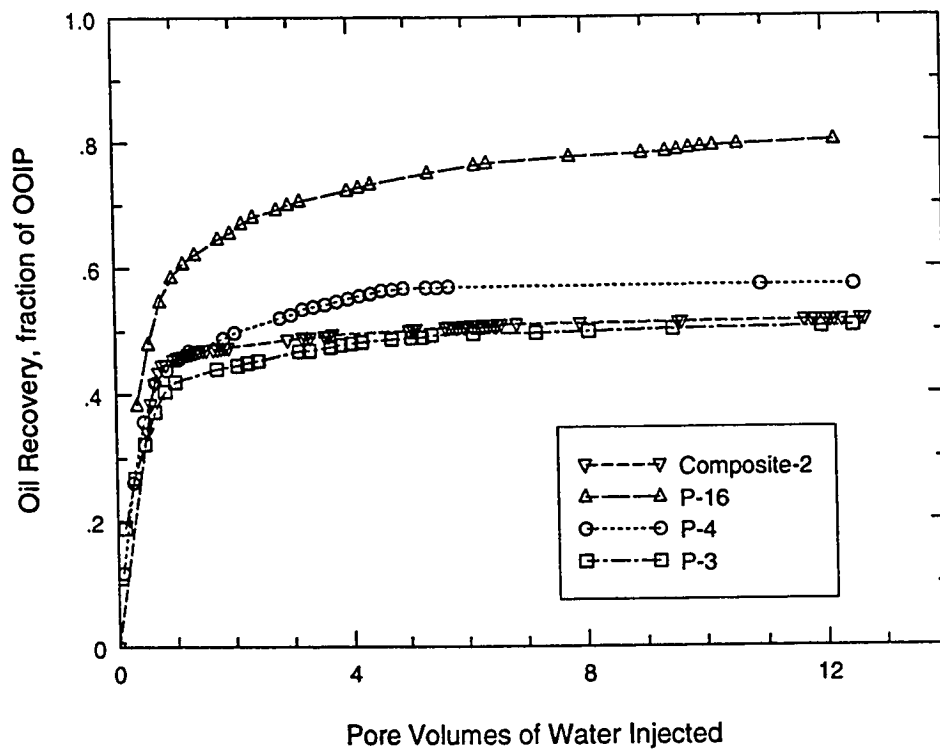


Figure 5.7: Recovery Performance Comparison of Composite-2

5.3 JBN Relative Permeabilities

Relative permeabilities of the individual plugs and composite cores were calculated using JBN method which does not take into account the capillary pressure and capillary end effects. The relative permeabilities of the individual samples and their composites are shown in Figures 5.8 to 5.14. The comparison of individual and composite relative permeabilities are shown in Figures 5.15 and 5.16. From these figures, it is clear that relative permeabilities for the composite are either higher or lower than the individual core plugs. It is also obvious from the comparison that an average relative permeability for the composite cannot be estimated from the individual plugs relative permeabilities.

According to Craig's [8] rule of thumb, if the crossover point saturation, where both the relative permeabilities are equal, is about 50 percent, then the rock sample will be neutral. It is evident that P-2 and P-12 are neutral wet, and their composite is slightly oil wet. The relative permeability to oil for the composite-1 (composed of P-2 and P-12) is lower than the individual plugs, P-2 and P-12 and the relative permeability to water is higher than the individual plugs. For core plugs P-3, P-4, P-16 and composite-2 the crossover points are around 40-50 percent water saturation making them also neutral wet. The k_{rw} for core plug P-12 and composite-1 show a linear increase after breakthrough and k_{ro} decreased slowly indicating a continuous production of oil until the end of displacement.

For composite-2, the k_{rw} increases sharply after breakthrough indicating that most of the oil was recovered at breakthrough.

5.4 Comparison of Experimental and Calculated Results

It was observed from the experimental results of recovery and differential pressure that the pressure peaks in the pressure differential curves did not occur at the breakthrough of the oil recovery for most of the samples. To investigate this, a simulation study was made in which JBN relative permeabilities were supplied to a one dimensional, two phase numerical simulation program as input and recovery and differential pressure were computed. The comparison of the experimental and calculated oil recovery and pressure differential is shown in Figures 5.17 to 5.30.

The shift in the pressure peak of the pressure differential curves is due to the following reasons. First, due to the heterogeneous nature of the carbonate rocks the displacement front is not uniform over the cross sectional area of the core sample and true breakthrough occurs somewhat later than the simulated, and second, the displacement in the actual conditions is not one dimensional while the simulated results assume one dimensional flow in homogeneous porous medium. Very little difference is found in oil recovery curves, as shown in the figures, between experimental and calculated results.

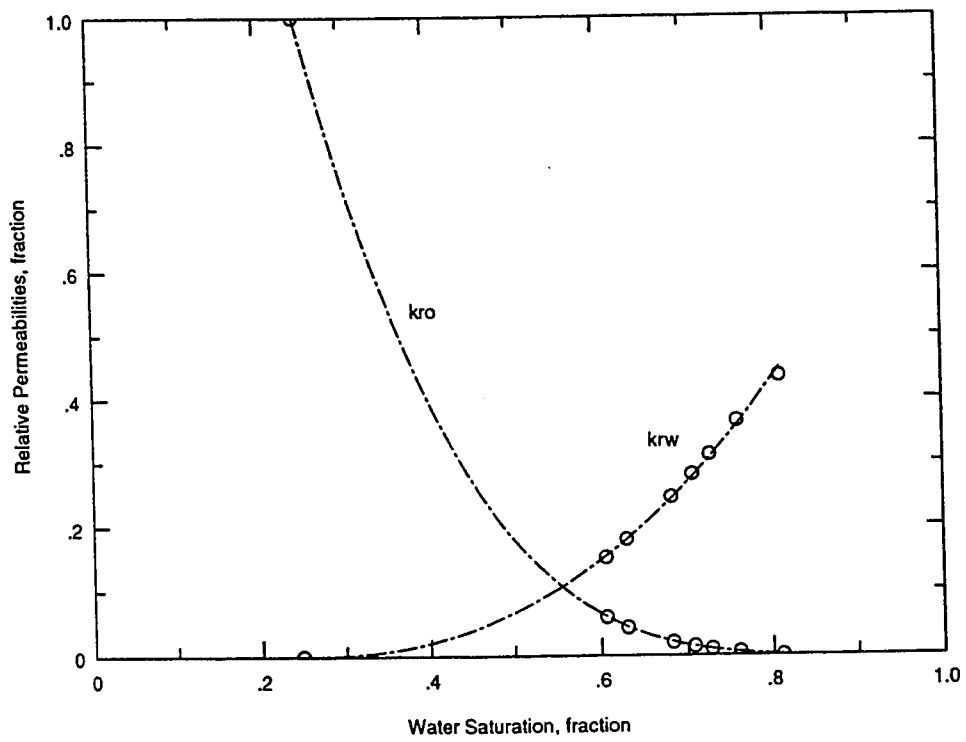


Figure 5.8: JBN Relative Permeabilities of Core Plug P-2

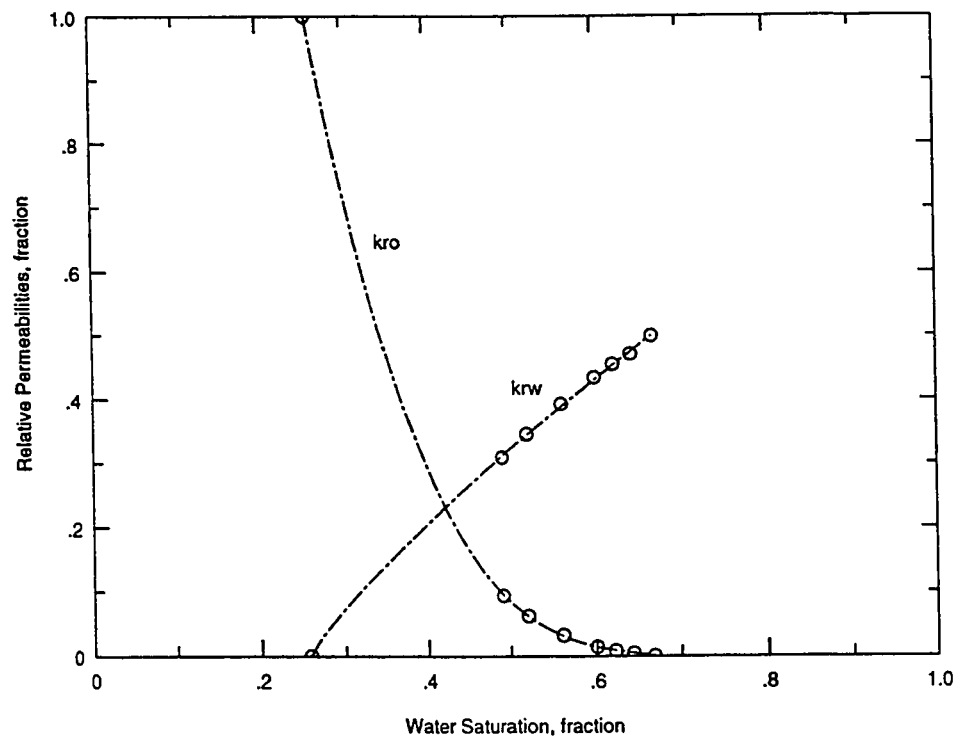


Figure 5.9: JBN Relative Permeabilities of Core Plug P-12

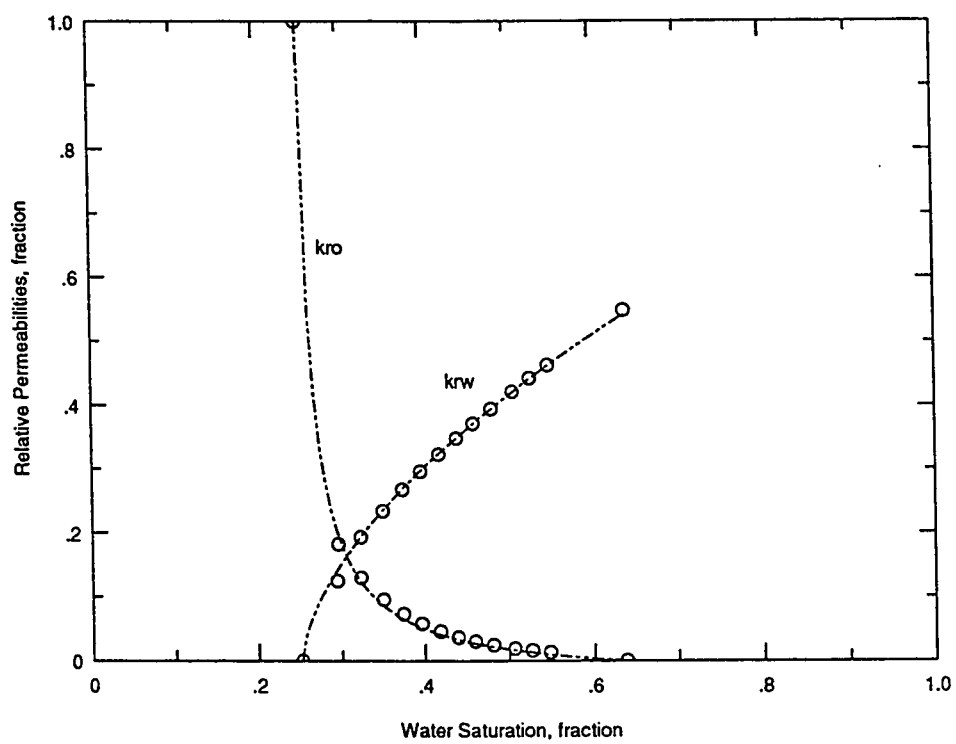


Figure 5.10: JBN Relative Permeabilities of Composite Core-1

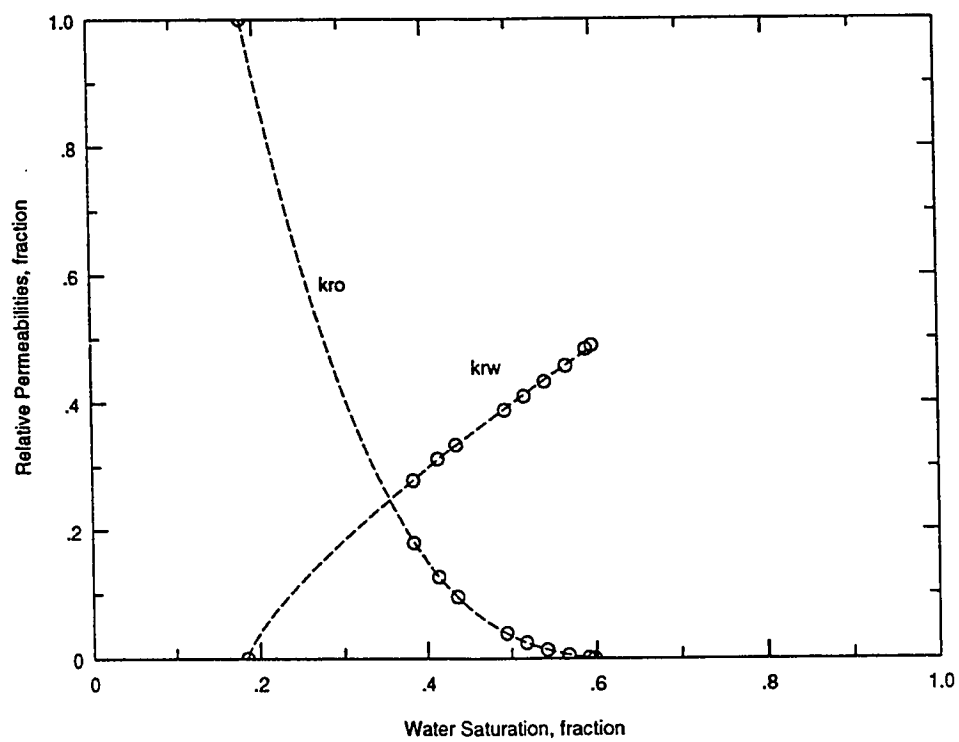


Figure 5.11: JBN Relative Permeabilities of Core Plug P-3

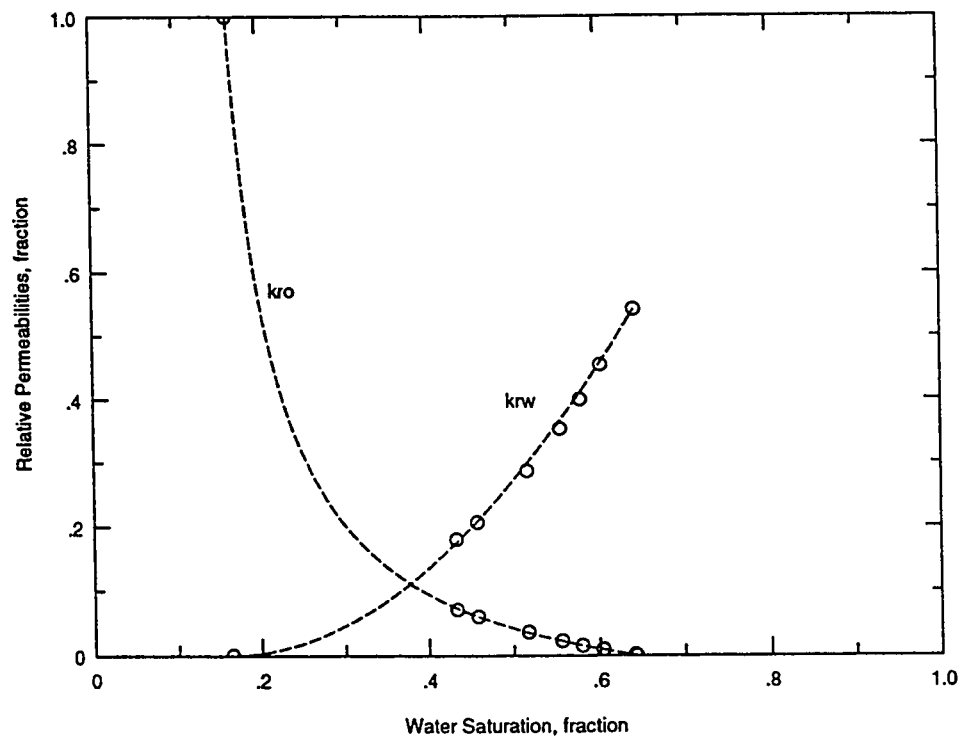


Figure 5.12: JBN Relative Permeabilities of Core Plug P-4

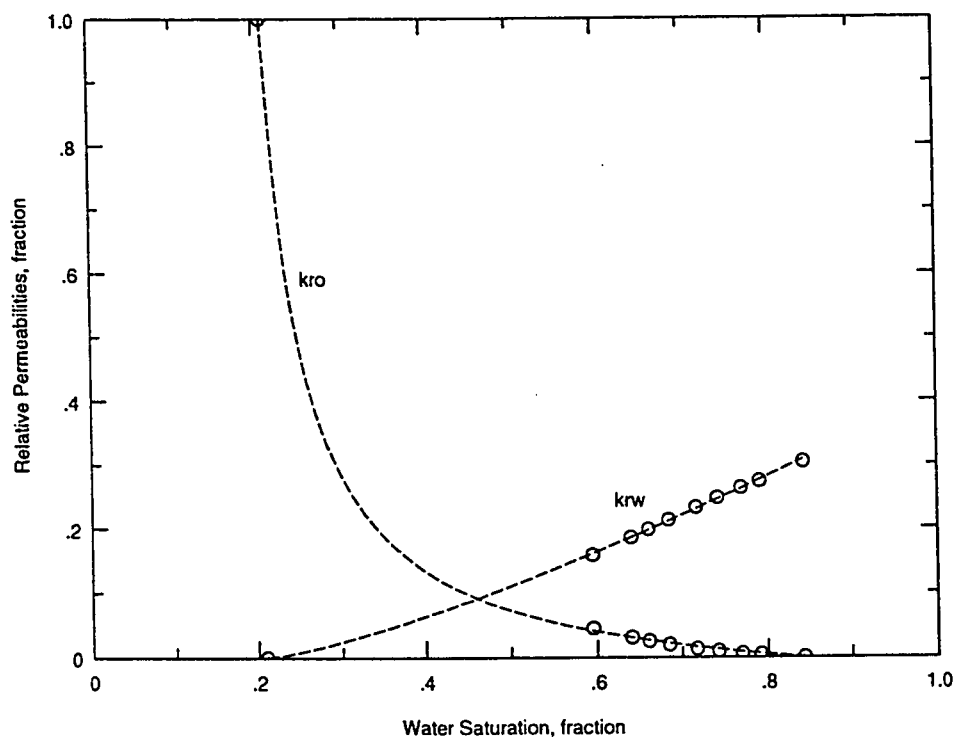


Figure 5.13: JBN Relative Permeabilities of Core Plug P-16

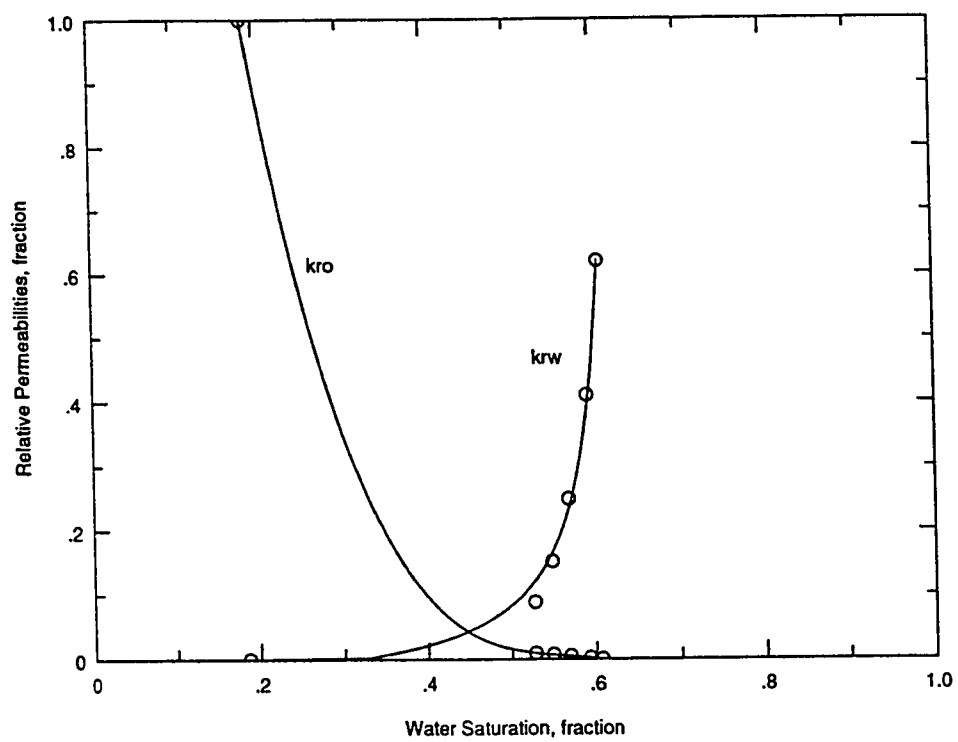


Figure 5.14: JBN Relative Permeabilities of Composite Core-2

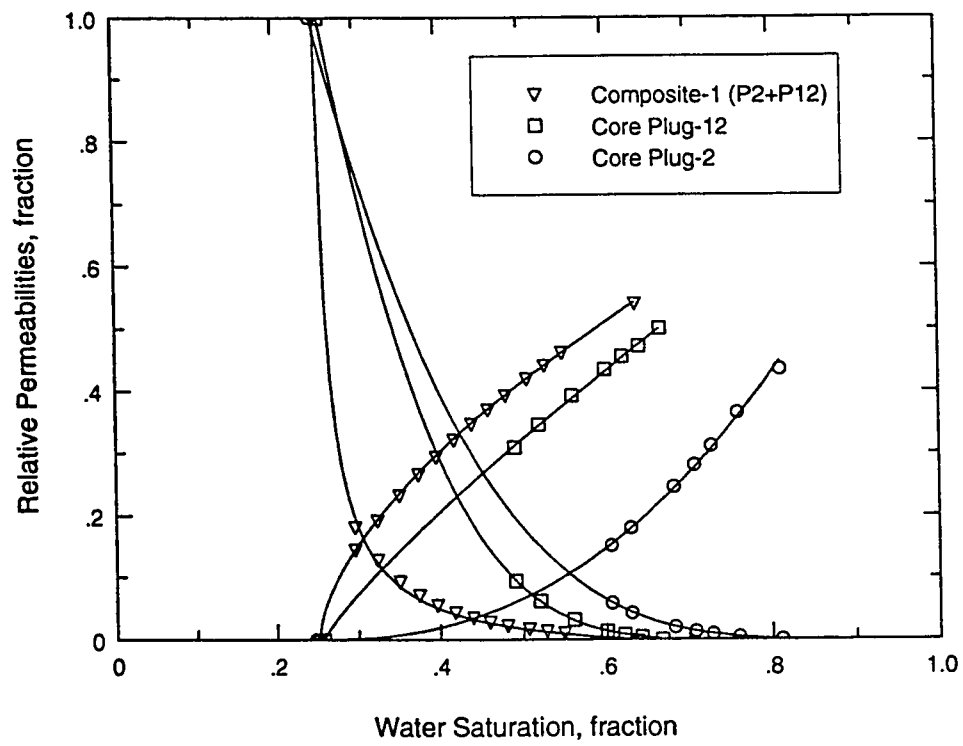


Figure 5.15: JBN Relative Permeabilities Comparison of Composite-1

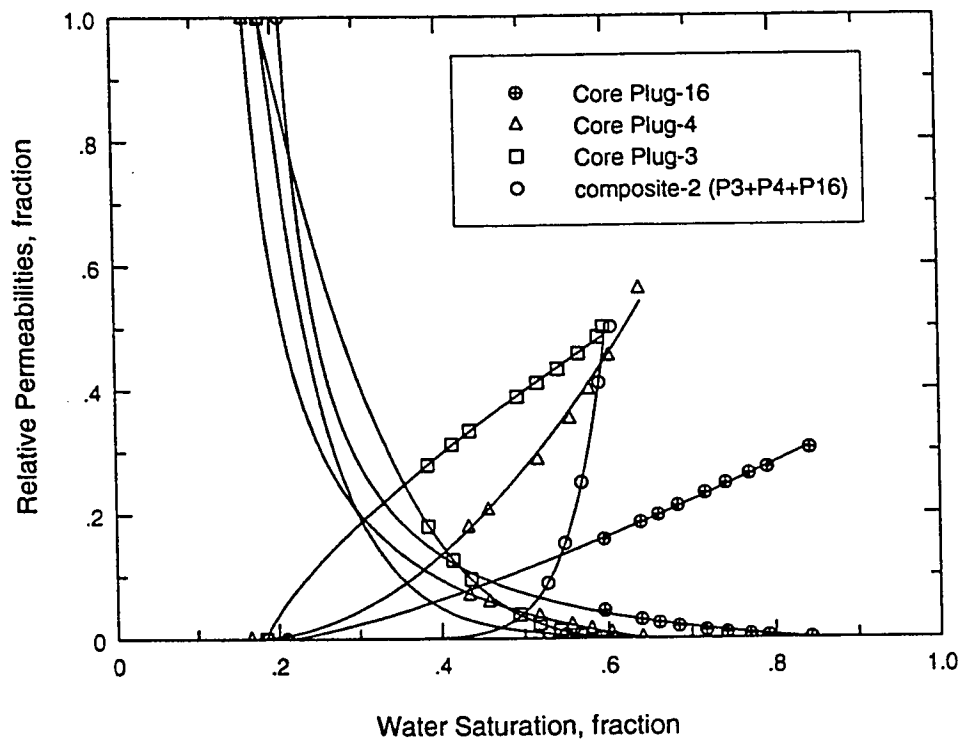


Figure 5.16: JBN Relative Permeabilities Comparison of Composite-2

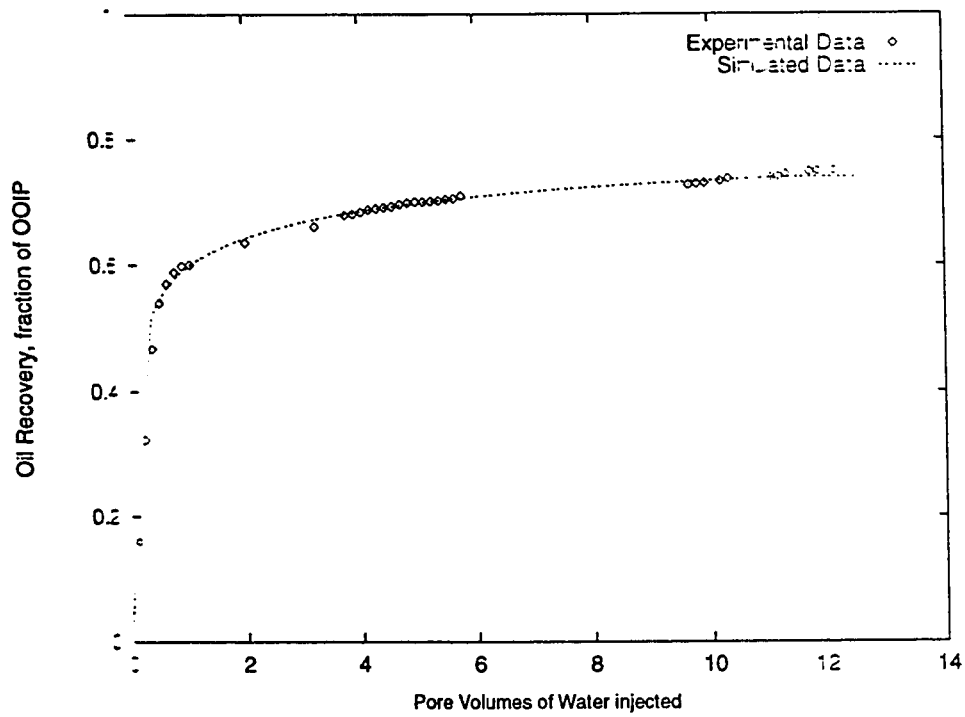


Figure 5.17: Recovery Performance for Core P-2

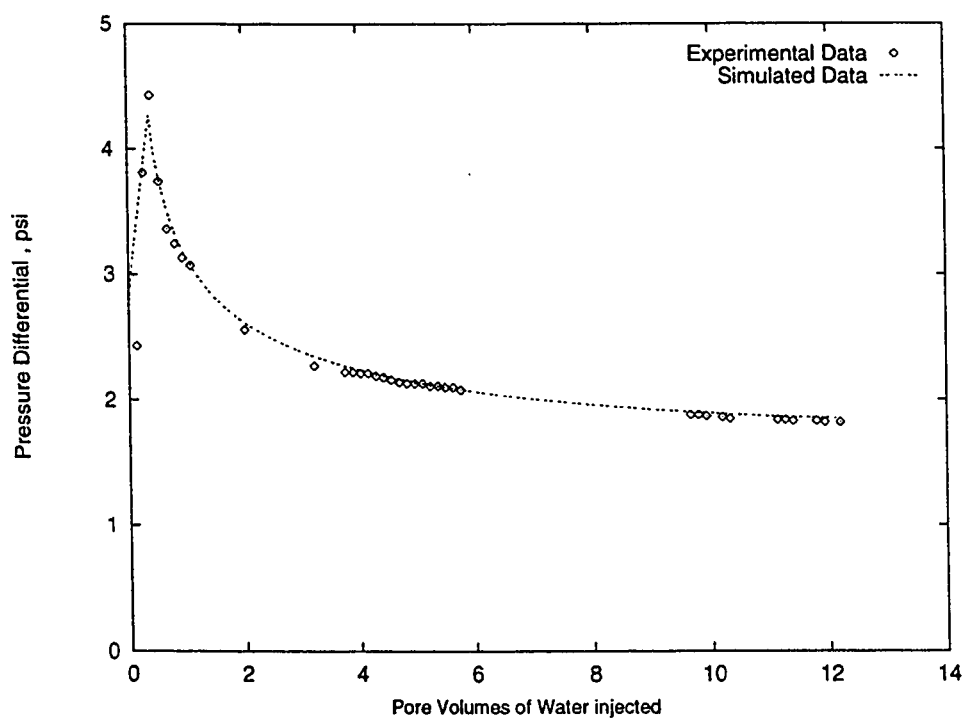


Figure 5.18: Pressure differential Curves for Core Plug P-2

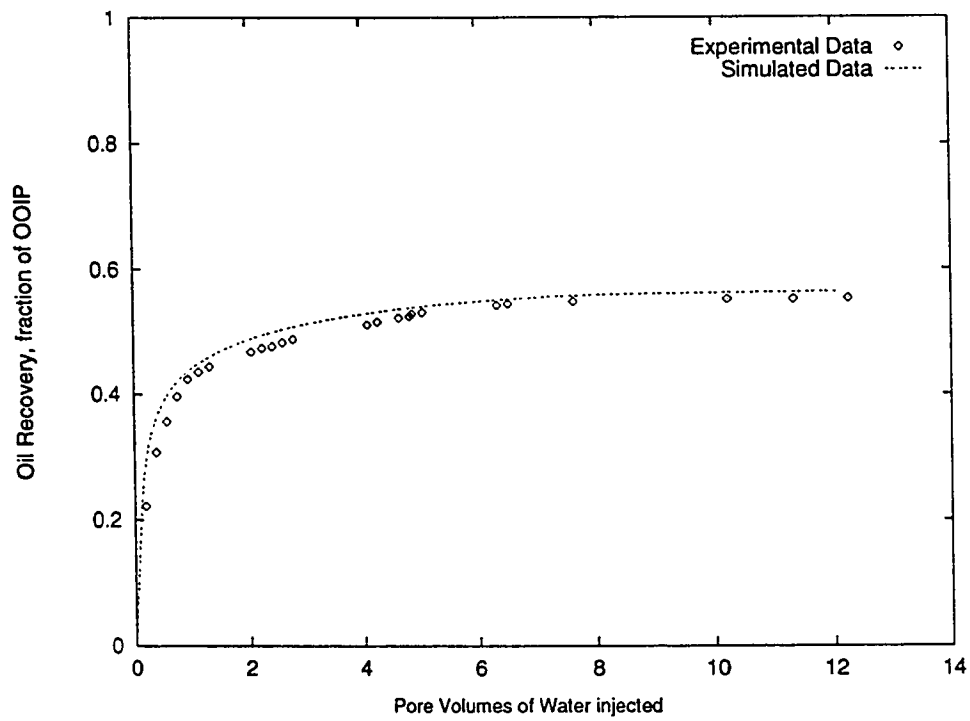


Figure 5.19: Recovery Performance for Core Plug P-12

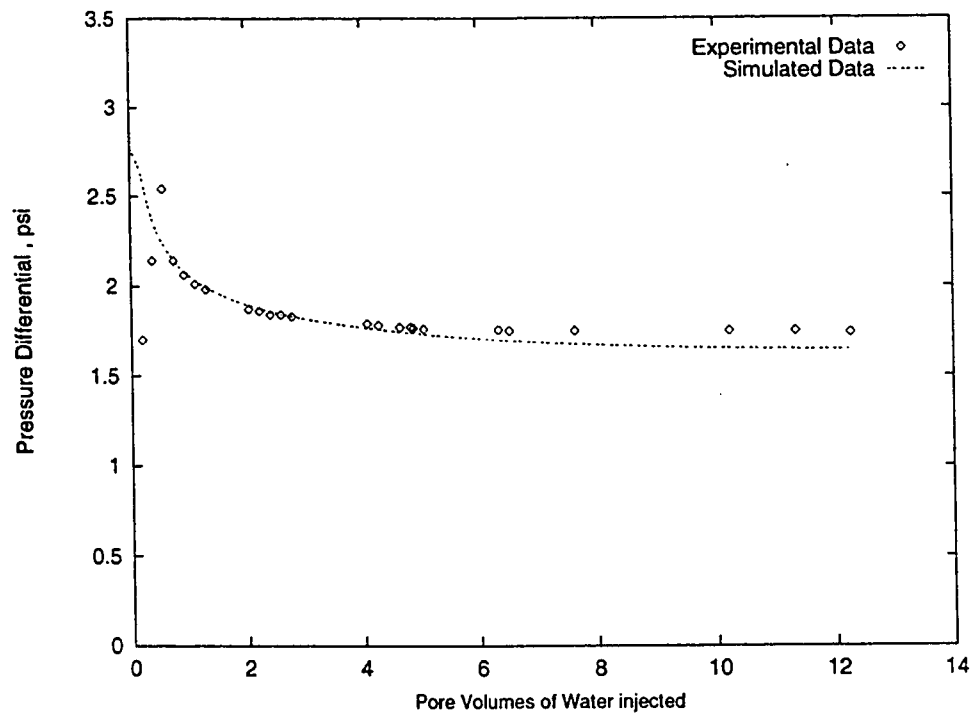


Figure 5.20: Pressure differential Curves for Core Plug P-12

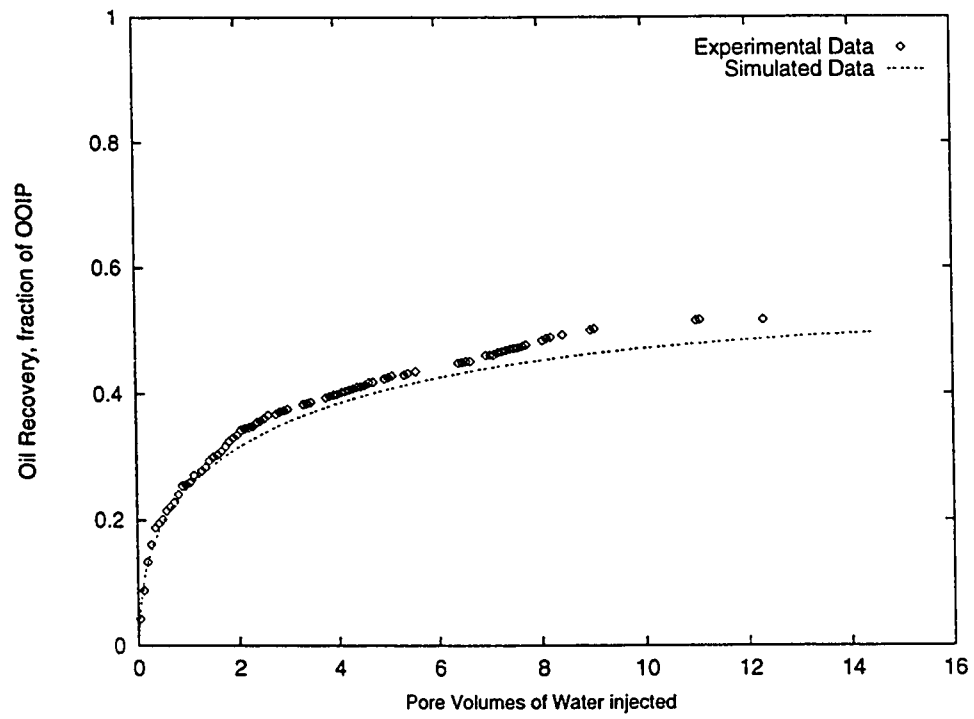


Figure 5.21: Recovery Performance for Composite-1

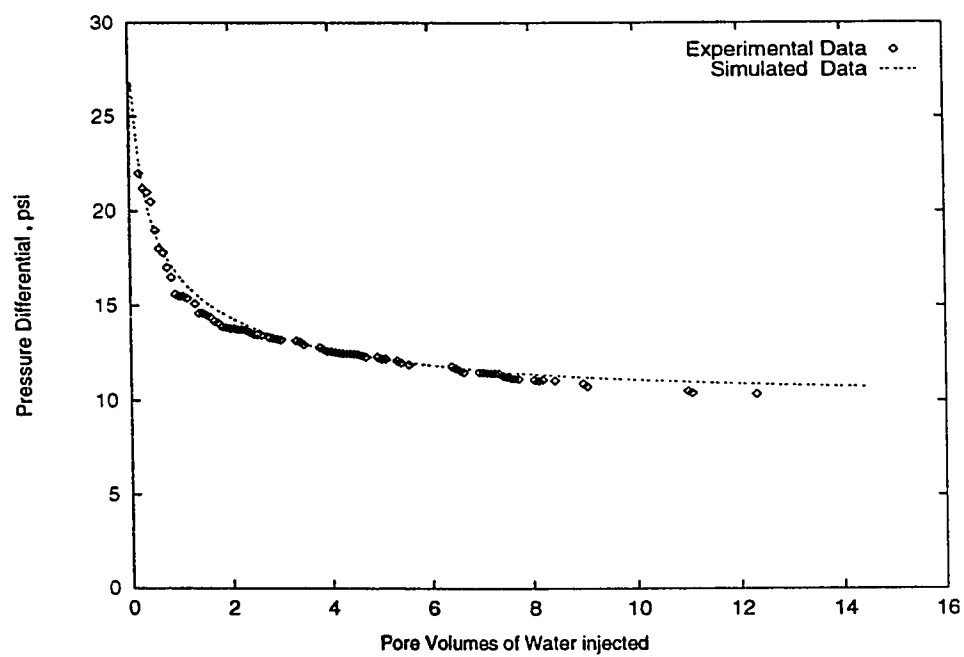


Figure 5.22: Pressure differential Curves for Composite-1

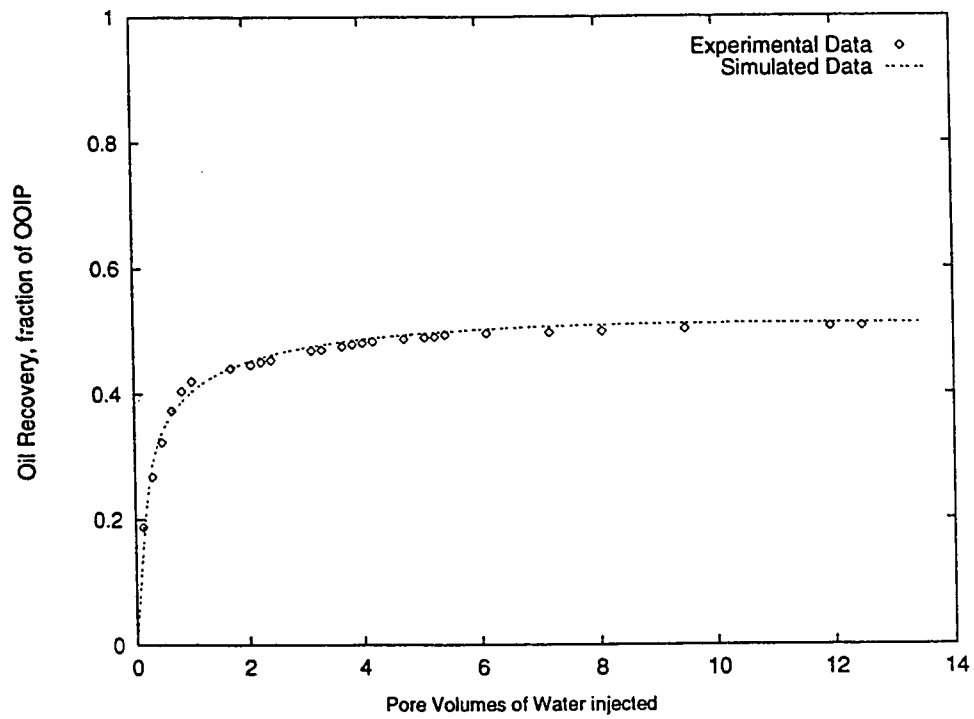


Figure 5.23: Recovery Performance Curves for Core Plug P-3

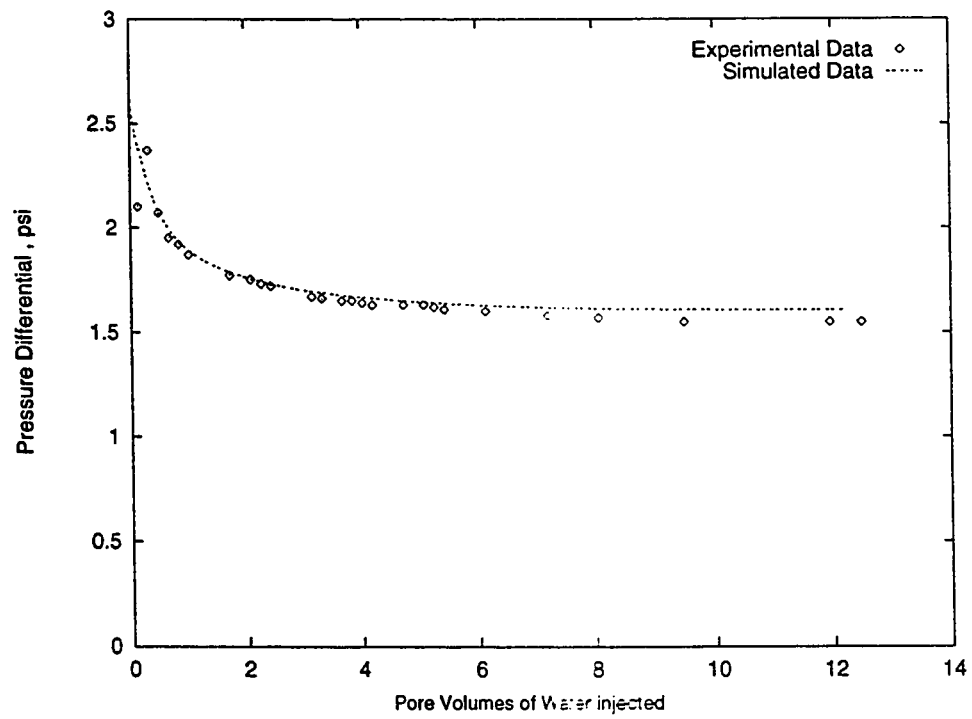


Figure 5.24: Pressure differential Curves for Core Plug P-3

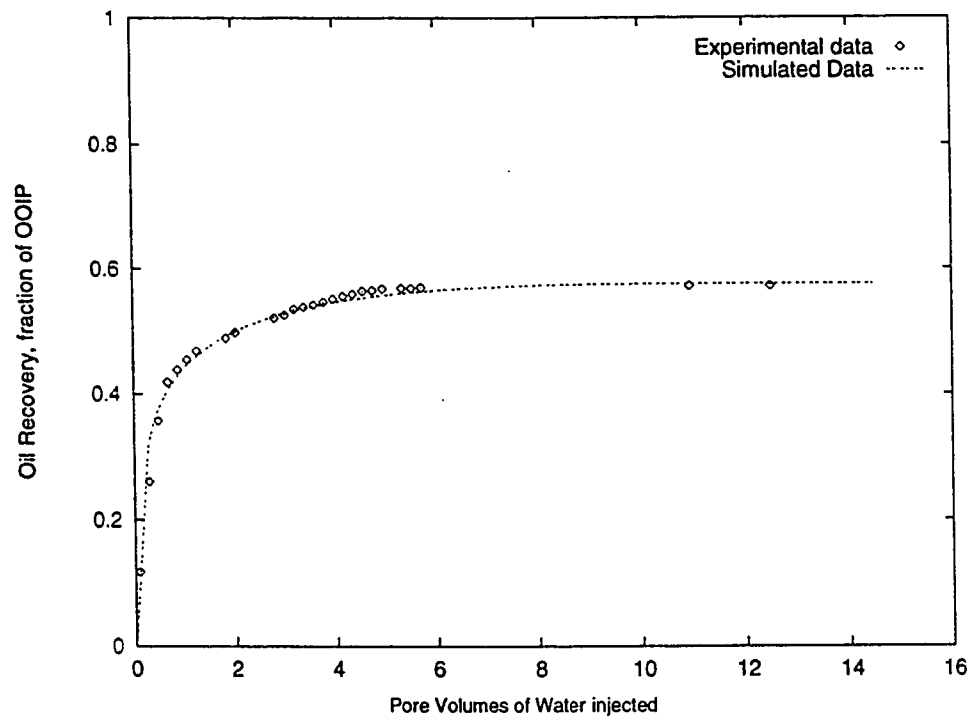


Figure 5.25: Recovery Performance Curves for Core Plug P-4

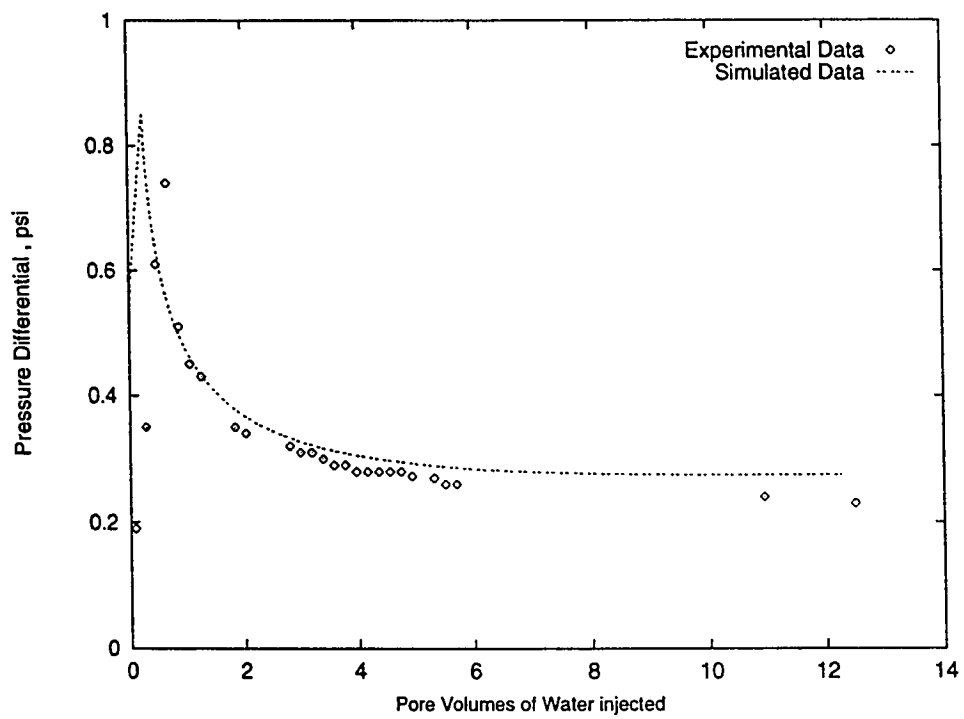


Figure 5.26: Pressure differential Curves for Core Plug P-4

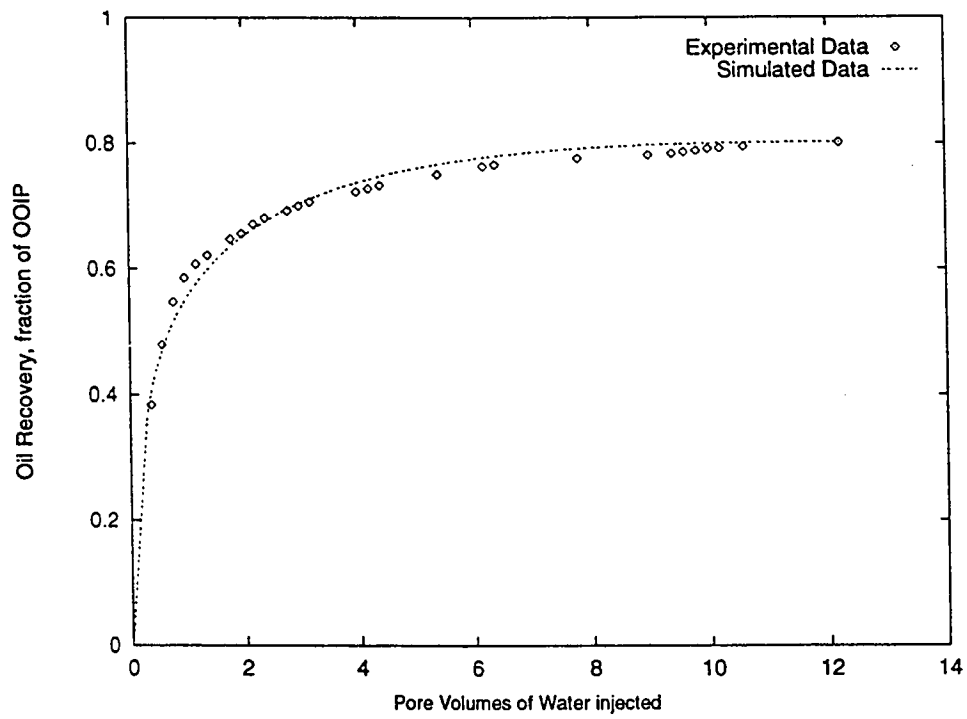


Figure 5.27: Recovery Performance Curves for Core Plug P-16

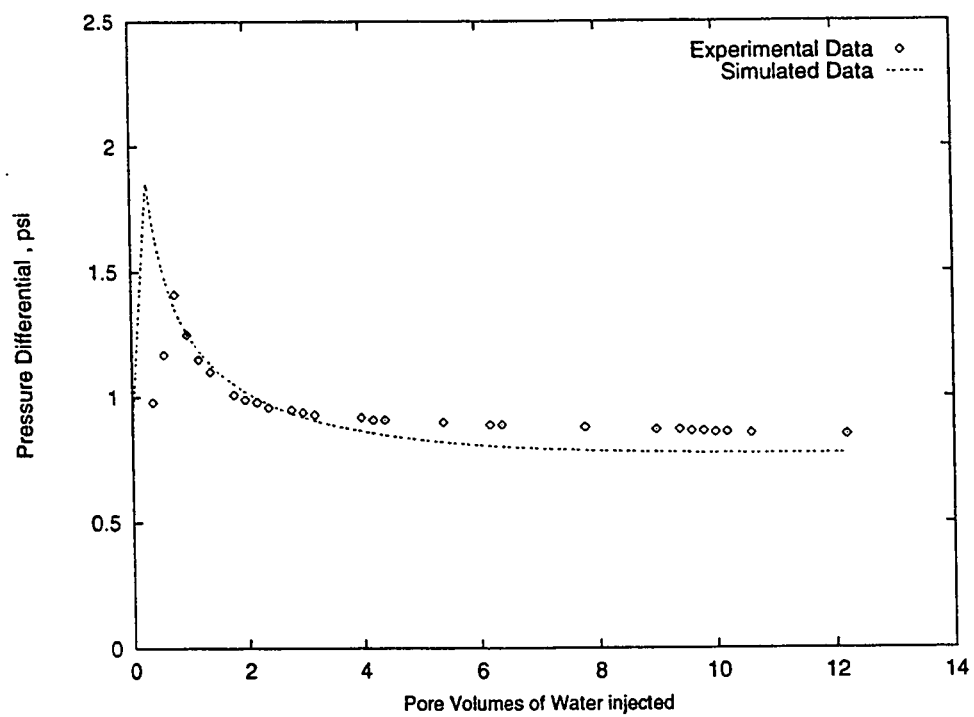


Figure 5.28: Pressure differential Curves for Core Plug P-16

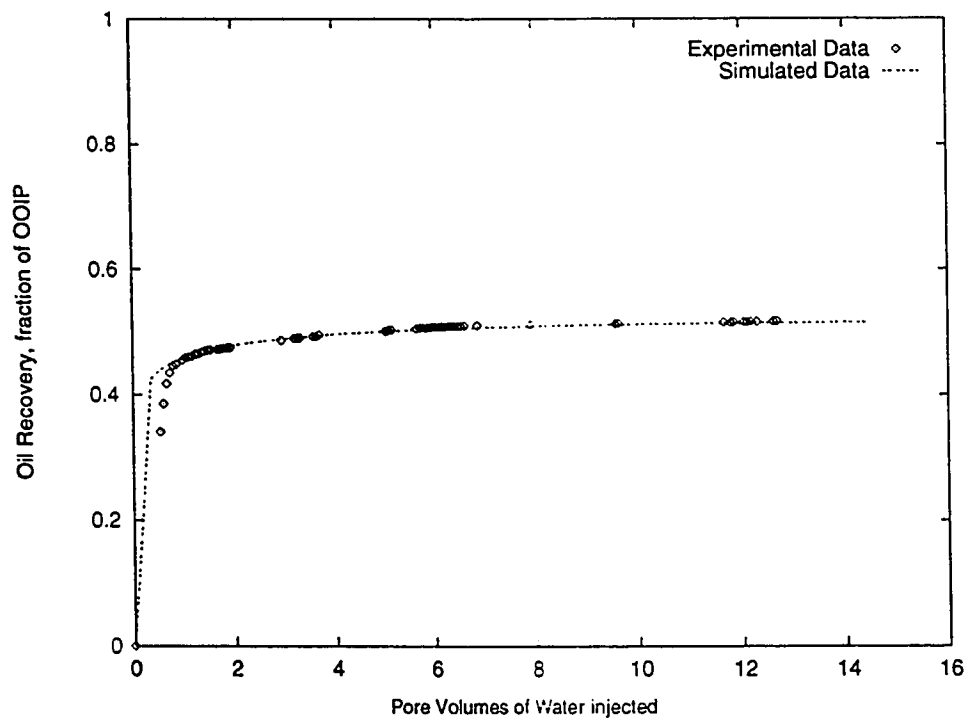


Figure 5.29: Recovery Performance Curves for Composite-2

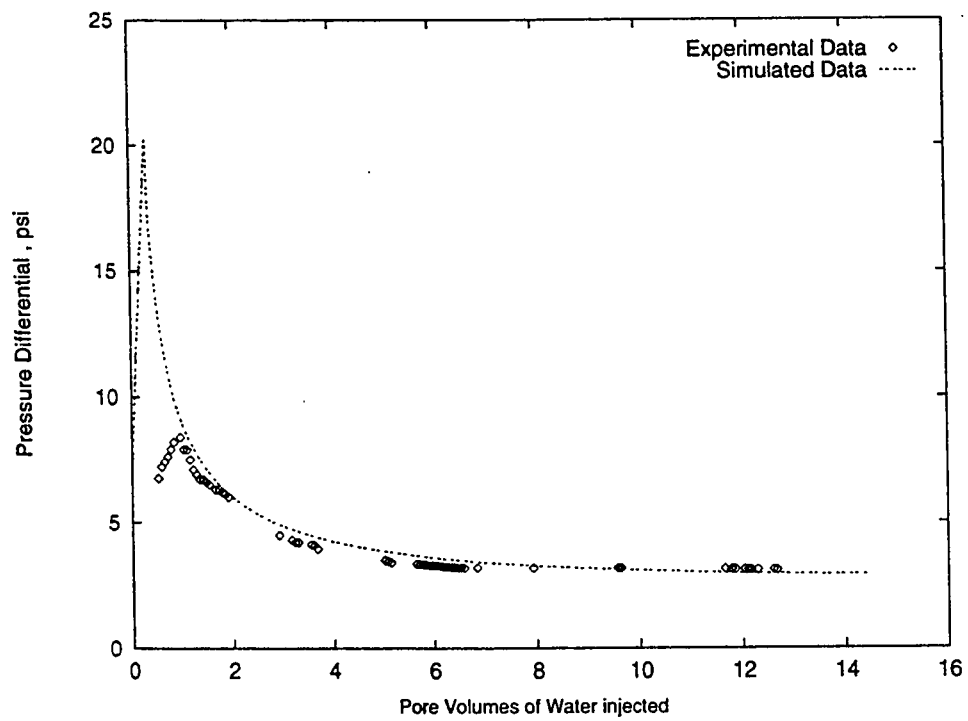


Figure 5.30: Pressure differential Curves for Composite-2

5.5 History Match Relative Permeabilities

The development of a simulation model along with the necessary input data in which some parameters are changed to match the calculated data and the observed data is referred to as history matching. The history matching approach is used to obtain relative permeabilities by taking into account capillary pressure and capillary pressure end effects.

In this study, the capillary pressure function from the brine drive curve and the estimated relative permeability curves were used as input into the simulation program to match the experimental data of oil recovery and differential pressure of core Plugs P-3, P-4 and composite-2. The following power law equations for k_{rw} and k_{ro} were used as the input relative permeability curves.

$$k_{rw} = A_w(S_w^*)^{N_w} \quad (5.1)$$

$$k_{ro} = (1 - S_w^*)^{N_o} \quad (5.2)$$

$$S_w^* = \frac{S_w - S_{wi}}{1 - S_{or} - S_{wi}} \quad (5.3)$$

The oil recovery and pressure differential matches for core plugs P-3 and P-4 are shown in Figures 5.31 to 5.35. The relative permeabilities obtained from the match for P-3 and P-4 are shown in Figures 5.33 and 5.36.

For the composite-2, the recovery and pressure differential matches are shown in Figures 5.37 and 5.38 respectively. A good match was obtained for the oil

recovery. However, the pressure differential data for this composite were not matched adequately. The relative permeabilities obtained from the match are higher than JBN relative permeabilities. This is due to the inclusion of capillary pressure end effects in the system during the history matching, while in the JBN method these effects are not incorporated.

5.6 Numerical Simulation

As discussed in the JBN relative permeability section, no average relative permeability curves were obtained from the individual plugs relative permeabilities. Therefore a simulation study was made to investigate the averaging process of the relative permeabilities. Two synthetic cases were studied in which a composite comprising two plugs (S1.S3) and the other consisted of three plugs with an additional plug S2. The rock and relative permeability data are shown in Table 5.3. The relative permeability data were modeled using equations 5.1 to 5.3.

Table 5.3: Input parameters for the simulation runs

Core Plug	Length cm	Area cm^2	ϕ frac.	k md	S_{wi} frac.	S_{or} frac.	A_w	N_w	N_o
S1	5.08	11.34	0.20	500	0.20	0.30	0.30	1.50	3.50
S2	5.08	11.34	0.20	500	0.20	0.30	0.45	1.75	3.00
S3	5.08	11.34	0.20	500	0.20	0.30	0.60	2.00	2.50

Two composites CP2-1 and CP2-2 were formed from plugs S1 and S3 in the

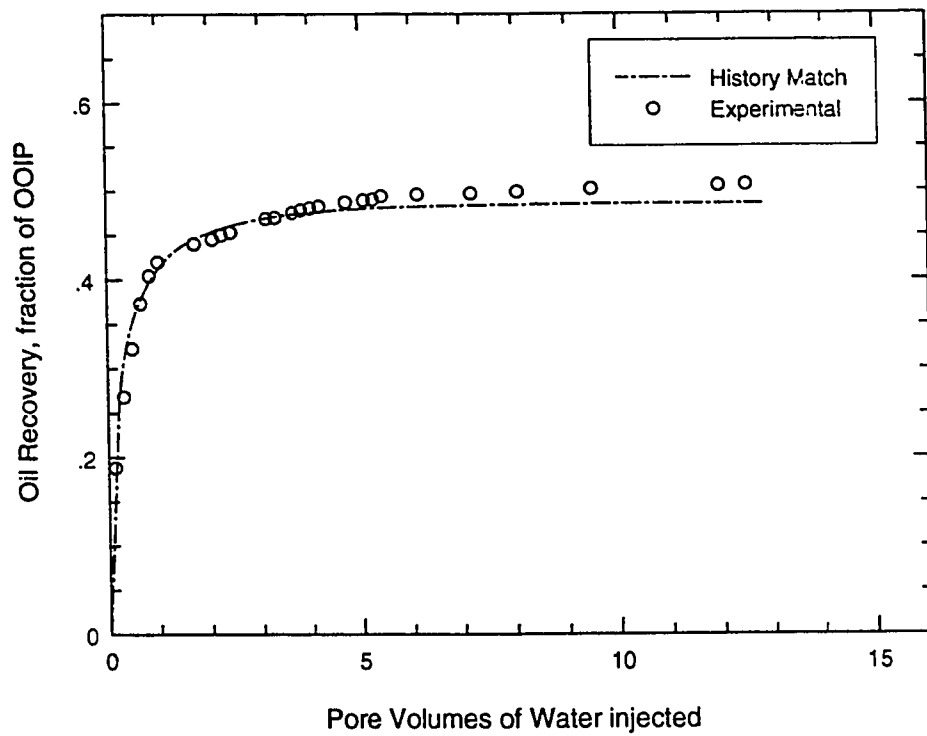


Figure 5.31: History Match Recovery for Core Plug P-3

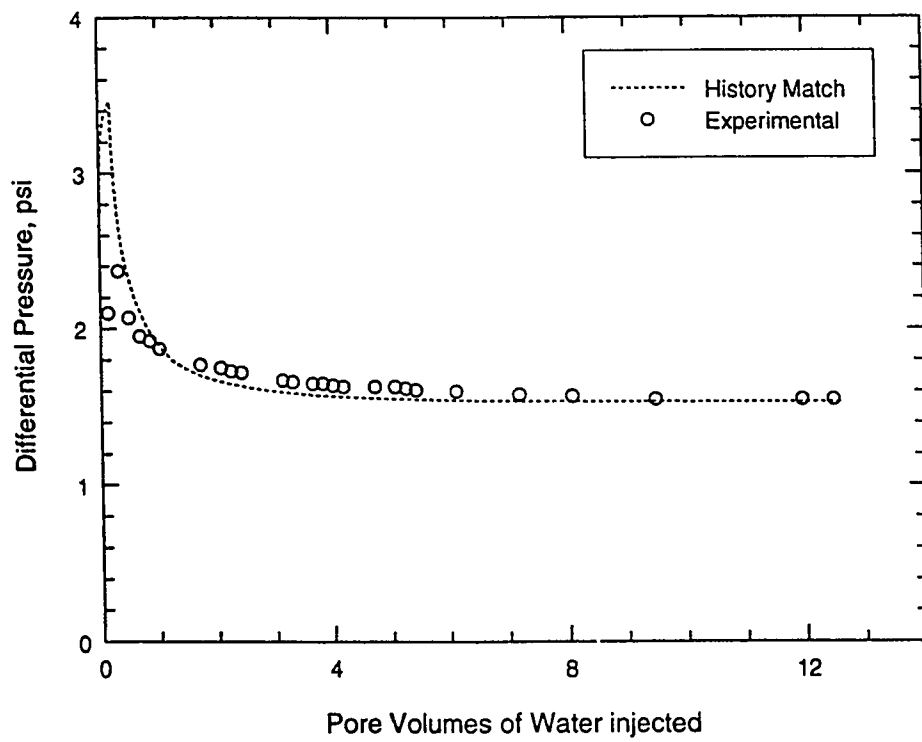


Figure 5.32: History Match Pressure drop for Core Plug P-3

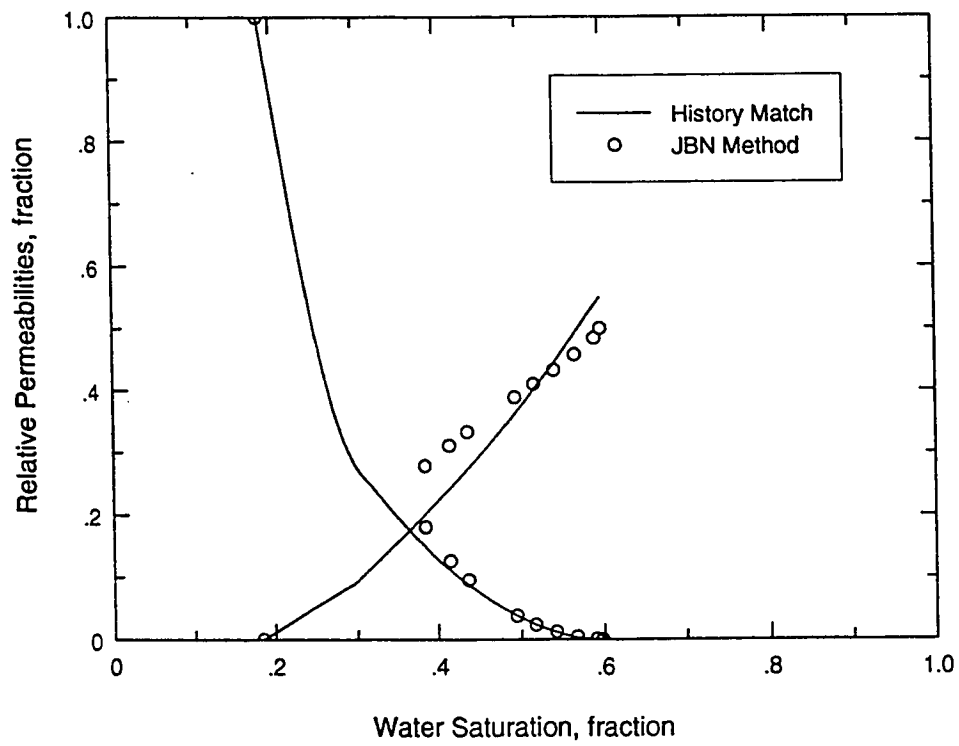


Figure 5.33: History Match Relative Permeabilities for Core Plug P-3

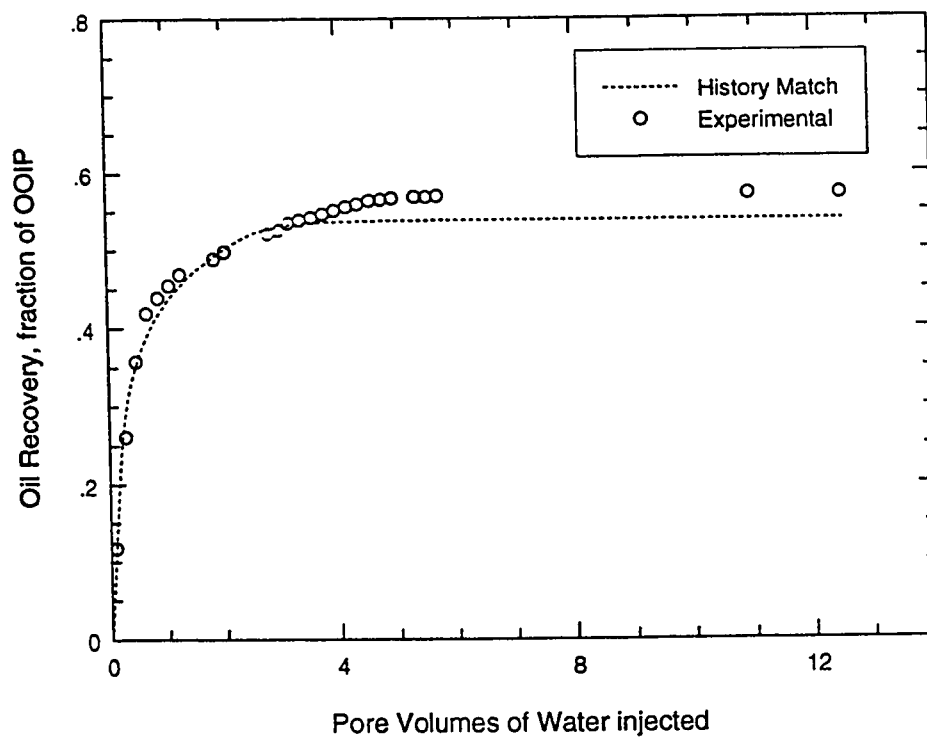


Figure 5.34: History Match Recovery for Core Plug P-4

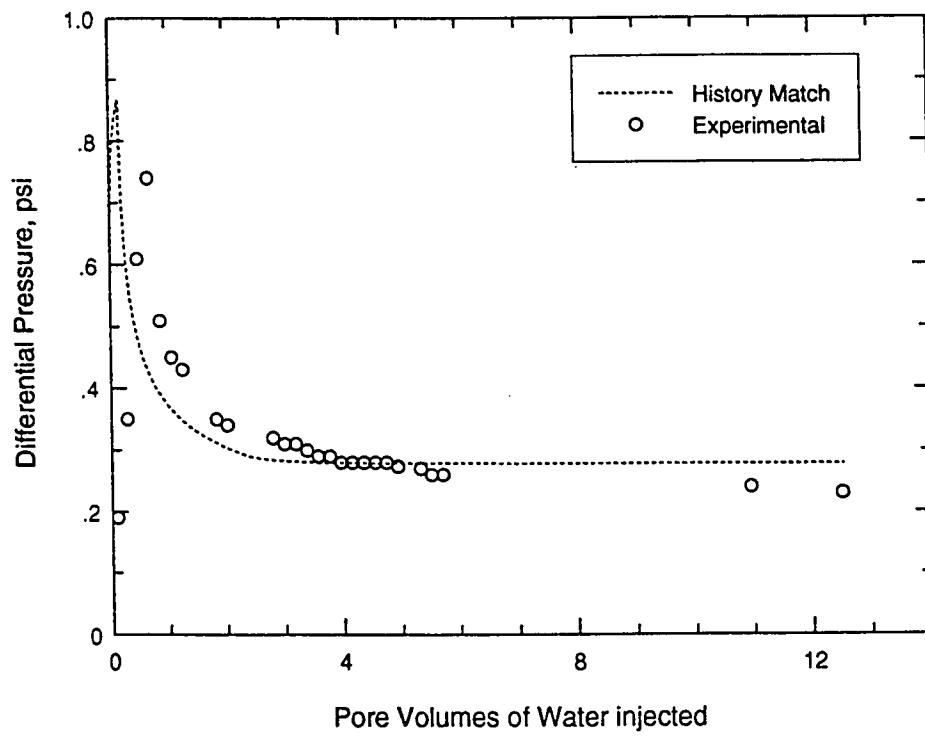


Figure 5.35: History Match Pressure drop for Core Plug P-4

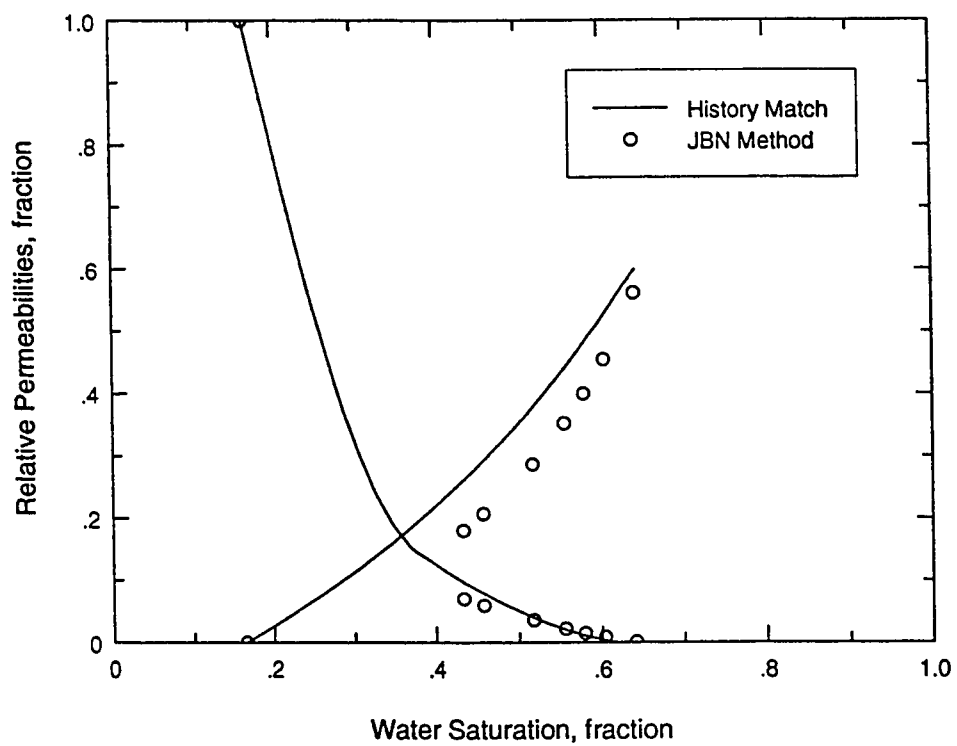


Figure 5.36: History Match Relative Permeabilities for Core Plug P-4

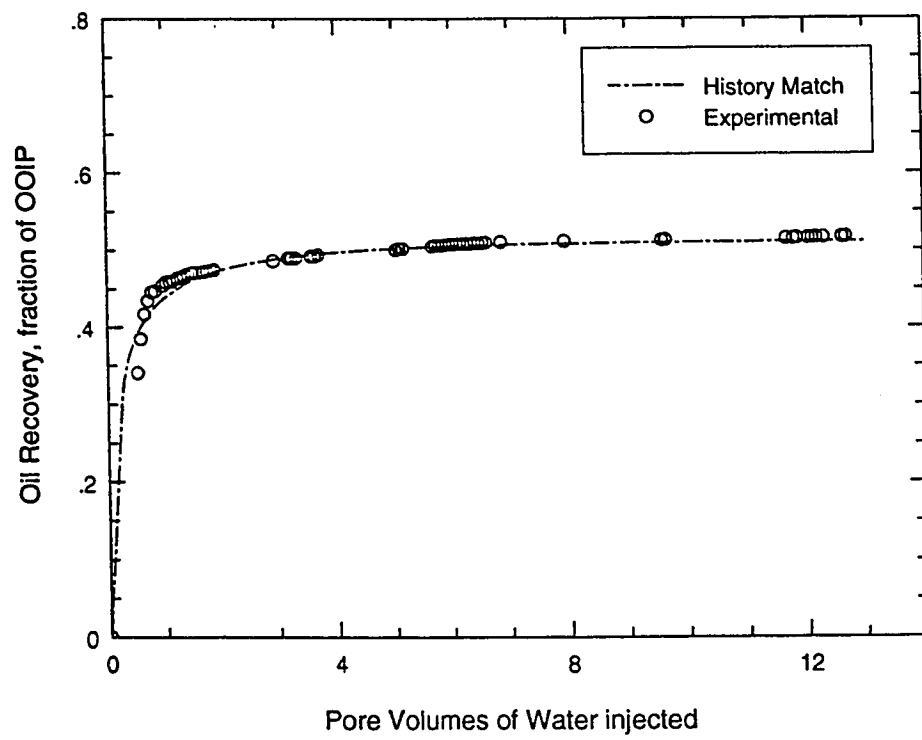


Figure 5.37: History Match Recovery for Composite-2

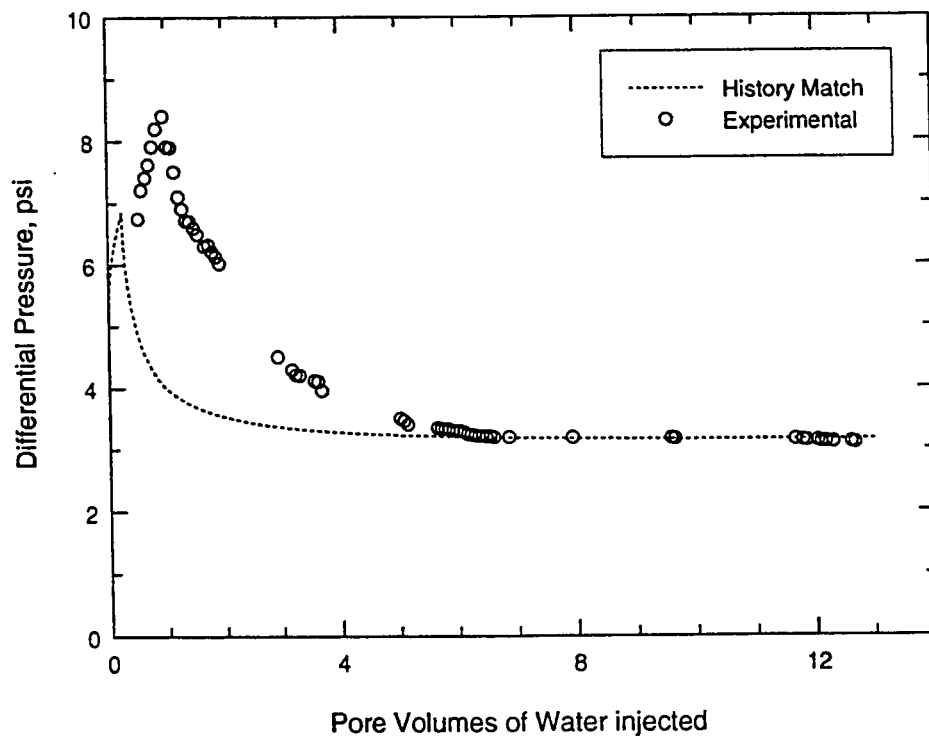


Figure 5.38: History Match Pressure drop for Composite-2

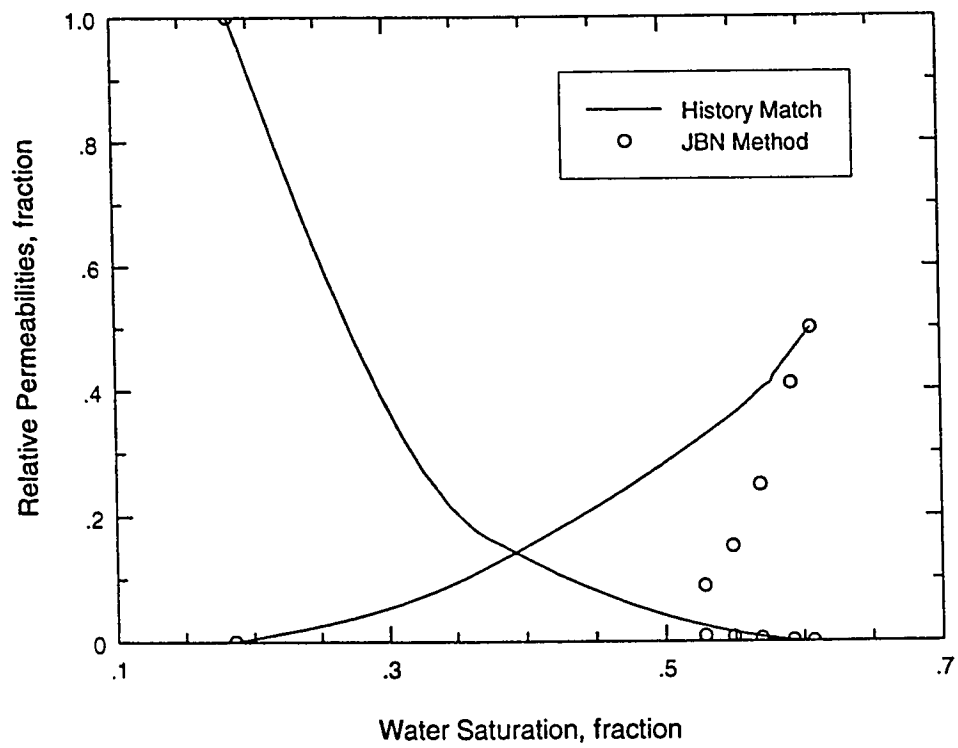


Figure 5.39: History Match Relative Permeabilities for Composite-2

order from inlet to outlet as S1,S3 and then S3, S1. Similarly three composites were formed using S1, S2, S3 as CP3-1 (S1, S2, S3), CP3-2 (S1, S3, S2), and CP3-3 (S2, S1, S3). The recovery performance of these composites was studied with and without including capillary pressure end effects at the outlet end of the system.

5.6.1 No Capillary Pressure Included

The simulation results without capillary pressure effects are shown in Figures 5.40 to 5.47. It is noticed that when capillary pressure is not included in the system, the order of the core plugs has no significant effect on the recovery performance of the composite core as shown in Figures 5.40 and 5.42. The pressure drop across the system is affected slightly due to different relative permeabilities of the core samples. The pressure drop for the composite is approximately the sum of the pressure drops for the individual plugs as shown in Figures 5.41 and 5.43. The oil recovery from the 2-plug composites is approximately the arithmetic average of the recoveries of the individual plugs. When plug S2 is added to plugs S1 and S3 to form a longer core, then the composite recovery is still in between the individual plugs.

To investigate the averaging of the relative permeabilities, the oil recovery and pressure drop data of the composites obtained from the simulation runs were analyzed to obtain relative permeabilities using JBN method. It is noticed that the calculated relative permeabilities of the composites are the same regardless of the ordering of the individual core plugs. The calculated values lie between the rela-

tive permeabilities of the individual plugs as shown in Figures 5.44 and 5.45. To determine the kind of average of the relative permeabilities of the composite cores, three averages; arithmetic, geometric and harmonic of input relative permeabilities were calculated and compared to the calculated values of the composites. It is noted that the harmonic average is closer to the calculated for the composite core than the arithmetic or geometric average as shown in Figures 5.46 and 5.47.

5.6.2 Capillary Pressure Included

When capillary pressure effects are incorporated in the simulation runs, the oil holdup at the outlet end causes an additional pressure drop resulting in an overall higher pressure drop of the system. After breakthrough, the pressure differential drops sharply to a stabilized value as shown in Figures 5.49 and 5.51 and the recovery of the composites is higher than that of the individual plugs as shown in Figures 5.48 and 5.50. There is a slight difference between the recovery of the three composite cores.

It is shown from the comparison in Figures 5.52 and 5.53 that the relative permeabilities to both oil and water, calculated using JBN method from numerical recovery data, decrease when capillary pressure is incorporated in the system. Due to the capillary end effects, the wetting phase holdup at the outlet end, the pressure differential is increased which causes the relative permeabilities to decrease. The comparison of relative permeabilities with and without capillary pressure end effects

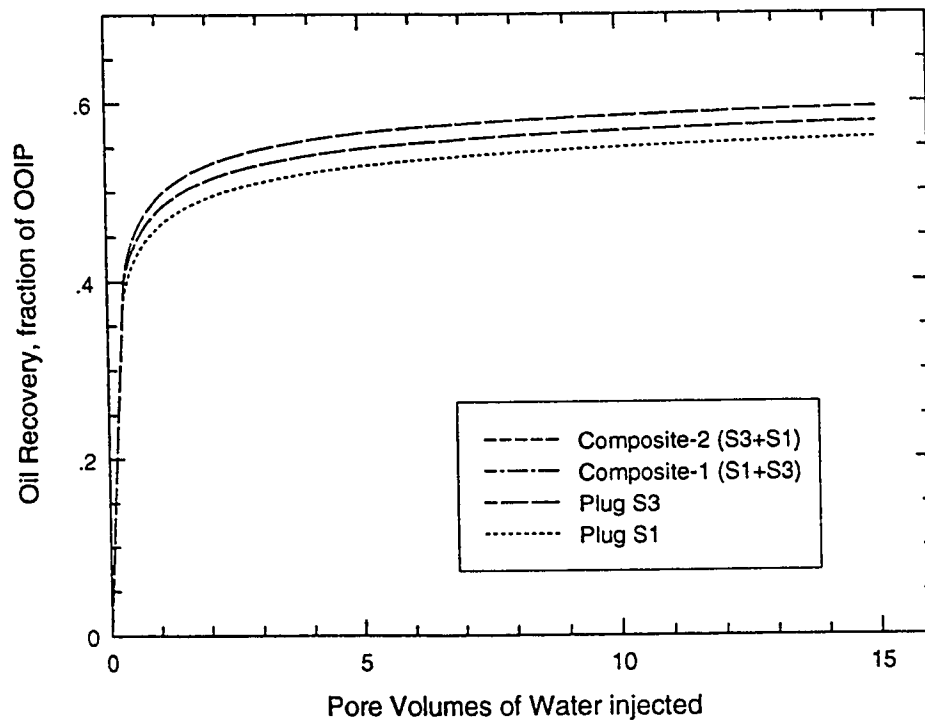


Figure 5.40: Recovery comparison for 2-plug composites without Capillary Pressure

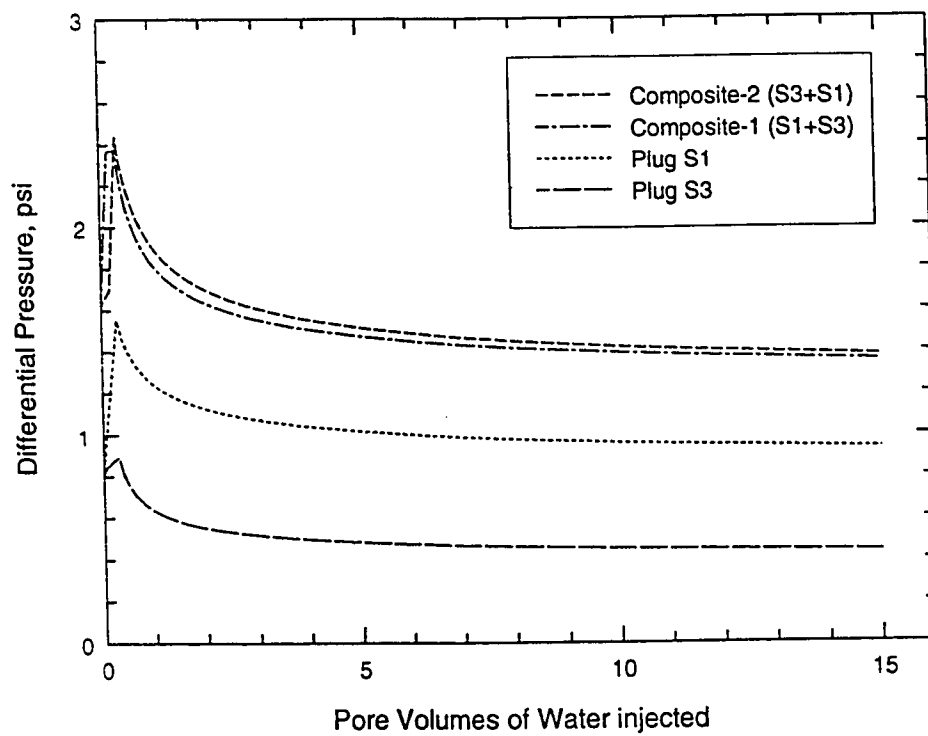


Figure 5.41: Pressure drop comparison for 2-plug composites without Capillary Pressure

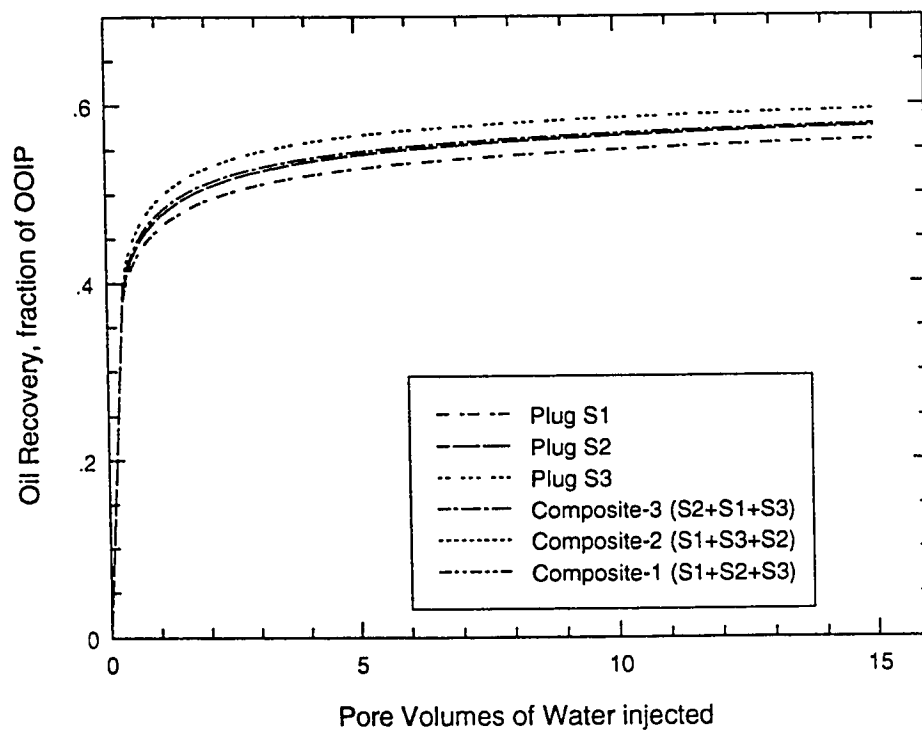


Figure 5.42: Recovery comparison for 3-plug composites without Capillary Pressure

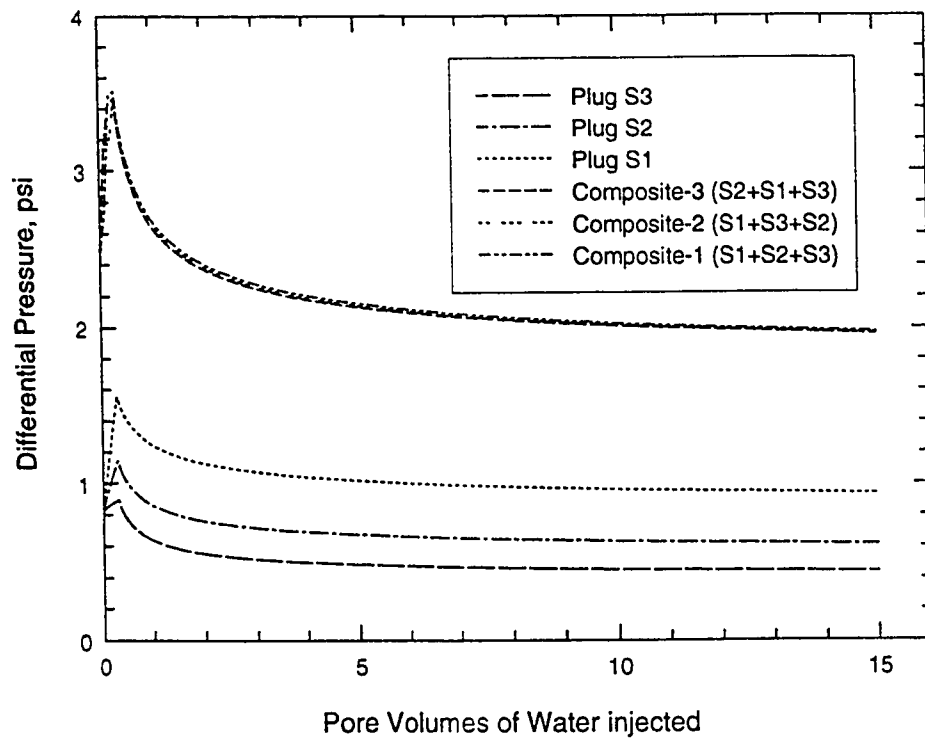


Figure 5.43: Pressure drop comparison for 3-plug composites without Capillary Pressure

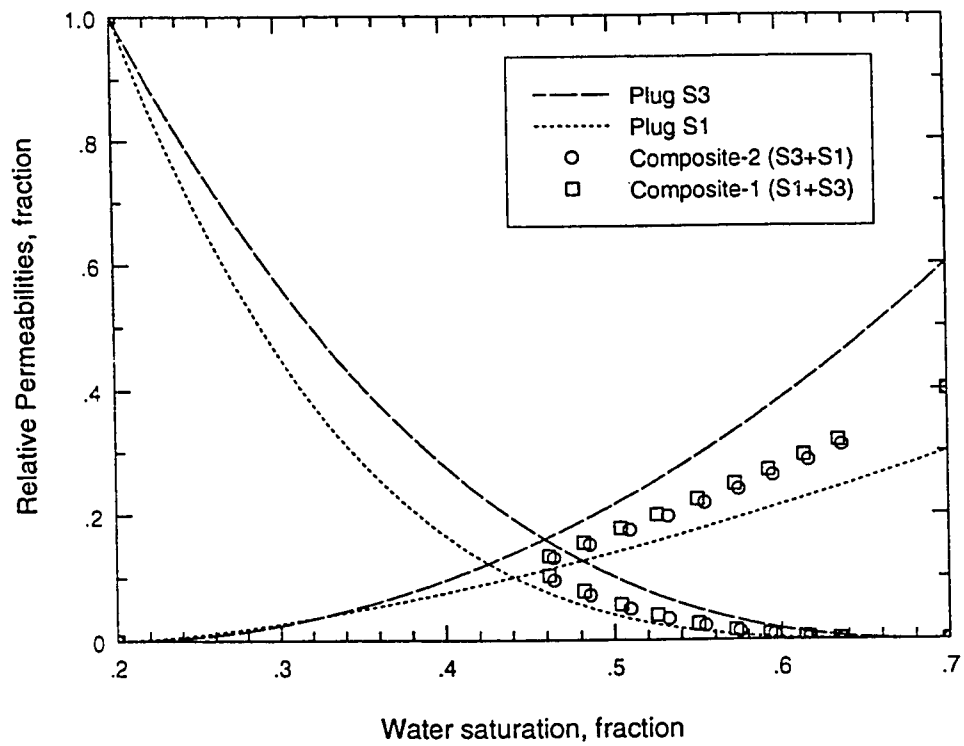


Figure 5.44: Relative permeabilities for 2-plug composites without Capillary Pressure

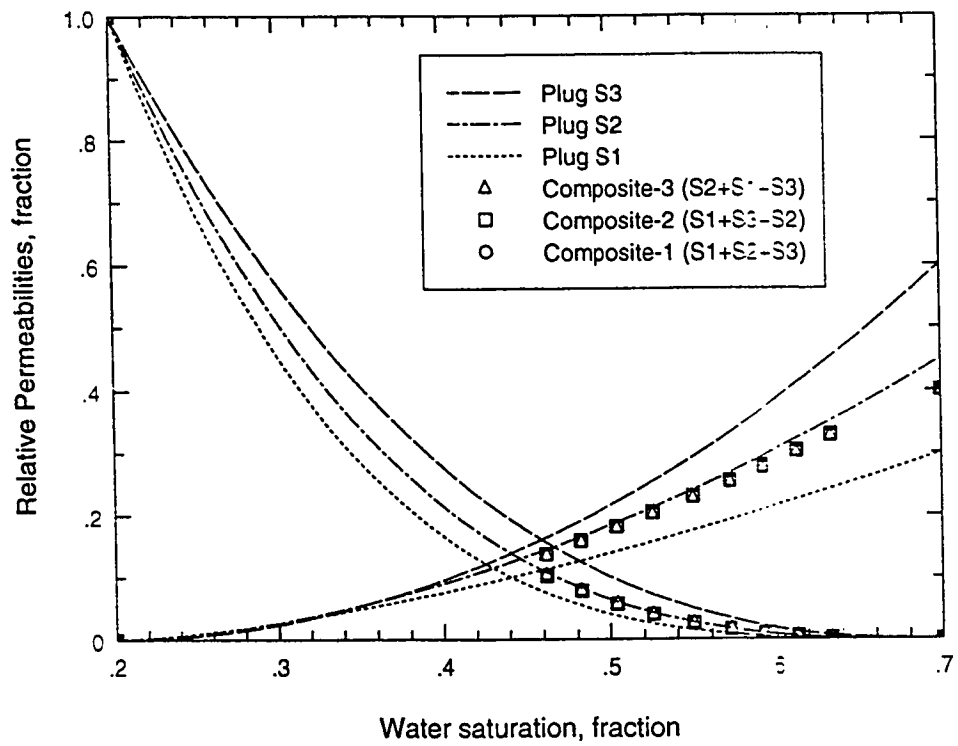


Figure 5.45: Relative permeabilities for 3-plug composites without Capillary Pressure

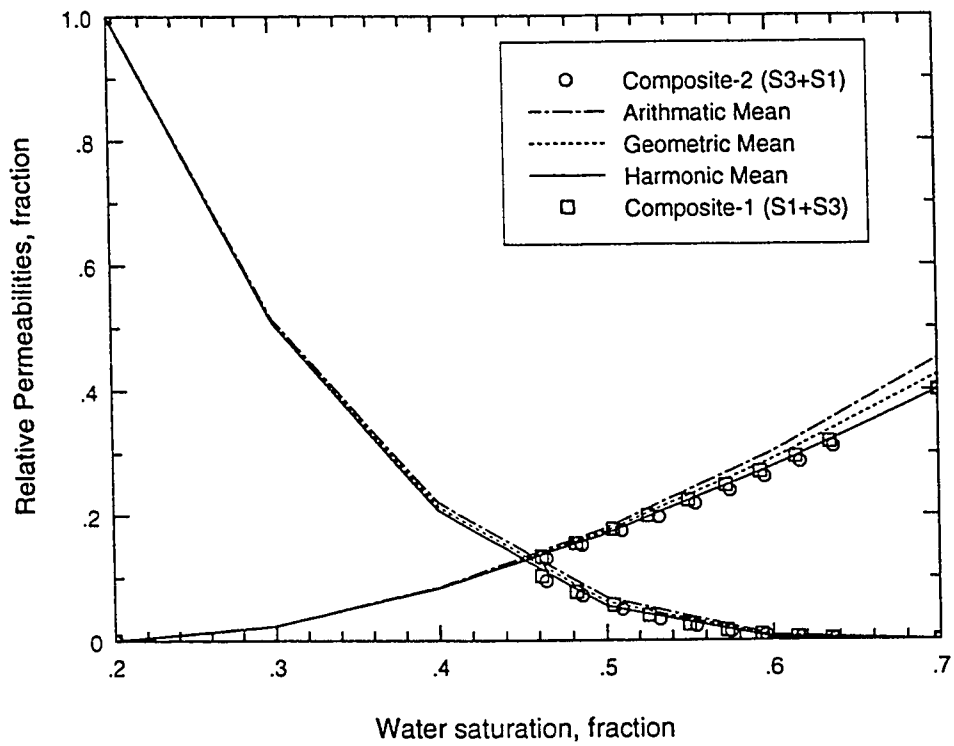


Figure 5.46: Averaging of relative permeabilities for 2-plug composites without Capillary Pressure

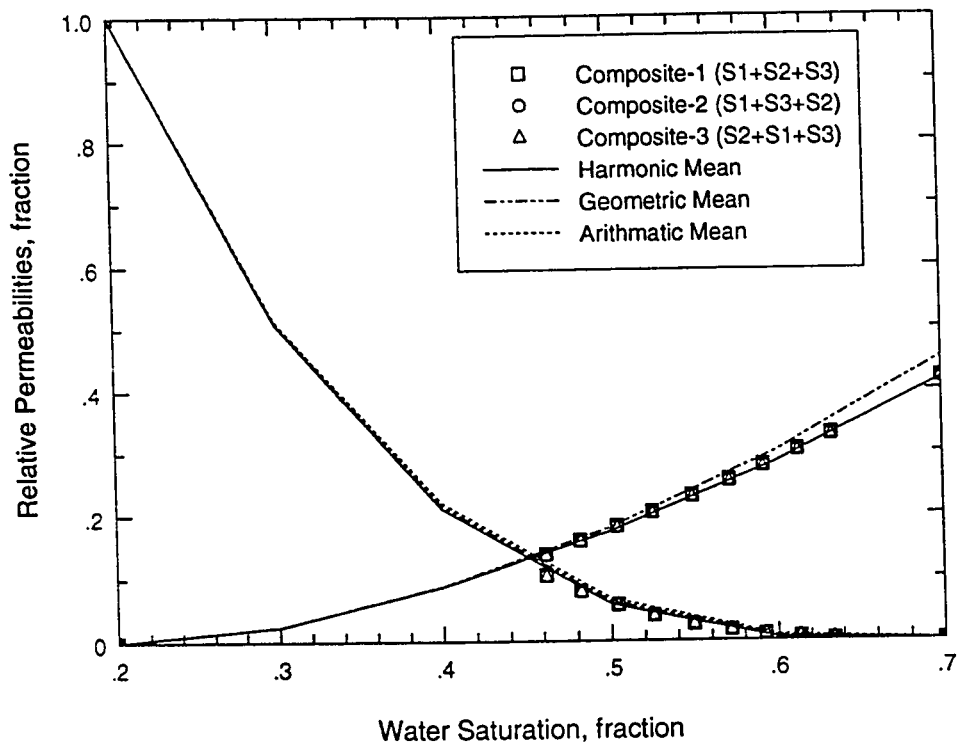


Figure 5.47: Averaging of relative permeabilities for 3-plug composites without Capillary Pressure

are shown in Figures 5.56 and 5.57. It is also noticed that the calculated values are lower than the expected harmonic average of the relative permeabilities of the individual plugs as shown in Figures 5.54 and 5.55.

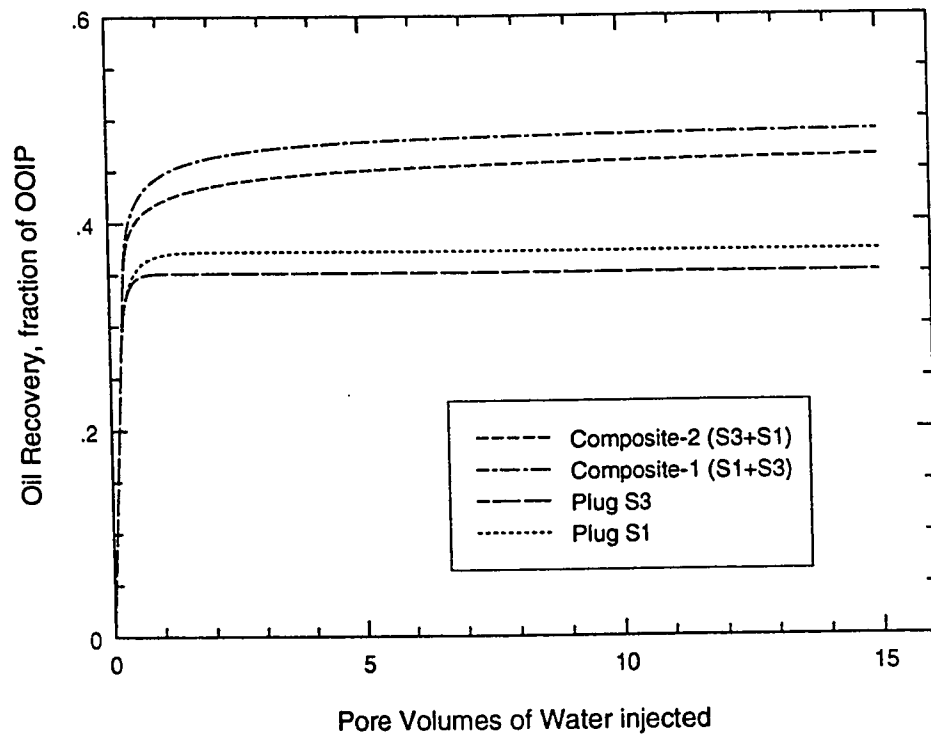


Figure 5.48: Recovery comparison for 2-plug composites with Capillary Pressure

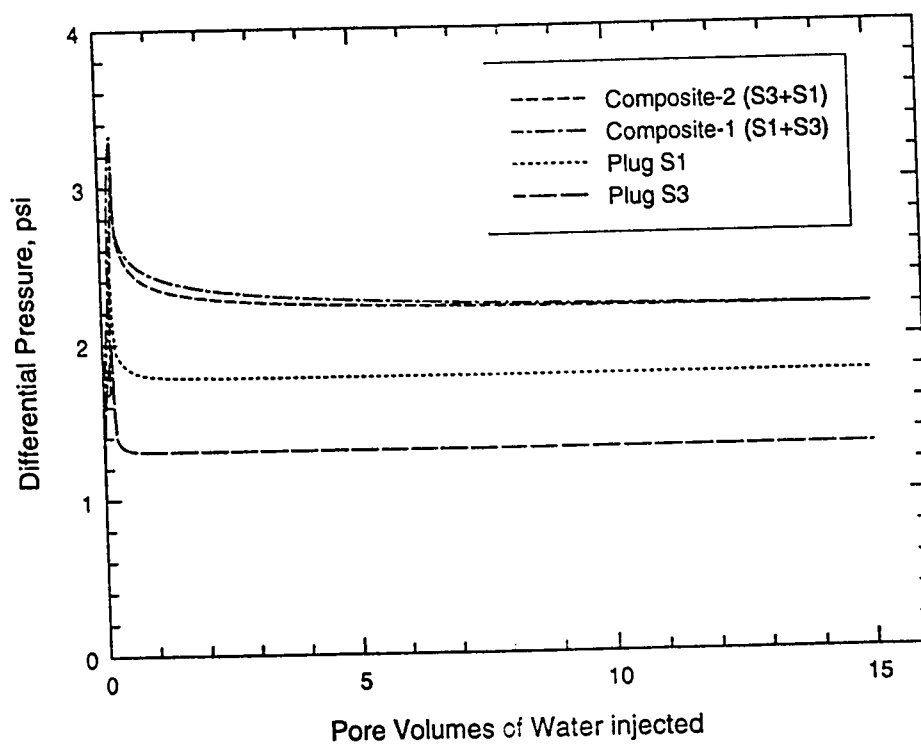


Figure 5.49: Pressure drop comparison for 2-plug composites with Capillary Pressure

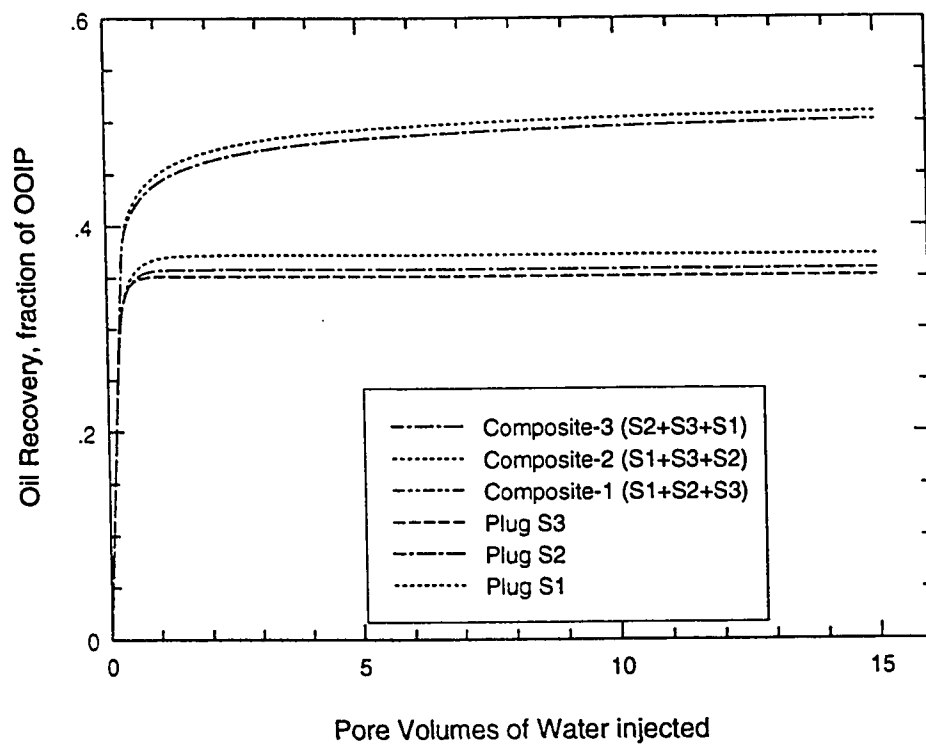


Figure 5.50: Recovery comparison for 3-plug composites with Capillary Pressure

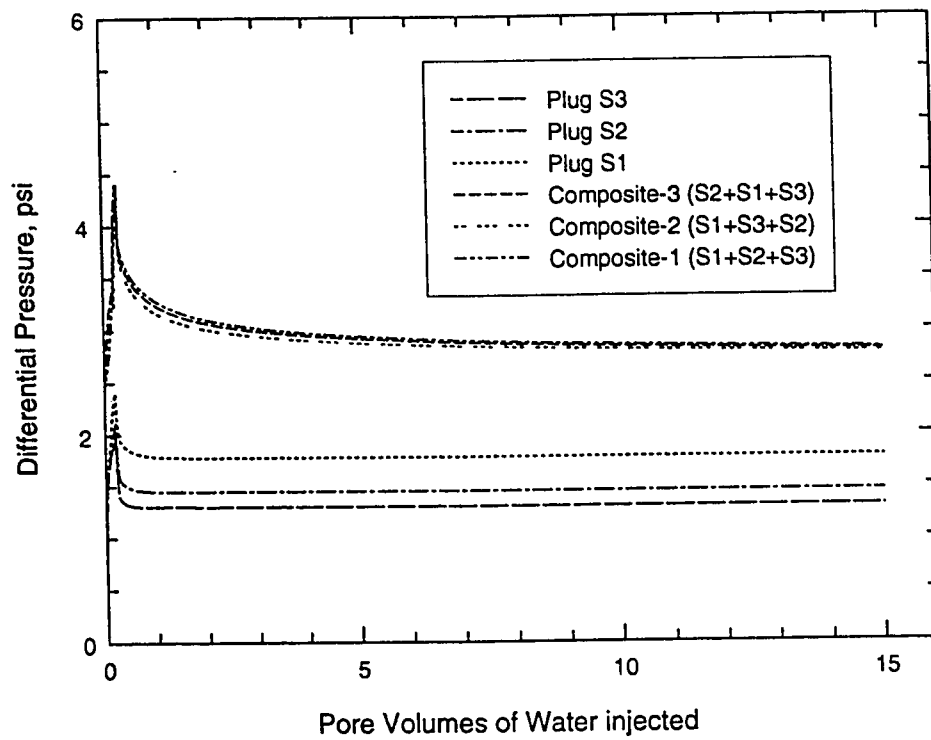


Figure 5.51: Pressure drop comparison for 3-plug composites with Capillary Pressure

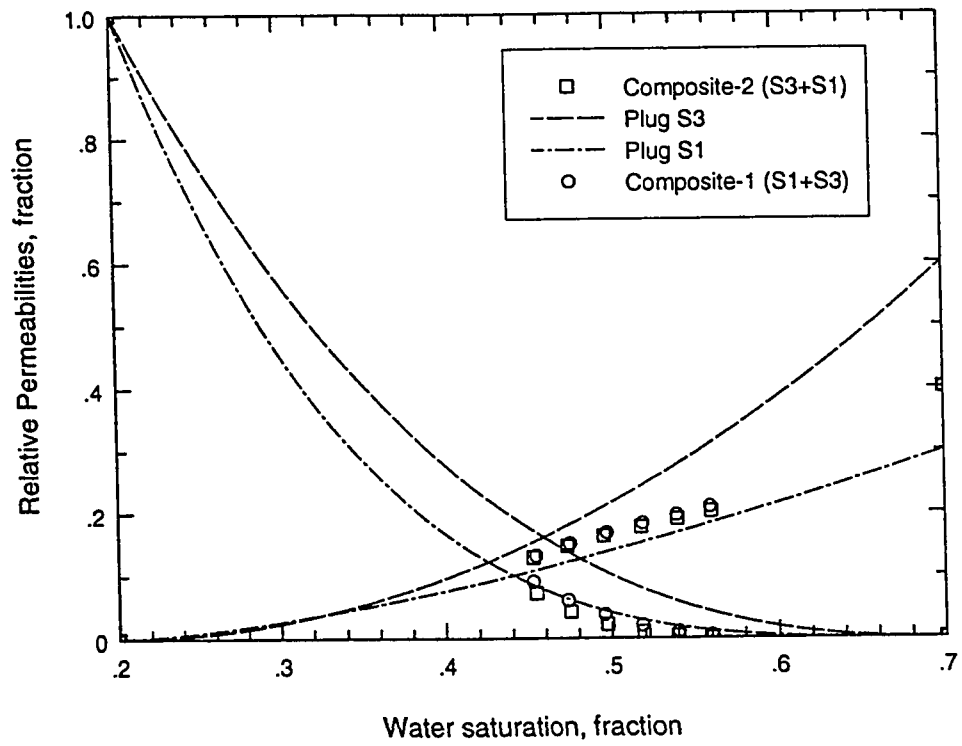


Figure 5.52: Relative permeabilities for 2-plug composites with Capillary Pressure

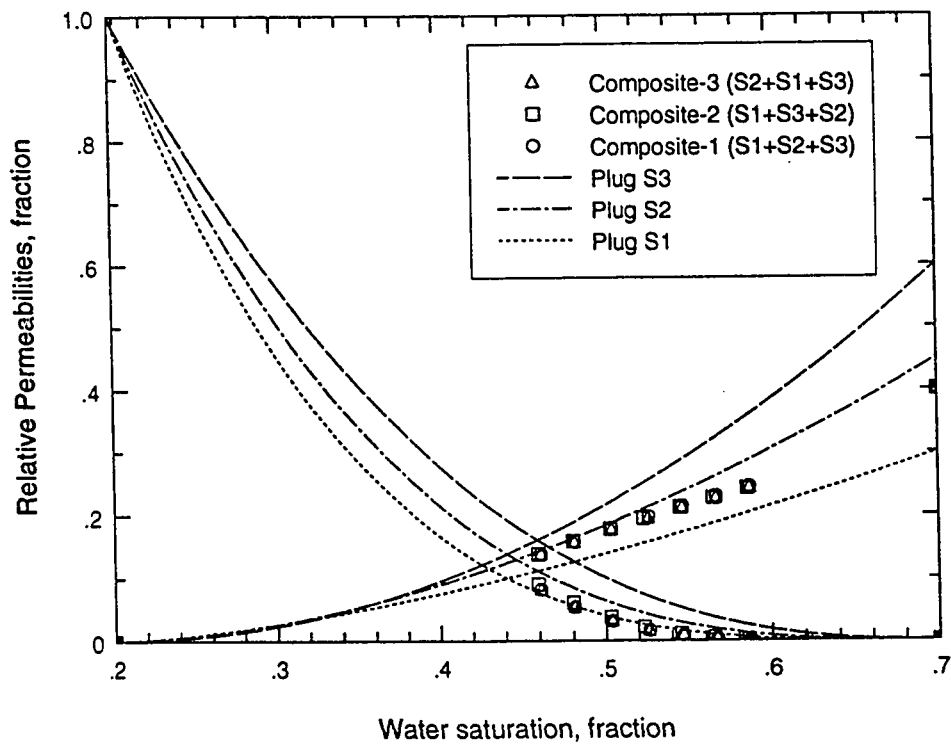


Figure 5.53: Relative permeabilities for 3-plug composites with Capillary Pressure

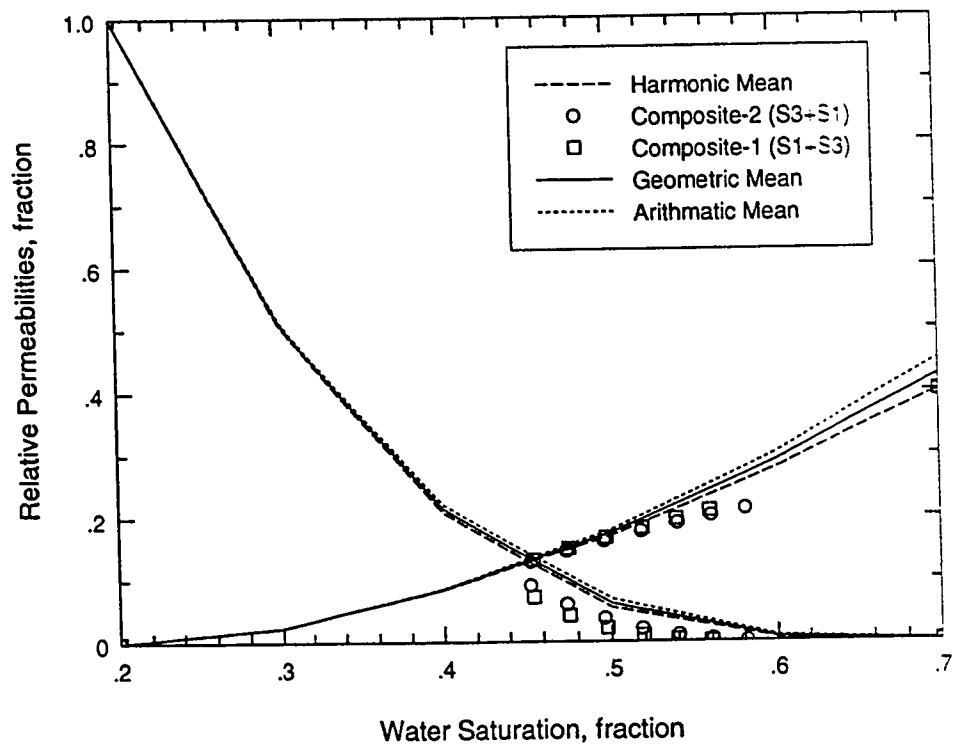


Figure 5.54: Averaging of relative permeabilities for 2-Plug composites with Capillary Pressure

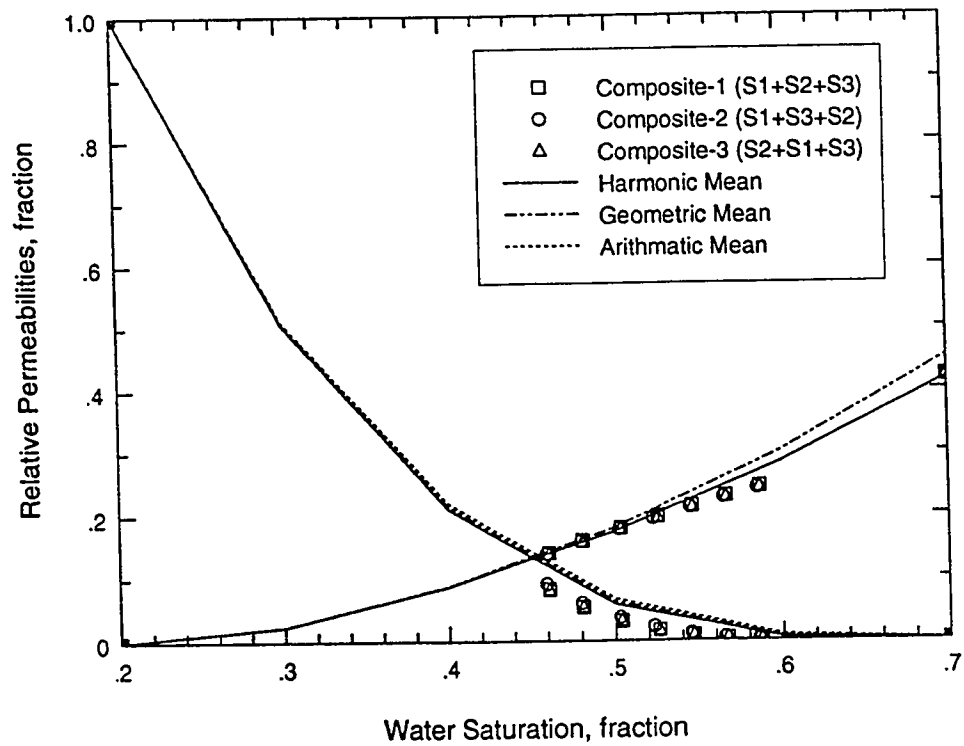


Figure 5.55: Averaging of relative permeabilities for 3-Plug composites with Capillary Pressure

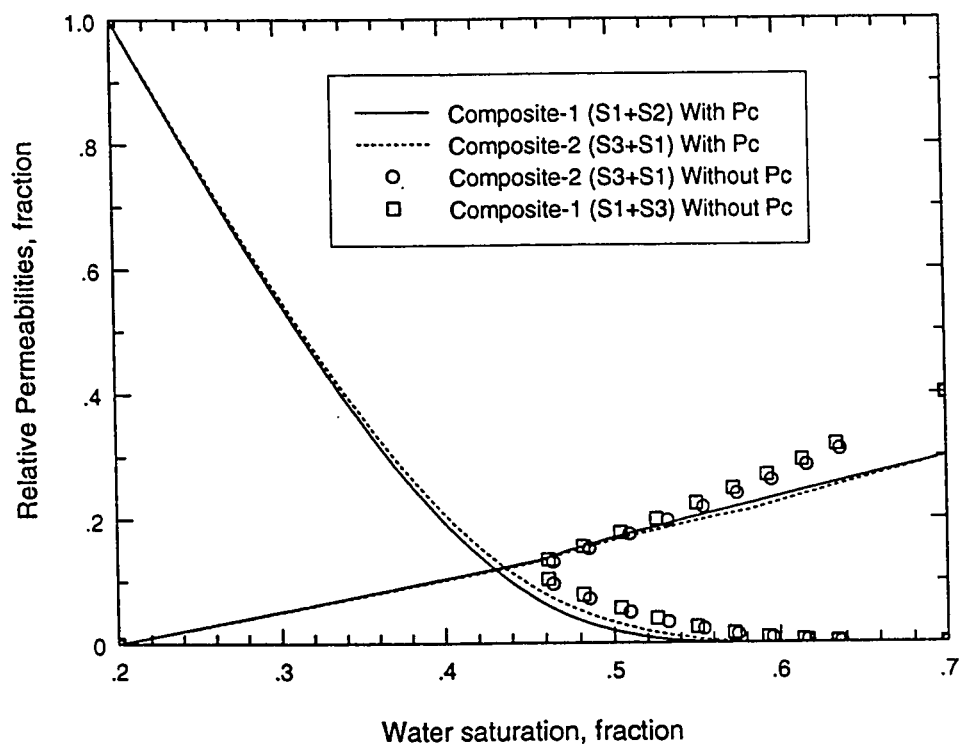


Figure 5.56: Comparison of relative permeabilities for 2-plug composites with and without Capillary Pressure

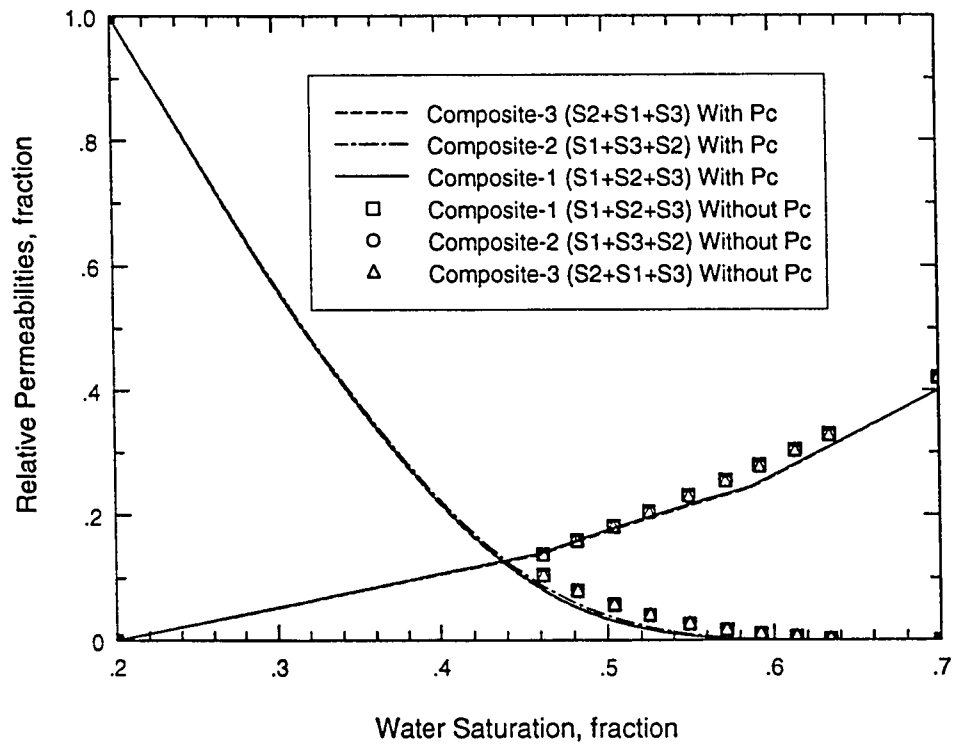


Figure 5.57: Comparison of relative permeabilities for 3-plug composites with and without Capillary Pressure

Chapter 6

CONCLUSIONS

6.1 Experimental

1. In this study, the experimental results showed that the oil recovery from composite cores is less than that of individual plugs due to the heterogeneous nature of the carbonate rocks which causes nonuniform front over the cross sectional area due to viscous fingering which causes an early breakthrough.
2. The JBN method might not be adequate for calculating relative permeabilities from displacement data subjected to viscous fingering and bypassing.

6.2 Numerical

1. Ordering of individual core plugs which might have different relative permeabilities does not have significant effect on the recovery performance of the

composite core if capillary pressure end effects are not significant.

2. Relative Permeability of a composite core is the harmonic average of the relative permeabilities of the individual plugs when capillary pressure end effects are not significant.

Nomenclature

L = Length of the sample , cm

A = Cross-sectional area, cm

q = Injection rate, cc/sec

k = Absolute permeability, md

P = Pressure differential across the core, psi

f = Fraction flow, fraction

S_{wi} = Irreducible water saturation, fraction

S_{or} = Residual oil saturation, fraction

\bar{S}_w = Average water saturation

S_{w2} = Water saturation at the outlet end

N_p = cumulative volume of oil produced

P_c = Capillary pressure, psi

f_o = fractional volume of oil flowing from core outlet

S_{wi} = irreducible water saturation

k_{rw} = relative permeability to water

k_{ro} = relative permeability to oil

μ_w = viscosity of water, cp

μ_o = viscosity of oil, cp

W_i = cumulative pore volumes of water injected

I_r = relative injectivity, $(q/p)/(q/p)_{base}$

dp/dx = Pressure gradient, atm/cm

Bibliography

- [1] Richardson, J.G., Kerver, J.K., Hafford, J.A. and Osaba, J.S.: "Laboratory Determination of Relative Permeability," Trans. AIME, (1952) 195, 187-196.
- [2] Rapoport, L.A. and Leas, W.J.: "Properties Of Linear Waterfloods," Trans., AIME (May 1953) 198, 139-148.
- [3] Johnson, E.F., Bossler, D.P. and Naumann, V.O.: "Calculation Of Relative Permeability From Displacement Experiments," Trans. AIME (1959) 216, 370-372.
- [4] Huppler, J.D.: "Waterflood Relative Permeabilities in Composite Cores," JPT (May 1969) 539-540.
- [5] Huppler, J.D.: "Numerical Investigation of the Effects of Core Heterogeneities on Waterflood Relative Permeabilities" SPEJ (December 1970) 381-392.
- [6] Jones, S.E. and Roszelle, W.O.: "Graphical Techniques for Determining Relative Permeability from Displacement Experiments," JPT (May 1978) 807-817.

- [7] Labastie A., Guy M., Jean, P.D. and Iffly R.: "Effect of Flowrate and Wettability on Water-Oil Relative Permeabilities and Capillary Pressure," paper SPE 9236 presented at the 55th Annual Fall Technical Conference and Exhibition of SPE, Dallas, Texas, September 21-24, 1980.
- [8] Craig, F.F. Jr.: *Reservoir Engineering Aspects of Waterflooding*, monograph series, SPE, Richardson, TX. (1971) 3
- [9] Hinkley. R.E. and Davis, L.A.: "Capillary Pressure Discontinuities and End Effects in Homogeneous Composite Cores : Effect of Flow Rate and Wettability," paper SPE 15596 presented at the 61st Annual Technical Conference and Exhibition of SPE, New Orleans, LA., October 5-8, 1986.
- [10] Heaviside. J., Brown, C.E. and Gamble, I.J.A.: "Relative Permeability for Intermediate Wettability Reservoirs ," paper SPE 16968 presented at the 62nd Annual Technical Conference and Exhibition of SPE Dallas, Texas, September 27-30, 1987.
- [11] Kossack. C.A., Aasen, J.O. and Opdal, S.T.: "Scaling-Up Laboratory Relative Permeabilities and Rock Hetrogenetics with Pseudo Functions for Field Simulations." paper SPE 18436 presented at the SPE Symposium on Reservoir Simulation in Houston, Texas, February 6-8, 1989.

- [12] Mohanty, K.K. and Miller, A.E. : "Factors Influencing Unsteady Relative Permeability of a Mixed-Wet Reservoir Rock." SPEFE, (September 1991) 349-358.
- [13] Arnyx, J.W., Bass, Jr.D. M. and Whiting, R.L.: *Petroleum Reservoir Engineering*, Macgraw Hill Book Company, 1960. 199-209 pp.
- [14] Anderson, W.G.: "Wettability Literature Survey- Part 1: Rock/Oil/Brine Interactions, and the effects of Core Handling on Wettability," JPT (October 1986) 1125-44.
- [15] Anderson, W.G.: "Wettability Literature Survey- Part 2: Wettability Measurement," JPT (November 1986) 1243-62.
- [16] Welge,H.J.: "A Simplified Method for Computing Oil Recovery by Gas or Water Drive," Trans., AIME (1952) 195.
- [17] Bobek, J.E., Mattax, C.C. and Danekas, M.O.: "Reservoir Rock Wettability-Its Significance and Evaluation," Trans., AIME (1958) 213. 155-60
- [18] Rajan, R.R. : "Theoretically Correct Analytical Solution for Calculating Capillary Pressure-Saturation from Centrifuge Experiments." SPWLA 27th annual logging symposium, June 9-13. 1986.
- [19] Miller, M.A.: "Effect of Temperature on Oil-Water Relative Permeabilities of Unconsolidated and consolidated sands." PhD dissertation, Stanford University, Stanford, California (1983).

- [20] Owens, W.W. and Archer, D.L. : "The Effect of Rock Wettability on Oil Water Relative Permeability Relationships," JPT, (July 1971)
- [21] Odeh, A.S. and Dotson, B.J. : "A Method for Reducing the Rate Effect on Oil and Water Relative Permeabilities Calculated from Dynamic Displacement Data," paper SPE 14417 presented at the 60th Annual Technical Conference and Exhibition of SPE, Las Vegas, Nevada, September 22-25, 1985.
- [22] Buckley, S.E. and Leverett, M.C.: "Mechanism of Fluid Displacement in Sands," Trans. AIME (1942) 146.
- [23] Donaldson, E.C., Civan, F. and WaqulAlam, M.: "Relative Permeabilities at Simulated Reservoir Conditions," SPERE (November 1988) 1323-1327.
- [24] Edmondson, T.A.: "Effect of Temperature on Waterflooding," JCPT (Oct.-Dec. 1965) 236-242.
- [25] Poston, S.W. et al : "The Effect of Temperature on Irreducible Water Saturation and Relative Permeability of Consolidated Sands," SPEJ (June 1970) 171-180.
- [26] Sinnokrot, A.A., Ramey, H.J.Jr., and Marsden, S.S.Jr.: "Effect of Temperature Level upon Capillary Pressure Curves," SPEJ (March 1971) 13-22.

- [27] Weinbrandt, M., Ramey, H.J.Jr. and Casse, F.J.: "The Effect of Temperature on Relative and Absolute Permeability of Sandstones," SPEJ (October 1975) 376-384.
- [28] Civan, F. and Donaldson, E.C.: "Relative Permeability from Unsteady-state Displacements with capillary Pressure Included," SPEFE (June 1989) 189-193.
- [29] Sandberg, C.R., Gournay, L.S. and Sippel, R.F.: "The Effect of Fluid Flow Rate and Viscosity on Laboratory Determinations of Oil-Water Relative Permeabilities," Trans. AIME (1958) 213, 36-43.
- [30] Wu, Y.S., Pruess, K. and Chen, Z.X.: "Buckley-Leverett Flow in Composite Porous Media," SPE Advanced Technology Series, Vol. 1, No.2, pp. 36-42.
- [31] Morrow, N.R. : *Interfacial Phenomena in Petroleum Recovery ,Surfactant Science Series*. Volume 36. Marcel Dekker, Inc.New York, 1991.
- [32] Watson, A.T., Kerig, P.D. and Otter, R.W.: "A Test for Determining Rock Property Nonuniformities in Core Samples." SPEJ (December 1985) 909-916.

Appendix A

Table A.1: Oil and Brine Drive of Core Plug-2

Centrifuge RPM	Oil Drive			Brine Drive		
	V_b cc	P_c psi	S_w fraction	V_o cc	P_c psi	S_w fraction
0.0	0.00	0.00	0.817	0.00	0.00	0.248
500.0	0.40	0.34	0.790	0.60	-0.70	0.288
700.0	0.50	0.67	0.784	1.50	-1.35	0.348
1000.0	2.25	1.36	0.666	3.20	-2.81	0.288
1200.0	3.75	1.96	0.566	4.00	-4.04	0.516
2000.0	6.50	5.45	0.382	6.25	-11.23	0.667
3000.0	7.50	12.27	0.315	7.00	-25.27	0.717
5000.0	8.00	34.07	0.281	7.50	-70.17	0.750
7000.0	8.30	66.78	0.261	7.75	-137.57	0.767
9000.0	8.50	110.39	0.248	8.00	-227.43	0.784

Table A.2: Oil and Brine Drive of Core Plug-12

Centrifuge RPM	Oil Drive			Brine Drive		
	V_b cc	P_c psi	S_w fraction	V_o cc	P_c psi	S_w fraction
0.0	0.00	0.00	0.785	0.00	0.00	0.258
500.0	0.30	0.34	0.757	0.70	-0.70	0.323
700.0	0.40	0.67	0.748	1.50	-1.35	0.397
1000.0	0.50	1.36	0.739	2.30	-2.81	0.471
1200.0	3.80	1.96	0.434	2.75	-4.04	0.512
2000.0	4.50	5.45	0.369	4.00	-11.23	0.628
3000.0	4.75	12.27	0.346	4.50	-25.27	0.674
5000.0	5.20	34.07	0.304	4.75	-70.17	0.697
7000.0	5.50	66.78	0.277	5.20	-137.57	0.739
9000.0	5.70	110.39	0.258	5.35	-227.43	0.752

Table A.3: Oil and Brine Drive of Core Plug-3

Centrifuge RPM	Oil Drive			Brine Drive		
	V_b cc	P_c psi	S_w fraction	V_o cc	P_c psi	S_w fraction
0.0	0.00	0.00	0.820	0.00	0.00	0.185
500.0	0.50	0.34	0.776	0.70	-0.70	0.247
700.0	0.70	0.67	0.758	2.50	-1.38	0.405
1000.0	1.00	1.36	0.732	3.50	-2.81	0.494
1200.0	4.80	1.96	0.397	4.00	-4.04	0.538
2000.0	5.50	5.45	0.335	5.25	-11.23	0.648
3000.0	5.80	12.27	0.309	6.25	-25.27	0.736
5000.0	6.50	34.07	0.247	7.20	-70.19	0.820
7000.0	6.80	66.78	0.220	7.50	-137.57	0.846
9000.0	7.20	110.39	0.185	7.75	-227.40	0.868

Table A.4: Oil and Brine Drive of Core Plug-4

Centrifuge RPM	Oil Drive			Brine Drive		
	V_b cc	P_c psi	S_w fraction	V_o cc	P_c psi	S_w fraction
0.0	0.00	0.00	0.843	0.00	0.00	0.165
500.0	0.40	0.34	0.805	1.75	-0.70	0.335
700.0	0.50	0.67	0.795	2.00	-1.38	0.359
1000.0	0.50	1.36	0.795	3.00	-2.81	0.456
1200.0	4.70	1.96	0.388	4.25	-4.04	0.577
2000.0	5.20	5.45	0.339	5.50	-11.23	0.698
3000.0	5.50	12.27	0.310	6.20	-25.27	0.766
5000.0	6.20	34.07	0.243	6.80	-70.19	0.824
7000.0	6.60	66.78	0.204	7.30	-137.57	0.872
9000.0	7.00	110.39	0.165	7.50	-227.40	0.892

Table A.5: Oil and Brine Drive of Core Plug-16

Centrifuge RPM	Oil Drive			Brine Drive		
	V_b cc	P_c psi	S_w fraction	V_o cc	P_c psi	S_w fraction
0.0	0.00	0.00	0.862	0.00	0.00	0.210
500.0	0.60	0.34	0.802	0.50	-0.70	0.260
700.0	0.80	0.67	0.782	1.50	-1.38	0.360
1000.0	0.80	1.36	0.782	2.50	-2.81	0.461
1200.0	4.60	1.96	0.401	3.00	-4.04	0.511
2000.0	5.30	5.45	0.330	4.20	-11.23	0.631
3000.0	5.50	12.27	0.310	4.50	-25.27	0.661
5000.0	6.00	34.07	0.260	5.00	-70.19	0.712
7000.0	6.25	66.78	0.235	5.70	-137.57	0.782
9000.0	6.50	110.39	0.210	6.00	-227.40	0.812

Appendix B

B.1 Wettability

Wettability is defined as the tendency of one fluid to spread on or adhere to a solid surface in the presence of other immiscible fluids. When the rock is water wet, there is a tendency for water to occupy the small pores and contact the majority of the rock surface. The non-wetting fluid will occupy the center of the large pores and form globules that extend over several pores [14].

Wettability is a major factor controlling the location, flow, and distribution of fluids in a reservoir. For core analysis to predict the behavior of the reservoir, the wettability of the core must be the same as the wettability of the undisturbed reservoir rock.[15] There are different quantitative methods of measuring wettability which are Contact Angle Method, Amott Method, and USBM Method.

B.1.1 USBM Method

The United States Bureau of Mines Method measures the average wettability of the core. This test is relatively rapid and also has an advantage that it is sensitive near neutral wettability but the USBM wettability index can only be measured on plug-size samples because samples must be spun in a centrifuge and it cannot determine whether a system has fractional or mixed wettability.

This test compares the work necessary for one fluid to displace the other. Because of the free-energy change, the work required for the wetting fluid to displace

the nonwetting fluid from the core is less than the work required for the opposite displacement. This work is related to the area under the capillary pressure curve.[15]

In the first step of the measurement, called brine drive, oil saturated cores are placed in brine and centrifuged at incrementally increasing speeds until there is no increase in volume of oil expelled from the cores. The speed is changed to a higher rotation rate without decelerating the centrifuge. Redistribution of the fluids (hysteresis) would occur if the centrifuge were slowed or stopped. Thus the subsequent values for water saturation would be too low. The capillary pressure is calculated from the rotational speed of the centrifuge by the following formula.

$$P_c = 7.9527 * 10^{-8} * N^2 * \Delta\rho * ((R_2)^2 - (R_1)^2) \quad (B.1)$$

where

P_c = Capillary pressure, psi

$\Delta\rho$ = Density difference between two fluids, gm/cc

R_2 = Outer arm length, cm.

R_1 = Inner arm length cm.

$R_2 - R_1$ = core Length, cm.

N = Revolutions per minute, RPMs

In the second step, the oil displaces brine and is called oil-drive, the cores are placed in oil filled buckets and centrifuged. At equilibrium, the capillary pressure

$P_c(r)$ at every position r , there is a corresponding value of water saturation $S_w(r)$ and both vary substantially from one end of the core to the other. Water saturation is calculated at the face of the core sample by using the method proposed by Rajan [18] as follows.

$$S_i(P_{ci}) = S_w(P_{ci}) + \frac{2R}{1+R} P_{ci} \frac{dS_w(P_{ci})}{dP_{ci}} + \frac{R}{1-R^2} \int_0^{P_{ci}} \left(\frac{1 - [1 - \frac{P_c}{P_{ci}}(1 - R^2)]^{1/2}}{[1 - \frac{P_c}{P_{ci}}(1 - R^2)]^{1/2}} \right)^2 \frac{dS_w(P_c)}{dP_c}$$

where

$S_i(P_{ci})$ = Brine saturation corresponding to P_{ci}

P_{ci} = Capillary pressure at the inlet face of the core, psi

$S_w(P_{ci})$ = Average brine saturation corresponding to P_{ci}

$R = R1/R2$

$R1$ = Radius to inlet face of the core from center of rotation, cm

$R2$ = Radius to outlet face of the core from center of rotation, cm

P_C = Capillary pressure at any point along the length of the core, psi

Both the oil-drive and brine-drive capillary pressures vs. average saturation are plotted. The USBM wettability index, W is calculated by

$$W = \log \frac{A_1}{A_2} \quad (B.2)$$

$A1$ = Area under the oil-drive curve

$A2$ = Area under the brine-drive curve

When W is greater than zero, the core is water-wet, if W is less than zero, the core is oil-wet. A wettability index near zero means the core is neutrally wet. The larger the value of W , the greater the wetting preference.

B.2 Johnson-Bossler-Naumann Method

The Buckley-Leverett [22] displacement theory is based on a material balance equation, which relates the rate of change of displacing phase saturation at a position x with the change in fraction flow with respect to distance at a given time,

$$\left(\frac{\delta S_w}{\delta t}\right)_x = -\left(\frac{q_t}{A_O}\right)\left(\frac{\delta f_w}{\delta x}\right)_t \quad (\text{B.3})$$

where water is assumed to be the displacing phase and oil the displaced phase. This equation is then transformed to obtain the rate of advance of a plane of constant saturation given by

$$\left(\frac{\delta x}{\delta t}\right)_{S_w} = -\left(\frac{q_t}{A_O}\right)\left(\frac{\delta f_w}{\delta S_w}\right)_t \quad (\text{B.4})$$

If gravitational and capillary forces are neglected, Darcy's Law gives

$$f_w = \frac{1}{1 + \frac{k_{ro} \mu_w}{k_{rw} \mu_o}} \quad (\text{B.5})$$

Welge [16] proposed a method of analyzing f_w versus S_w data by constructing a tangent cord, from $(S_{wi}, f_w(S_{wi}))$ to the fractional flow curve. The height of the front is identified by the saturation corresponding to the point of tangency and its speed is proportional to the slope of tangent line. The average saturation at water

breakthrough is the saturation where tangent intersects the line at $f_w=1$. Welge derived the following equations:

$$\bar{S}_w - S_{w2} = f_o W_i \quad (\text{B.6})$$

$$1 + \frac{k_{rw}}{k_{ro}} \frac{\mu_o}{\mu_w} = \frac{1}{f_o} \quad (\text{B.7})$$

The importance of this method is that the saturation at the outlet face can be calculated from the average core saturation. Since average saturation can be determined from material balance as,

$$\bar{S}_w = S_{wi} + \frac{N_p}{V_p} \quad (\text{B.8})$$

and f_o can be measured directly from the effluent production. The above equations provide an easy and convenient method of calculating relative permeability ratio. Theory of individual relative permeabilities determination was presented by Johnson Bossler and Naumann [3]. They derived the following equations:

$$I_r = \frac{(q/\Delta P)}{(q/\Delta P)_{base}} \quad (\text{B.9})$$

$$\frac{f_o}{k_{ro}} = \frac{d(1/W_i I_r)}{d(1/W_i)} \quad (\text{B.10})$$

$$f_o = \frac{1}{1 + \frac{k_{rw}}{k_{ro}} \frac{\mu_o}{\mu_w}} \quad (\text{B.11})$$

$$f_o = \frac{N_p}{W_i} \quad (\text{B.12})$$

$$S_{w2} - S_{wi} = N_p - W_i f_o \quad (\text{B.13})$$

Vita

Name: Ashiq Hussain

Permanent Address: 117-G, Bogaram Street,
Mianwali 42200, Pakistan

Date of Birth: September 15, 1963

Secodary Education: Government Central Model High
School, Mianwali

Higher Education: University of Engineering and
Technology, Lahore, Pakistan

Major: Petroleum Engineering

Date of Degree, B.Sc.(ENGG.): February, 1988

Date of Degree, M.S.(ENGG.): April, 1995